Molecular and isotopic composition showing source and in-reservoir phase fractionation of crude oils and condensates in the Surma basin, NE Bangladesh

Doctoral Dissertation

20125207

September, 2015

HOSSAIN MD. Ashique

Division of Earth and Planetary System Science

Department of Natural History Sciences

Graduate School of Science

Hokkaido University

Contents

Chapter 1.

Geochemical characteristics of crude oils and condensates from the Surma basin, NE Bangladesh

Chapter 2.

Carbon and hydrogen isotope composition of individual *n*-alkane in crude oils and condensates from the Surma basin, NE Bangladesh

List of Tables and Figures

List of Tables

List of Figures

List of Figures

Chapter 1

Geochemical characteristics of crude oils and condensates

Abstract

The origin and source rocks of crude oils and condensates from seven oil and gas fields located in the Surma basin, Bangladesh were investigated based on saturated and aromatic hydrocarbon distributions. The relative compositions of pristane, phytane and adjacent *n*-alkanes suggest that the source rock was deposited in a non-marine setting. The abundance and similar distribution of biphenyls, cadalene and bicadinanes in most of the crude oils and condensates indicates a significant supply of higher-plant derived organic matter to the source rocks. Maturity levels of oils and condensates from the Surma basin were estimated based on the alkylnaphthalenes, alkylphenanthlenes, and diamondoids, correspond to calculated vitrinite reflectance (R_c) values of 1.0–1.3%. R_c (%) values indicating hydrocarbon expulsion from the source rock at a comparatively high maturity level. The R_c values of oils from the Titas field in the southern margin of the Surma basin are relatively low (0.8–1.0%). Some oils were severely biodegraded. The similar distribution of diamondoid hydrocarbons in both biodegraded and non-biodegraded oils indicated similar type of source rocks and similar maturity levels to those of oils from the Surma basin.

Although the geochemical data set for the Oligocene and older sedimentary sequences is limited, the top of the Eocene Kopili Shale to lower Jenam Shale of early Oligocene sedimentary rocks rich in terrigenous organic matter are identified as possible source rocks. The relative abundance of C_7 aromatic, cyclic, and straight chain hydrocarbons in oil and condensates and other molecular parameters inferred diversity of the petroleum from waxy crude oils to condensates in the study area. This diversity of the petroleum was likely due to evaporative fractionation, resulting in residual waxy oils and lighter condensates which subsequently underwent tertiary migration and re-accumulation. Evaporative fractionation is thought to be due to modification of the reservoir structure occurred during and after the Pliocene, when large-scale tectonic deformation occurred in and around the Bengal Basin.

1. Introduction

Bangladesh covers most part of the Bengal Basin. Surma basin, a sub-basin of the Bengal Basin lies in the northeastern part of Bangladesh, evolved from a pre-Oligocene passive continental margin to a foreland basin associated with the Indo-Burman and Himalayan mobile belts. The basin is filled by thick (12–16 km) Late Mesozoic and Cenozoic sedimentary succession (Johnson and Alam, 1991). Hydrocarbons that produced in Bangladesh (primarily gas and gas-associated condensates) have been discovered in the Mio-Pliocene Surma Group, but the source of these hydrocarbons remains ambiguous. Although a number of geochemical studies have been performed (Hiller and Elahi, 1984; Alam and Pearson, 1990; Ahmed et al., 1991; Ismail and Shamsuddin, 1991; Shamsuddin and Abdullah, 1997; Curiale et al., 2002; Hossain et al., 2009; Takeda et al., 2011), few studies have evaluated the source rocks in the Surma basin based on the geochemical characteristics of the crude oils and condensates.

It was reported that, oils and condensates in the Surma basin may have been generated by source rocks in the Oligocene Jenam Formation which was deposited in a deltaic environment (Ahmed et al., 1991). Condensates from the southern margin of the Surma basin are thought to be sourced from marine-influenced terrestrial organic matter (Ahmed et al., 1991). Alam and Pearson (1990) reported the occurrence of bicadinanes and oleanane in waxy oils from the basin, and suggested that the bicadinanes were formed from the polymerized resin of *Dipterocarpaceae* or similar angiosperms during source rock maturation. Curiale et al. (2002) also suggested corresponding differences in source rock organic matter between oils from the northern and central Surma basin and those from the south, on the basis of the *n*-alkane distribution, pristane/phytane ratio and the presence and abundance of bicadinane. Migration-induced compositional variation in oil/condensates and increasing wax content with depth have also been suggested (Curiale et al., 2002). These studies proposed that prospective source units are the Oligocene Jenam Formation in the north to central Surma basin and the Miocene Bhuban Formation in the south. However, previous studies did not include detailed investigations of low molecular weight hydrocarbons, cyclic saturate hydrocarbons or polycyclic aromatic hydrocarbons which can be used to characterize oils/condensates, and their sources.

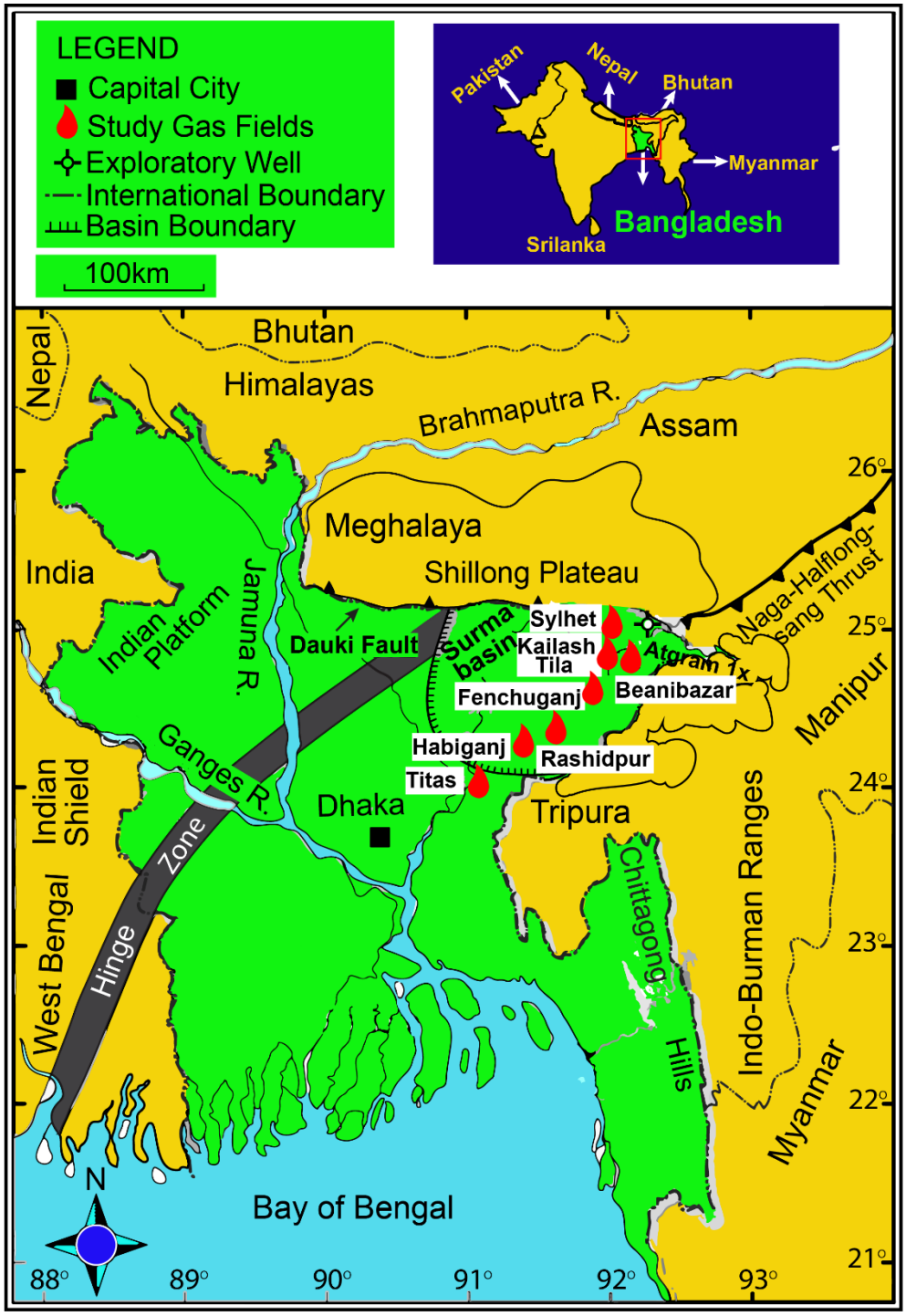

Fig. 1. Oil and gas field locations in the Surma basin and the major tectonic elements of Bangladesh and surrounding areas (modified after Hossain *et al*., 2014).

Age (approx.)	Group	Formation	Lithology	Environment of deposition
Holocene	Dihing	Alluvium		
Pleistocene		Dihing		Relatively thin subaerial local deposits[b].
Late Pliocene	Dupi Tila	Upper Dupi Tila		Probably braided, fluvial system to meandering river deposits[a] ; lake-river plain[c] ; fluvial-deltaic[d] ; continental-fluvietile[e].
		Lower Dupi Tila		
Mid-Pliocene	Tipam	Girujan Clay		
		Tipam Sandstone		
Early Pliocene-Miocene	Surma	UMS Upper (Bokabil)		Pro-delta and delta-front deposits of large mud-rich delta system[a]; fluvial-deltaic to estuarine[d]; deltaic to shallow marine[e].
		Lower (Bhuban)		
Oligocene	Barail	Renji Jenam Laisong		Fluvial, delta to pro-delta deposits[a]; marine to estuarine[e]; deltaic with marine incursions[d].
Paleocene-Eocene	Jaintia	Kopili Shale		Transition of basinal to shallow-marine[a]; shallow-marine to marine, shallow-marine to carbonate and deltaic to slope deposition (from bottom upwards) [b]; deep basinal[d]; marine[e].
		Sylhet Limestone		
		Tura Sandstone		
Pre-Paleocene	Undifferentiated sedimentary rocks on the continental basement complex.			

Sand, silt, clay; Clay; Shale; Sandstone; Coal; Limestone; Unconformity; UMS- Upper Marine Shale.

a- Johnson and Alam, 1991; **b**- Alam et al., 2003; **c**- Imam, 2005; **d**- Curiale et al, 2002; e- Alam, 1989.

Fig.2. Generalized stratigraphic succession of the Surma basin, Bangladesh, with schematic lithology (not to scale); modified after Hossain *et al.*, 2014.

In the present study, taking into account the geochemical characteristics, including distributions of low molecular weight saturate and aromatic hydrocarbons, *n*-alkanes, diamondoids, alkylnaphthalenes, biphenyls and phenanthrenes, potential source rocks for the crude oils and condensates in the Surma basin were investigated

2. Study area and the adjoining geologic settings

Bangladesh is bordered by the Indian shield to the NW and west, the Shillong Plateau to the north, the Indo-Burman Ranges to the east, and the Bay of Bengal in the south (Fig. 1). The present-day platformal shelf of western Bangladesh was originally part of eastern Gondwana together with India, Australia, and Antarctica (Shamsuddin and Abdullah, 1997). India began to separate from Australia and Antarctica during the Early Cretaceous, drifting north and then NE, and finally colliding with the Asian plate (Shamsuddin and Abdullah, 1997; Curiale et al., 2002; Imam, 2005). In terms of structure, Bangladesh can be divided into a stable shelf in the NW and west, underlain by Precambrian continental crust; and a deep basin in the south and east in which there is a very thick sedimentary succession (Uddin and Lundberg, 2004). The deep basin area can be further divided into an unfolded platform flank in the west, and to the east the Chittagong-Tripura fold belt (Shamsuddin and Abdullah, 1997). The NE–SW trending Hinge Zone separates the stable shelf and deep basin (Fig. 1), and may mark the transition from continental to oceanic crust (Alam et al., 2003).

The Bengal Basin had a complex sedimentary and tectonic history between Eocene and Recent times. Rapid uplift of the Himalayas to the north and the Indo-Burman Ranges in the east, slow subsidence of the western platform area and rapid subsidence of the foredeep in the south took place simultaneously. The Bengal delta, the largest delta in the world, formed in response to a huge influx of detrital material derived from the rising Himalayas and transported by the Ganges and Brahmaputra rivers (Johnson and Alam, 1991). Large-scale tectonic movements occurred along the east-west trending Dauki thrust fault (Fig. 1) during the Pliocene and in the Himalaya and Indo-Burman Ranges, resulting in the formation of anticlinal folds and structural traps (Alam, 1989; Imam and Hussain, 2002). The Surma basin, also known as the Sylhet trough, is located in NE Bangladesh (Fig. 1) and basin evolved from a pre-Oligocene passive continental margin

to a foreland basin associated with the Indo-Burman and Himalayan fold belts. The basin is bounded by the Dauki Fault and Shillong Plateau to the north, the Indian platform to the west and the Chittagong-Tripura fold belt of the Indo-Burman Ranges to the east; it is separated from the Patuakhali depression by the Tangail-Tripura High to the south (Shamsuddin and Abdullah, 1997). The basin has a thick sedimentary fill (up to 12–16 km) comprising Upper Mesozoic to upper Cenozoic deposits (Johnson and Alam, 1991).

Geology of the Surma basin

Wells drilled in the Surma basin have not penetrated sedimentary strata older than Oligocene. At the base of the sedimentary succession (Fig. 2), the Paleocene–Early Eocene Tura Sandstone Formation has been encountered by wells in western Bangladesh and is composed of freshwater to mixed-marine sandstones and shales within coal seams. The formation is thought to be equivalent to the Jalangi Formation of West Bengal. During the Middle–Late Eocene, an extensive marine transgression over the shelf area resulted in deposition of the nummulitic Sylhet Limestone in the west and open-marine shale-rich facies in the east (Alam, 1989; Shamsuddin and Abdullah, 1997). The top of the Sylhet Limestone represents the deepest seismic reflector in the Surma basin (Hiller and Elahi, 1984). The overlying Eocene Kopili Formation in the Surma basin passes gradually from open-marine up to estuarine facies (Banerji, 1981).

The overlying pre-Oligocene Disang Group can be divided into lower and upper units in the Naga Hills of India and the eastern Surma basin (Rao, 1983). The Sylhet Limestone and Kopili Shales are thought to be equivalent to the upper portion of the Disang Group (Shamsuddin and Abdullah, 1997). Oligocene rocks of the Barail Group crop out on the eastern and northern margins of the Surma basin near the Dauki Fault zone and Oligocene rocks have been encountered in the subsurface by wells Rashidpur #2 and Atgram #IX (Johnson and Alam, 1991). Most of the stable shelf area was exposed during a marine regression during the Oligocene, and the Barail Group is interpreted as a marine to estuarine deposit in the foredeep area (Alam, 1989). Rocks of the Barail Group crop out over a wide area in the NE Surma basin having an off-lap relationship with the underlying Kopili Formation (Banerji, 1984). The Barail Group comprise sediments

Table I. General geochemical characteristics of the crude oils and condensates. T, toluene; MCH, methylcyclohexane; Pr, pristane; Ph, phytane (Hossain *et al*., 2014).

Serial no.	Well name	Field name	Depth (m)	Formation	*n* C_7/MCH	Toluene/*n* C_7	Pr/*n* C_{17}	Ph/*n* C_{18}	Pr/Ph
1	Sylhet #7	Sylhet	1874-1886 1901-1908	Upper Bhuban	0.18	8.47	2.09	0.37	11.00
2	Sylhet #7		2020-2033	Bhuban	0.20	8.60	1.55	0.22	7.99
3	Kailash Tila #1	Kailash Tila	2941-2948	Bhuban	0.27	4.37	1.43	0.22	9.71
4	Kailash Tila #2		2252-2265	Bokabil	0.19	7.95	1.74	0.25	11.93
5	Kailash Tila #2+6		2252-2265	Bokabil	0.18	6.59	1.51	0.26	9.00
6	Kailash Tila #2		2724-2732	Bhuban	0.27	4.70	1.37	0.23	7.91
7	Kailash Tila #2		2927-2930	Bhuban	0.24	6.25	1.51	0.25	7.95
8	Kailash Tila #4		2930-2958	Bhuban	0.25	5.81	1.66	0.27	9.60
9	Beanibazar #1+2 (heavy)	Beanibazar	3451-3465	Bokabil	0.31	2.96	1.26	0.21	7.05
10	Beanibazar #1+2 (light)				0.39	0.94	nd	nd	nd
11	Fenchuganj #2	Fenchuganj	2578.6-2581.6	Upper Bhuban	0.16	9.09	1.51	0.29	7.23
12	Fenchuganj #2+3		2768-2781		0.22	7.67	1.61	0.29	8.13
13	Fenchuganj #2		3068.5-3072.5 3074.5-3083.5		0.22	9.88	0.84	0.13	5.30
14	Rashidpur #1	Rashidpur	1401-1418 1421-1445	-	nd	nd	nd	nd	nd
15	Habiganj #1	Habiganj	1417-1428	Lower Bokabil	nd	nd	nd	nd	nd
16	Habiganj #3+4		1328-1487(3) 1363-1489(4)		nd	nd	nd	nd	nd
17	Titas #1	Titas	2617-2769	Upper Bhuban	0.37	3.33	1.05	0.30	5.92
18	Titas #5		2921-3052	Bhuban	0.34	4.13	1.04	0.30	5.38
19	Titas #8		3293-3551	Bhuban	0.19	7.90	1.10	0.36	5.36
20	Titas #10		3473-3680	Bhuban	0.26	4.97	1.10	0.34	5.50

derived from the rising eastern Himalayas, which were deposited in environments ranging from fluvial to deltaic and pro-deltaic from north to SE (Johnson and Alam, 1991). The subsidence rate of the basin during the Miocene increased markedly in response to loading caused by encroachment from the west of the Indo-Burman Ranges, associated with the eastward subduction of the Indian plate beneath the Burmese plate. The Surma Group was deposited during this time period and is composed of sediments mostly derived from the eastern Himalayas (Johnson and Alam, 1991). The top of the Surma Group, known as the "Upper Marine Shale", provides a prominent seismic marker and stratigraphic reference level in the Surma basin, and represents the last marine incursion (Hiller and Elahi, 1984). The Surma basin subsided rapidly during the Miocene – Plio-Pleistocene, resulting in the deposition of the fluvial Tipam and Dupi Tila Formations. South-directed overthrusting of the Shillong Plateau contributed to this subsidence. The absence of Pliocene and younger strata from the Shillong Plateau suggests that it formed an uplifted block during the Pliocene (Johnson and Alam, 1991).

3. Materials and Methods

3.1. Samples

A set of total 20 crude oil and condensate samples (Table 1) were collected from seven oil and gas fields located in the Surma basin (Fig. 1): Beanibazar, Fenchuganj, Kailash Tila, Sylhet, Rashidpur, Habiganj and Titas. The four samples from the Titas gas field represent the southern margin of the basin. All the investigating samples were provided by the joint study between Bangladesh Petroleum Institute (BPI) / Bangladesh Oil, Gas & Mineral Corporation (Petrobangla) / Bangladesh Petroleum Exploration & Production Company Limited (BAPEX), Bangladesh and Mitsui Oil Exploration Company Limited (MOECO) / JGI Inc. and Hokkaido University, Japan.

3.2. Experimental

All the oil/condensate samples were analyzed as whole oil, and most of the samples were separated into saturated and aromatic hydrocarbon fractions and analyzed using gas chromatography and gas chromatography-mass spectrometry (GC and GC-MS). Detail experimental methods are discussed in the following

3.2.1. Gas chromatography (GC)

To get the quantitative information of individual components existed in oil/condensate samples, all the samples were analyzed by whole oil gas chromatography (GC) using HP6890 instrument equipped with a fused silica capillary column DB35MS (30 × 0.25 mm, J&W). Saturate fractions were separated using silica gel (60, Merck) column chromatography and analyzed by GC. The oven temperature of the GC was initially programmed to 40ºC and held isothermally for 4 minutes; it was then programmed to 300ºC at a rate of increase of 5ºC/min and held isothermally for 19 min. Helium was used as carrier gas with a flow rate of 1.5 ml/min. Relative concentrations of *n*-alkane and acyclic isoprenoids (pristane and phytane) were determined from peak areas of the whole oil and saturate fraction flame ionization detector (FID) chromatograms by GC.

3.2.2. Gas chromatography-mass spectrometry (GC-MS)

To identify and evaluate the saturate and aromatic hydrocarbons as well as biomarkers, all the samples were analyzed as whole oil, and saturate and aromatic fraction of most of the oil/condensate samples have been analyzed by gas chromatography-mass spectrometry (GC-MS) using HP6890/HP5973 instruments equipped with a fused silica capillary column DB35MS (30 × 0.25 mm, J&W). The oven temperature of the GC-MS was initially programmed to 40ºC and held isothermally for 5 minutes; subsequently, it was programmed to 300ºC at a rate of increase of 4ºC/min and held isothermally for 5 minutes. Helium was used as carrier gas with a flow rate of 0.6 ml/min. Identification of individual compounds was performed using a mass spectra data library together with the retention times in published literature.

Relative concentrations of polycyclic aromatic hydrocarbons (PAHs) and cyclic saturate hydrocarbons (mainly adamantanes) were precisely calculated based on peak areas in the whole oil and saturate fraction total ion current (TIC) chromatograms by GC-MS. Considering the availability of published literature (e.g. Trolio et al., 1999; Mrkic et al., 2011), a DB5HT fused silica capillary column (30 × 0.25 mm, J&W) was also used for GC-MS analysis to identify the isomers of the PAHs and cyclic saturated hydrocarbons.

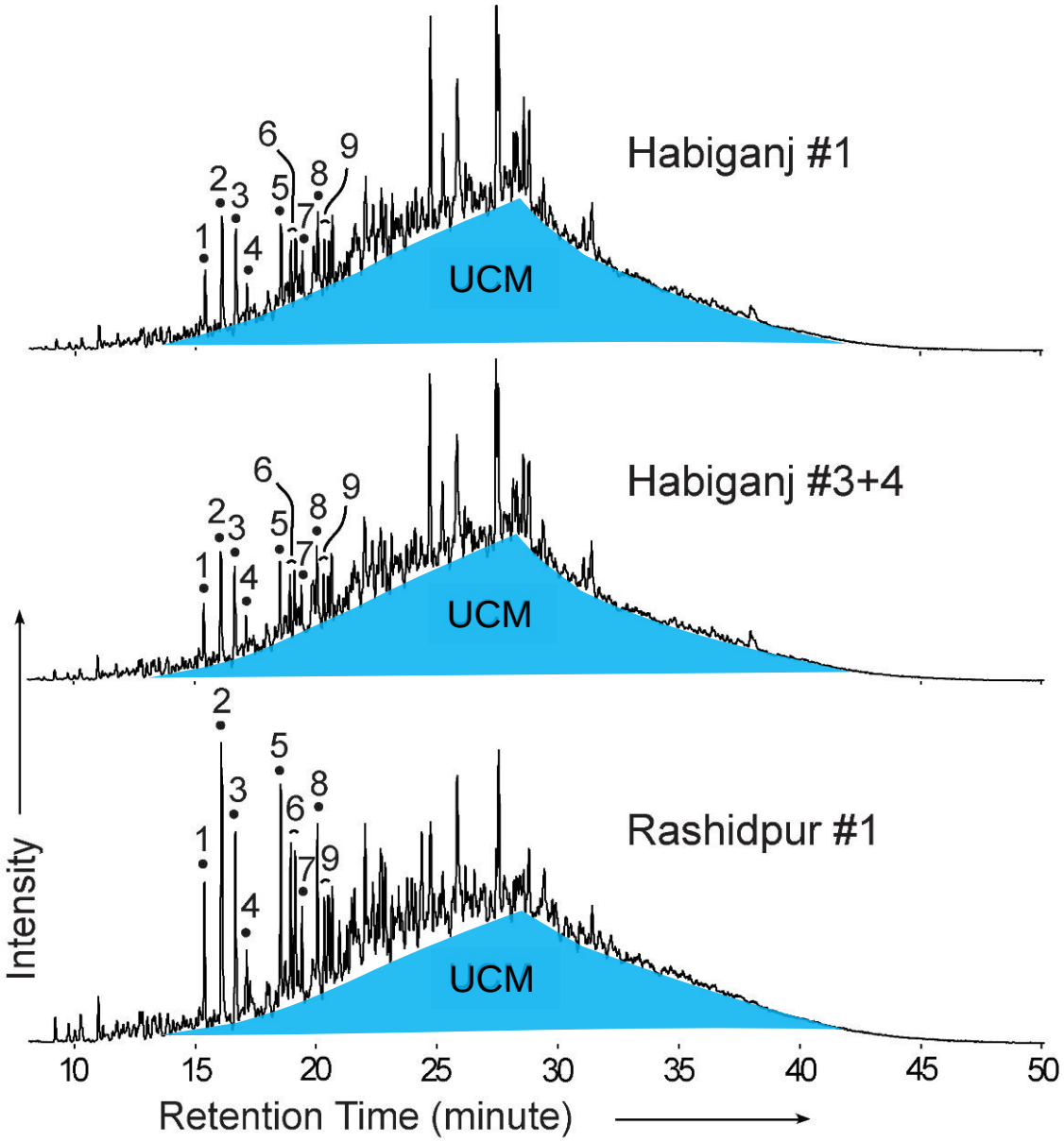

Fig.3. Whole oil TIC chromatograms of the severely biodegraded oils (Hossain et al., 2014). 1, adamantane; 2, 1-methyladamantane; 3, 1,3-dimethyladamantane; 4, 1,3,5-trimethyladamantane; 5, 2-ethyladamantane; 6, 1,4-dimethyladamantane (cis + trans); 7, 1,3,6-trimethyladamantane; 8, 1,2-dimethyladamantane; 9, 1,3,4-trimethyladamantane (cis + trans).

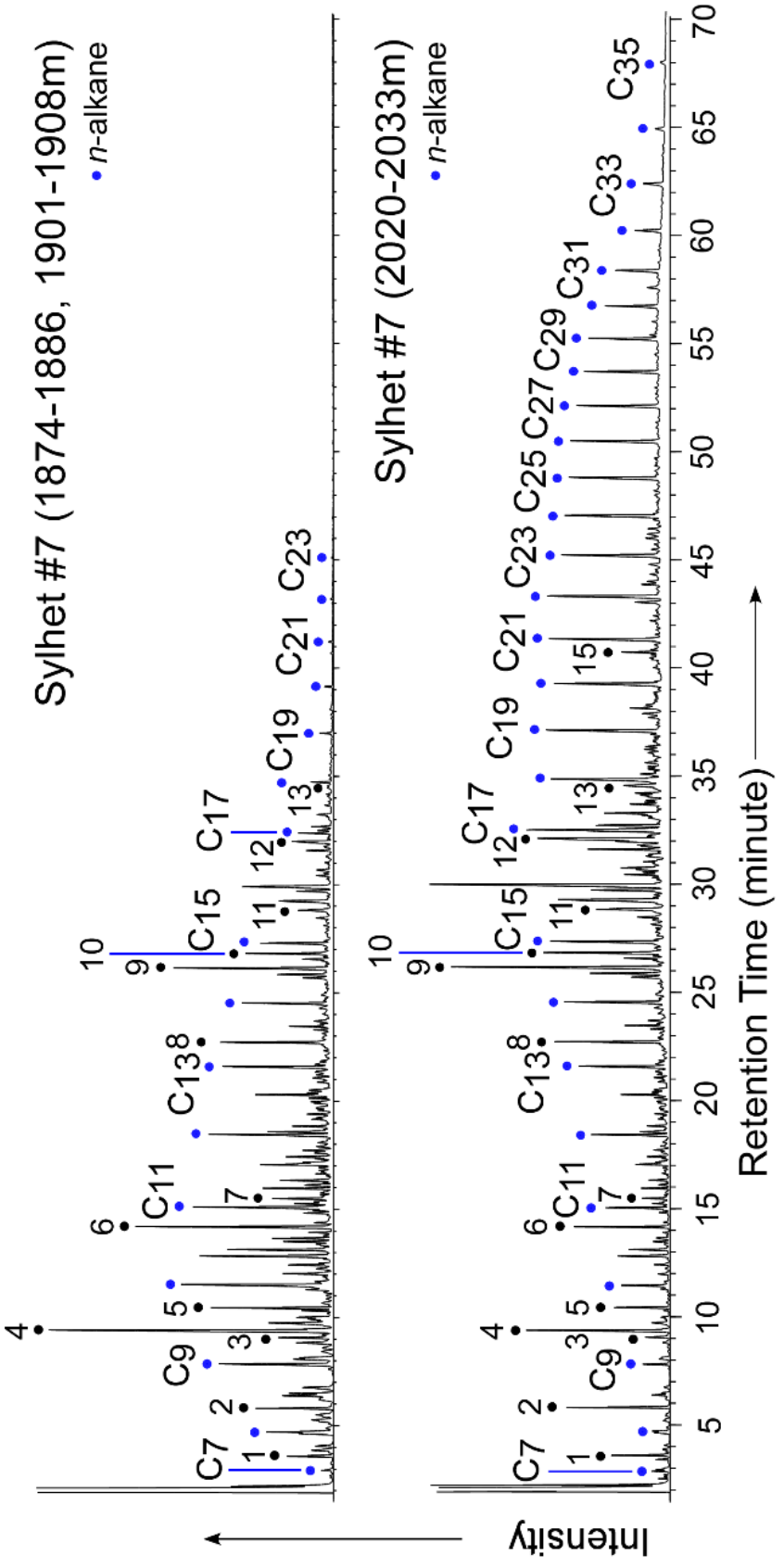

Fig. 4. Field wise (from north to south) whole oil FID chromatograms. Identification of important peaks: 1, methylcyclohexane; 2, toluene; 3, ethylbenzene; 4, meta + para-xylene; 5, ortho-xylene; 6 + 7, trimethylbenzene; 8, naphthalene; 9, 2-methylnaphthalene; 10, 1-methylnaphthalene; 11, biphenyl; 12, pristane; 13, phytane; 14, cadalene; 15, phenanthrene.

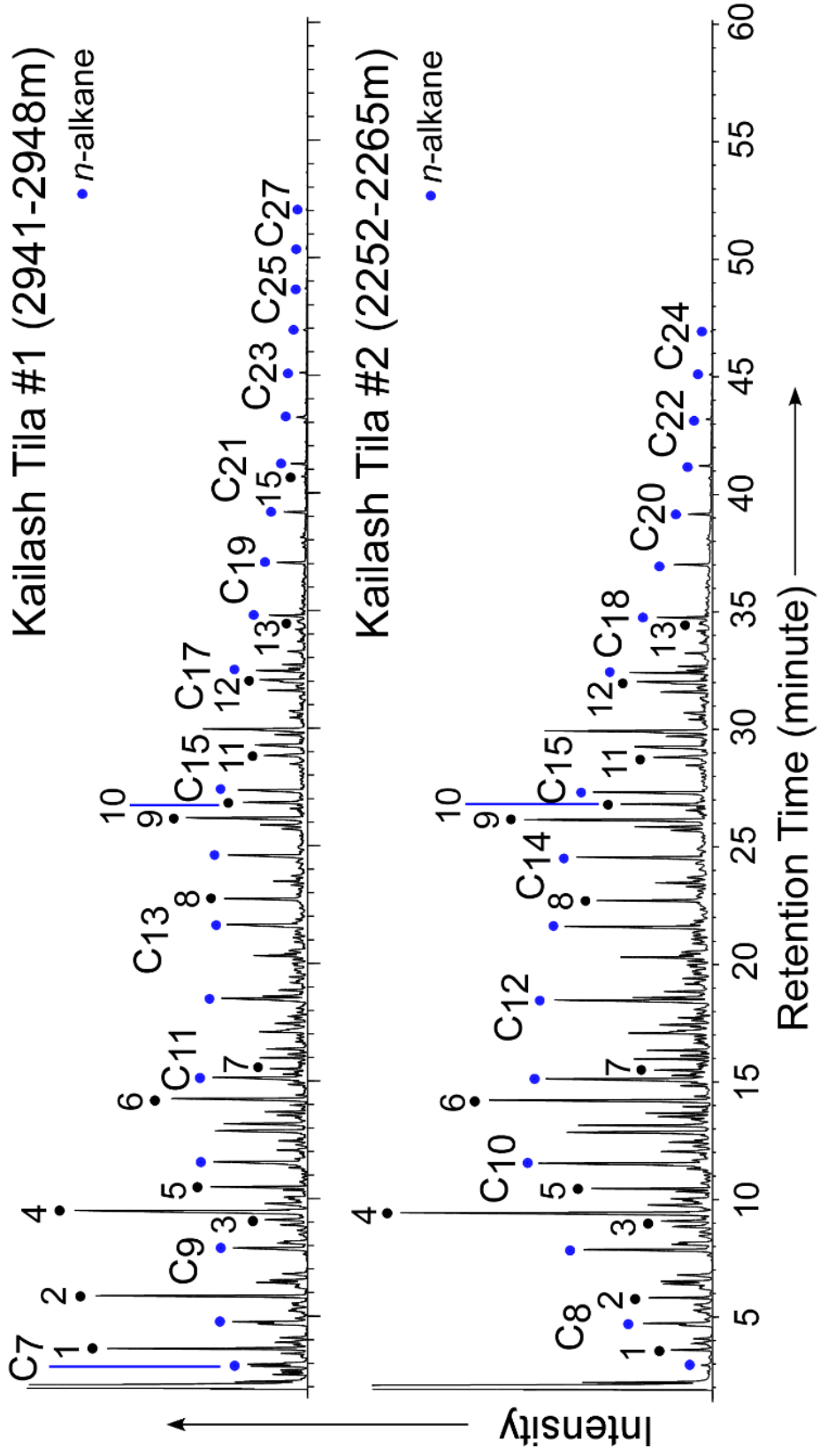

Continue Fig. 4.

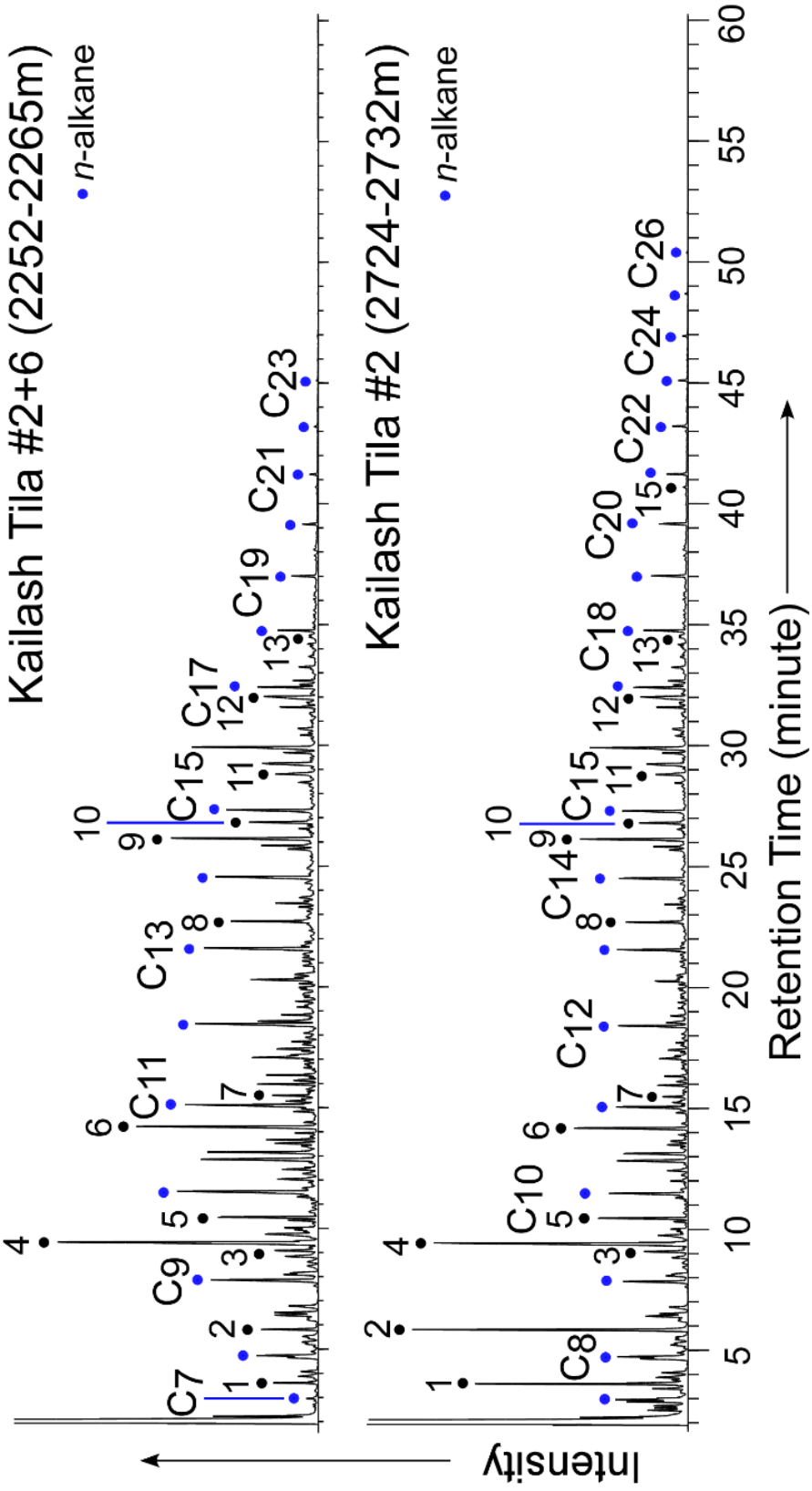

Continue Fig. 4.

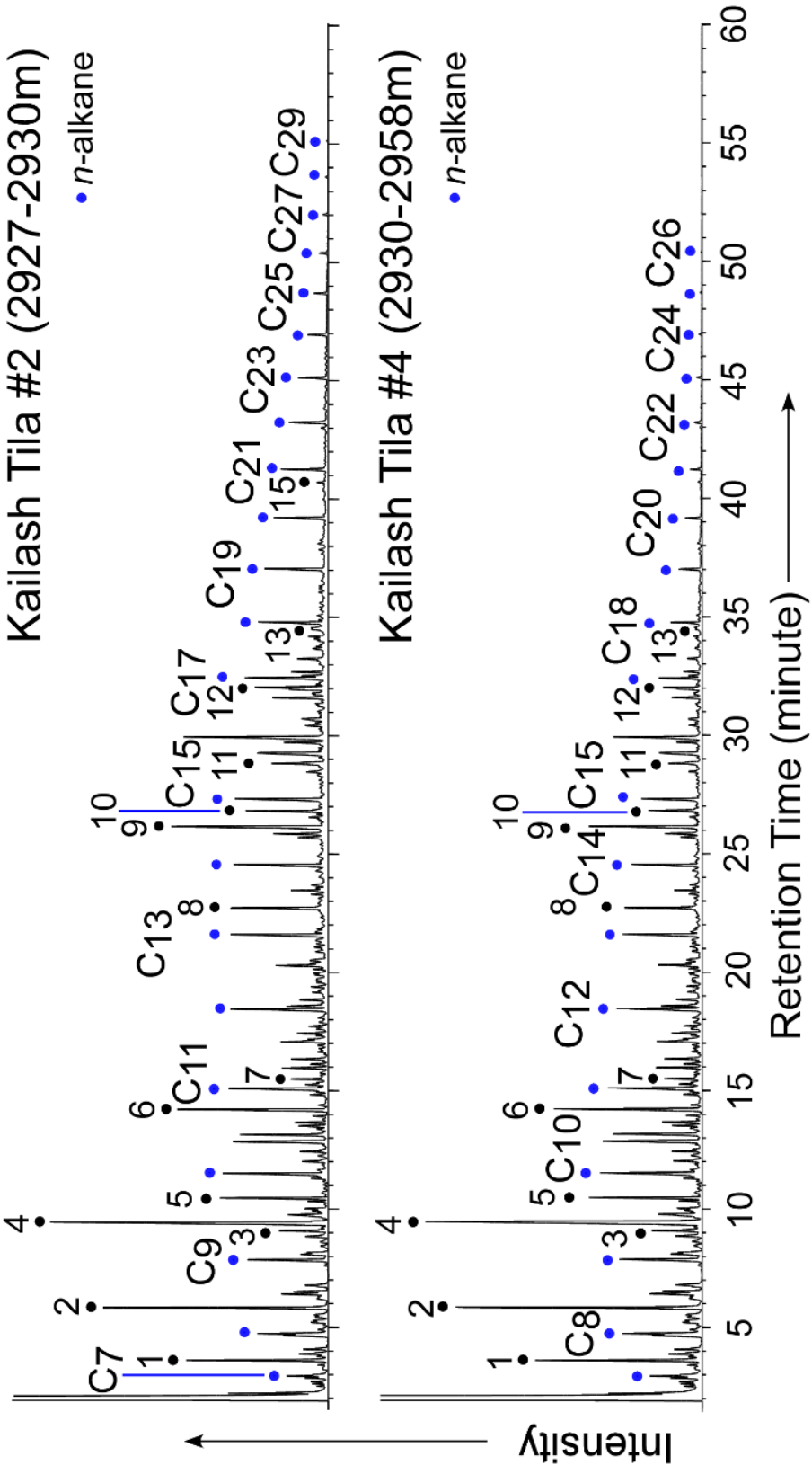

Continue Fig. 4.

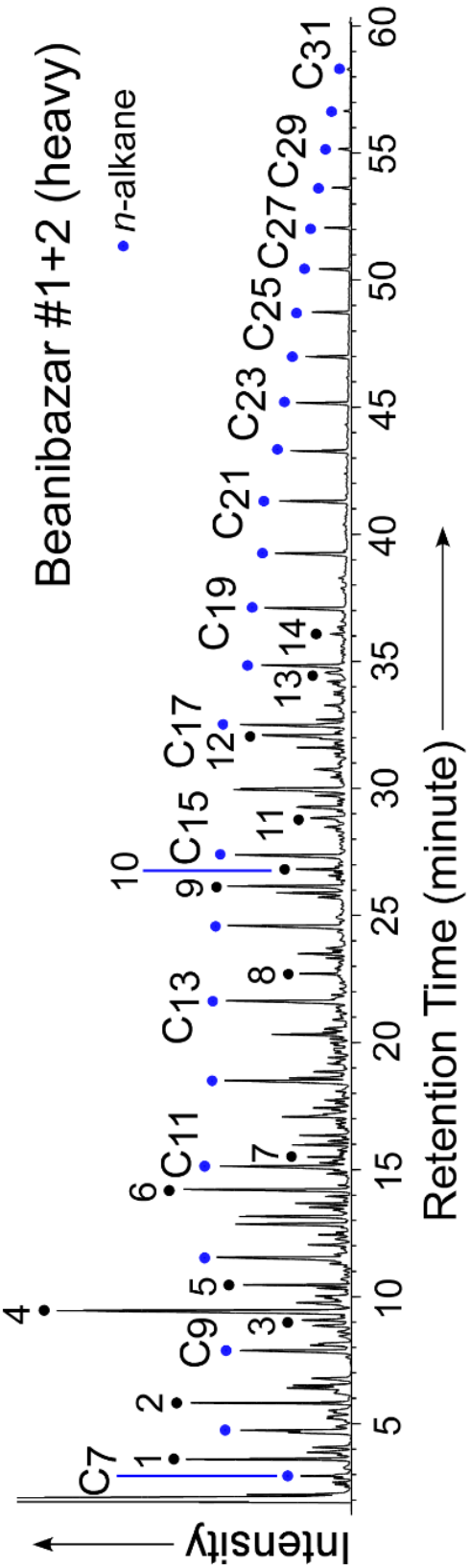

Continue Fig. 4.

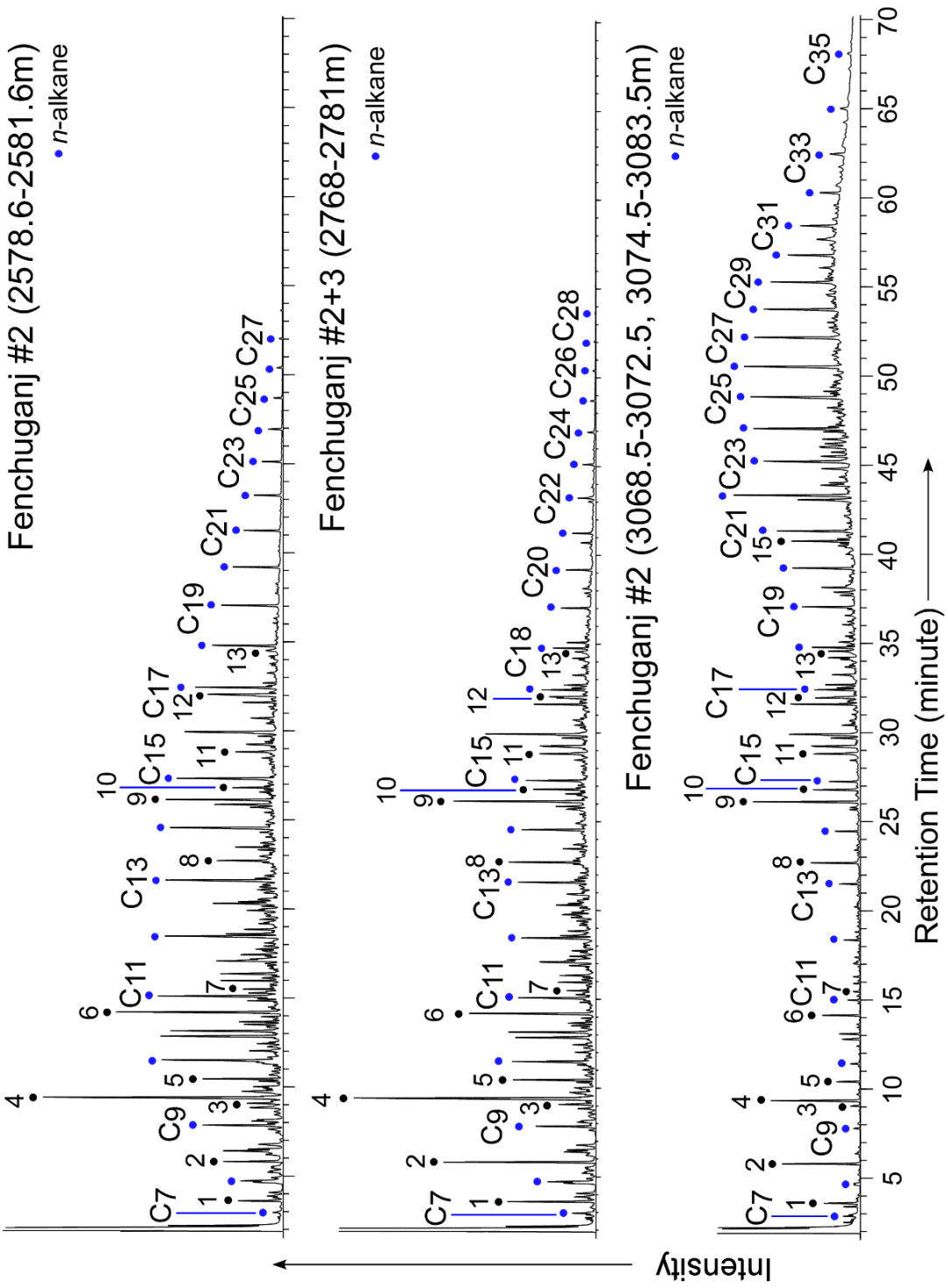

Continue Fig. 4.

Continue Fig. 4.

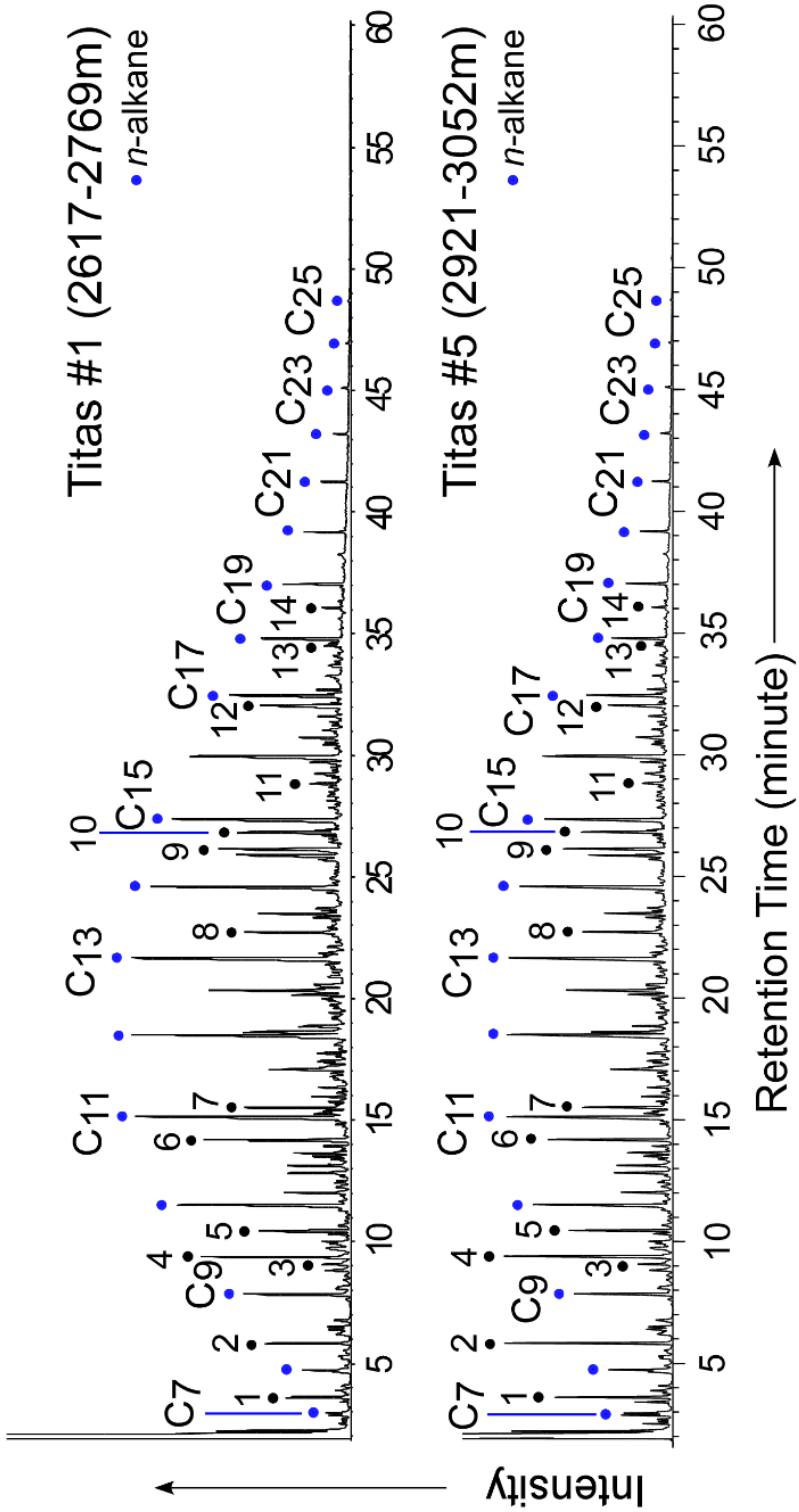

Fig. 4. Field wise (from north to south) whole oil FID chromatograms. Identification of important peaks: 1, methylcyclohexane; 2, toluene; 3, ethylbenzene; 4, meta + para-xylene; 5, ortho-xylene; 6 + 7, trimethylbenzene; 8, naphthalene; 9, 2-methylnaphthalene; 10, 1-methylnaphthalene; 11, biphenyl; 12, pristane; 13, phytane; 14, cadalene; 15, phenanthrene.

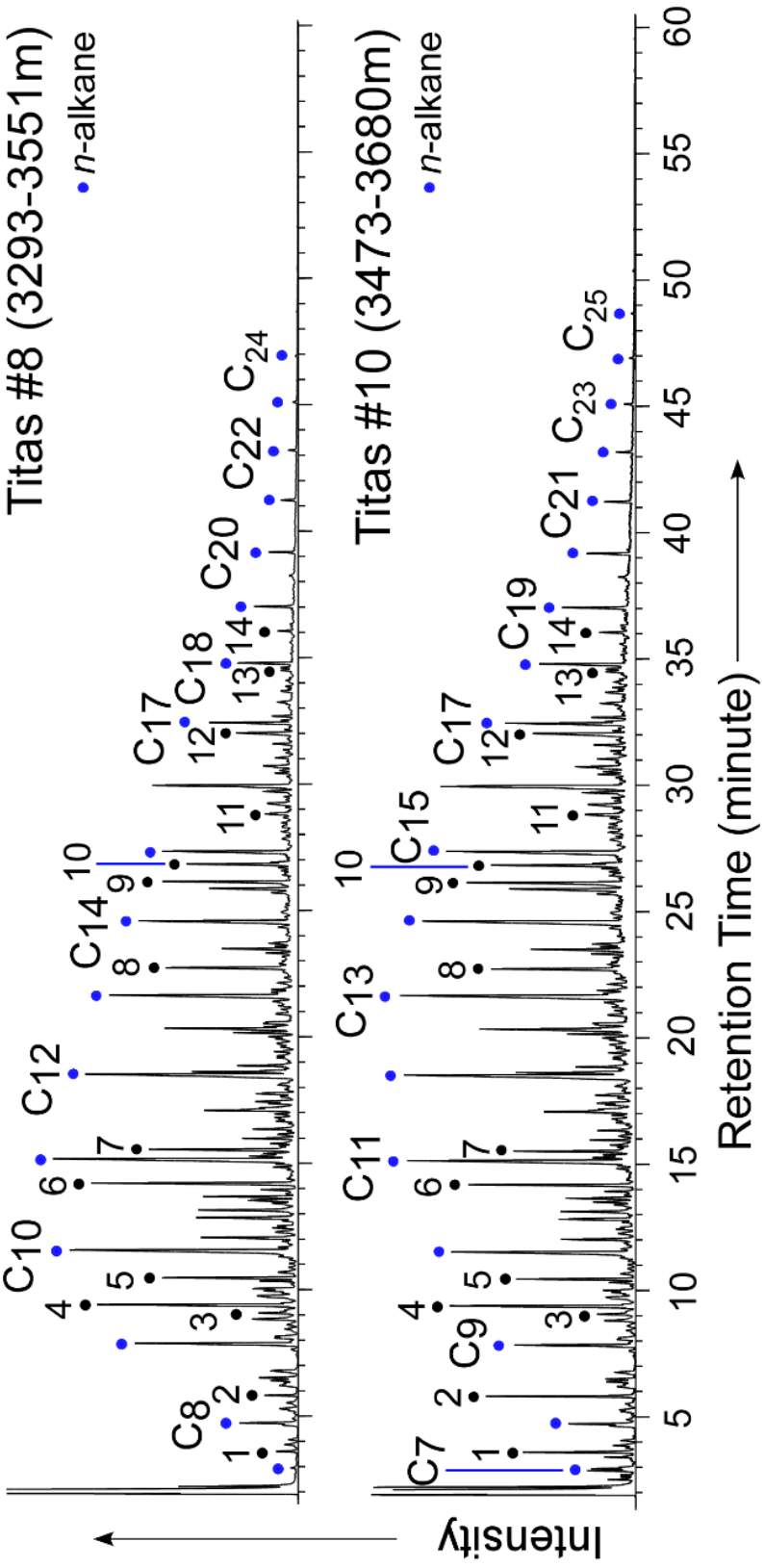

Continue Fig. 4.

Table 2. Relative abundance (%) of *n*-alkanes calculated from whole oil FID chromatograms (Hossain *et al*., 2014).

Well name	Depth (m)	C_7	C_8	C_9	C_{10}	C_{11}	C_{12}	C_{13}	C_{14}	C_{15}	C_{16}*	C_{17}	C_{18}	C_{19}	C_{20}	C_{21}	C_{22}	C_{23}	C_{24}	C_{25}	C_{26}	C_{27}	C_{28}	C_{29}	C_{30}	C_{31}	C_{32}	C_{33}	C_{34}	C_{35}	Total
Sylhet #7	1874-1886 1901-1908	0.7	6.1	11.8	18.9	15.4	13.5	11.5	8.7	7.1	0.0	2.6	1.5	0.9	0.5	0.3	0.2	0.1	0.0	0.0	0.0	0.0	0.0	0.0	0.0	0.0	0.0	0.0	0.0	100
Sylhet #7	2020-2033	0.4	0.6	0.9	2.0	2.2	3.0	4.0	4.9	5.5	0.0	6.7	6.2	5.6	5.9	6.2	6.5	5.6	5.2	4.7	4.5	4.2	3.5	3.2	2.5	2.3	1.4	1.2	0.6	0.4	100
Kailash Tila #1	2941-2948	4.1	5.8	8.6	13.3	11.8	10.9	10.5	9.5	8.8	0.0	5.0	3.8	2.9	1.8	1.1	0.9	0.5	0.3	0.2	0.1	0.1	0.0	0.0	0.0	0.0	0.0	0.0	0.0	0.0	100
Kailash Tila #2	2252-2265	0.4	4.0	9.0	15.0	14.2	12.8	12.1	10.6	9.6	0.0	4.8	3.3	2.0	1.1	0.6	0.3	0.1	0.1	0.0	0.0	0.0	0.0	0.0	0.0	0.0	0.0	0.0	0.0	0.0	100
Kailash Tila #2+6	2252-2265	0.6	4.7	9.9	15.9	13.7	12.9	11.9	10.1	9.0	0.0	4.5	3.0	1.8	1.0	0.5	0.3	0.1	0.0	0.0	0.0	0.0	0.0	0.0	0.0	0.0	0.0	0.0	0.0	0.0	100
Kailash Tila #2	2724-2732	6.7	8.0	8.5	10.4	8.6	8.6	8.8	8.4	8.6	0.0	6.0	5.0	3.8	2.9	2.1	1.7	1.0	0.6	0.3	0.2	0.0	0.0	0.0	0.0	0.0	0.0	0.0	0.0	0.0	100
Kailash Tila #2	2927-2930	2.4	4.9	6.5	9.4	8.2	8.5	8.8	8.7	9.2	0.0	6.9	6.1	5.3	4.0	3.3	2.8	1.8	1.3	0.9	0.5	0.3	0.2	0.1	0.0	0.0	0.0	0.0	0.0	0.0	100
Kailash Tila #4	2930-2958	4.3	8.2	10.5	14.6	12.0	11.0	10.0	8.5	7.3	0.0	4.1	3.1	2.1	1.4	1.0	0.8	0.5	0.3	0.2	0.1	0.0	0.0	0.0	0.0	0.0	0.0	0.0	0.0	0.0	100
Beanibazar #1+2 (heavy)	3451-3465	2.2	4.8	6.5	9.3	8.3	7.8	8.1	8.3	7.9	0.0	7.1	5.4	4.7	3.8	3.4	2.8	2.3	1.9	1.6	1.3	1.0	0.7	0.5	0.3	0.2	0.0	0.0	0.0	0.0	100
Beanibazar #1+2 (light)		nd	nd	nd	nd	nd	nd	nd	nd	nd	nd	nd	nd	nd	nd	nd	nd	nd	nd	nd	nd	nd	nd	nd	nd	nd	nd	nd	nd	nd	0
Fenchuganj #2	2578.6-2581.6	0.5	3.3	6.6	10.5	11.2	10.6	10.9	10.7	10.2	0.0	6.4	5.1	3.9	3.1	2.2	1.6	1.2	0.8	0.6	0.4	0.2	0.0	0.0	0.0	0.0	0.0	0.0	0.0	0.0	100
Fenchuganj #2+3	2768-2781	2.0	5.4	7.3	12.1	9.3	9.6	10.3	9.6	10.9	0.0	6.0	4.5	3.1	2.7	2.1	2.0	1.2	0.8	0.5	0.3	0.2	0.1	0.0	0.0	0.0	0.0	0.0	0.0	0.0	100
Fenchuganj #2	3068.5-3072.5 3074.5-3083.5	0.4	0.3	0.3	0.5	0.6	0.6	0.9	1.0	1.5	0.0	3.2	2.4	2.8	3.5	4.4	7.8	6.6	7.6	8.7	8.5	8.6	8.0	8.0	4.9	4.3	2.5	1.2	0.7	0.4	100
Rashidpur #1	1401-1418 1421-1445	nd	nd	nd	nd	nd	nd	nd	nd	nd	nd	nd	nd	nd	nd	nd	nd	nd	nd	nd	nd	nd	nd	nd	nd	nd	nd	nd	nd	nd	0
Habiganj #1	1417-1428	nd	nd	nd	nd	nd	nd	nd	nd	nd	nd	nd	nd	nd	nd	nd	nd	nd	nd	nd	nd	nd	nd	nd	nd	nd	nd	nd	nd	nd	0
Habiganj #3+4	1328-1487(3) 1363-1489(4)	nd	nd	nd	nd	nd	nd	nd	nd	nd	nd	nd	nd	nd	nd	nd	nd	nd	nd	nd	nd	nd	nd	nd	nd	nd	nd	nd	nd	nd	0
Titas #1	2617-2769	0.9	2.0	4.6	9.8	13.1	14.6	15.1	13.3	10.8	0.0	5.8	3.7	2.7	1.6	0.9	0.5	0.3	0.2	0.1	0.0	0.0	0.0	0.0	0.0	0.0	0.0	0.0	0.0	0.0	100
Titas #5	2921-3052	2.0	3.3	5.8	10.5	13.1	14.4	14.2	12.5	10.1	0.0	5.3	3.3	2.4	1.5	0.8	0.5	0.3	0.2	0.1	0.0	0.0	0.0	0.0	0.0	0.0	0.0	0.0	0.0	0.0	100
Titas #8	3293-3551	0.2	2.5	8.5	16.5	16.9	15.1	12.5	10.1	7.7	0.0	3.9	2.4	1.7	1.0	0.5	0.3	0.2	0.1	0.0	0.0	0.0	0.0	0.0	0.0	0.0	0.0	0.0	0.0	0.0	100
Titas #10	3473-3680	1.1	2.2	4.6	9.7	12.7	14.5	15.0	13.5	10.9	0.0	5.9	3.7	2.9	1.5	0.8	0.5	0.3	0.2	0.1	0.0	0.0	0.0	0.0	0.0	0.0	0.0	0.0	0.0	0.0	100

*, Probably coeluted with other compound

DB35MS is a moderately polar capillary column has been used to control the solvent delay 1.5 minutes to detect the lower molecular weight compounds e.g. C_7 compounds. Quantification of *n*-alkanes and PAHs was performed using chromatograms obtained by the whole oil analysis to avoid the evaporative loss of components in the laboratory.

4. Results and discussion

4.1 Petroleum geochemical characteristics of the oils

4.1.1. Biodegradation

Among the 20 samples, three (Rashidpur #1, Habiganj #1, and Habiganj #3+4) were found to be severely biodegraded. In these three samples, *n*-alkanes, acyclic isoprenoids, aromatic hydrocarbons i.e. naphthalenes, biphenyls and phenanthrenes were completely removed and a large unresolved complex mixture (UCM) was detected (Fig. 3). However, diamondoid hydrocarbons mainly adamantane and alkyladamantanes were detected as major compounds in these three samples (Fig. 3). The diamondoid hydrocarbons are thought to be generated by the rearrangement of polycyclic hydrocarbons under thermal stress (Wingert, 1992). Therefore, they are resistant enough to further thermal stress and biological degradation compared to other petroleum components such as straight-chain and branched alkanes (Wingert, 1992). The compositional characteristics of these biodegraded oils represent level 3–5 on the biodegradation scale (Grice et al., 2000; Wenger et al., 2002). These severely biodegraded oils were derived from shallow reservoirs less than 1500 m deep (Table 1). Traces of *n*-alkanes (C_7–C_{11}) and lower molecular weight aromatic hydrocarbons (toluene and xylenes) were detected in sample Beanibazar #1 + 2 (light), probably due to the effects of water washing and biodegradation. Except for these four biodegraded oil samples, the other 16 samples were considered to be non-biodegraded oils.

4.1.2. Source rock organic matter

The distribution of *n*-alkanes in oils from the Surma basin in general range from C_7–C_{35} with maxima at around C_{10}-C_{13} (Table 2, Figs. 4). Variations in *n*-alkane distribution were observed, particularly in Fenchuganj #2 (3068.5–3083.5 m) and

Sylhet #7 (2020–2033 m). These two oils are waxy at room temperature and rich in long-chain (>C_{20}) *n*-alkanes, with maxima at around C_{25}-C_{27} and C_{22} in Fenchuganj #2 and Sylhet #7, respectively, suggesting a higher land plant origin (Tegelaar et al., 1989). Oils from Beanibazar #1+2 (heavy) well were also rich in long-chain *n*-alkanes. All the oils and condensates contained abundant aromatic hydrocarbons such as benzene, toluene, xylenes, naphthalenes, cadalene, biphenyls and phenanthrenes.

Biphenyls are bicyclic aromatic hydrocarbons, probably generated from a phenol coupling reaction (Alexander et al., 1994a; Trolio et al., 1996). Alkylbiphenyl are highly abundant and their distribution in all the study samples were very similar, with 3-methylbiphenyl being highly abundant compared to 4-methylbiphenyl (Fig. 6). Biphenyls are often detected in coal extracts (Mair and Mayer, 1964; Yew and Mair, 1966; White and Lee, 1980), suggesting that the crude oils and condensates in the Surma basin may have originated from organic matter derived from coal or coaly shale. However Cumbers et al. (1987) identified alkylbiphenyls in extracts from Middle Cambrian sedimentary rocks, demonstrating that biphenyls are not exclusively derived from higher plants.

Naphthalene (N) and alkylnaphthalenes such as methylnaphthalenes (MNs), dimethylnaphthalenes (DMNs) and trimethylnaphthalenes (TMNs) were detected in all the oil/condensate samples (Fig. 7). 2-MN was abundant and decreased in the order MNs>DMNs>N>TMNs, except in oils from Fenchuganj #2 (3068.5–3083.5 m), Sylhet #7 (2020–2033 m) and Beanibazar #1+2 (heavy), where a decreasing order DMNs>MNs>N>TMNs or DMNs>MNs>TMNs>N was observed. The methylated naphthalene distributions may be influenced by the effects of source, thermal stress and biodegradation (Van Aarssen et al., 1999). Diversity in the relative distribution of naphthalene and alkylated naphthalenes was observed. Marine oils tend to be rich in tetramethylnaphthalenes (TeMNs) compared to MNs or N (TMNs>DMNs>TeMNs> MNs>N), whereas terrestrial oils are poor in TeMNs compared to MNs or N (DMNs>MNs>TMNs> N>TeMNs) (Zhang et al., 2010). Alkylnaphthalenes in all the samples in the present study tended to be rich in DMNs and MNs compared to TMNs, similar to the alkylnaphthalene distribution in terrestrial oils described by Zhang et al. (2010). The 1,2,5-TMN was detected at trace levels or was not detected.

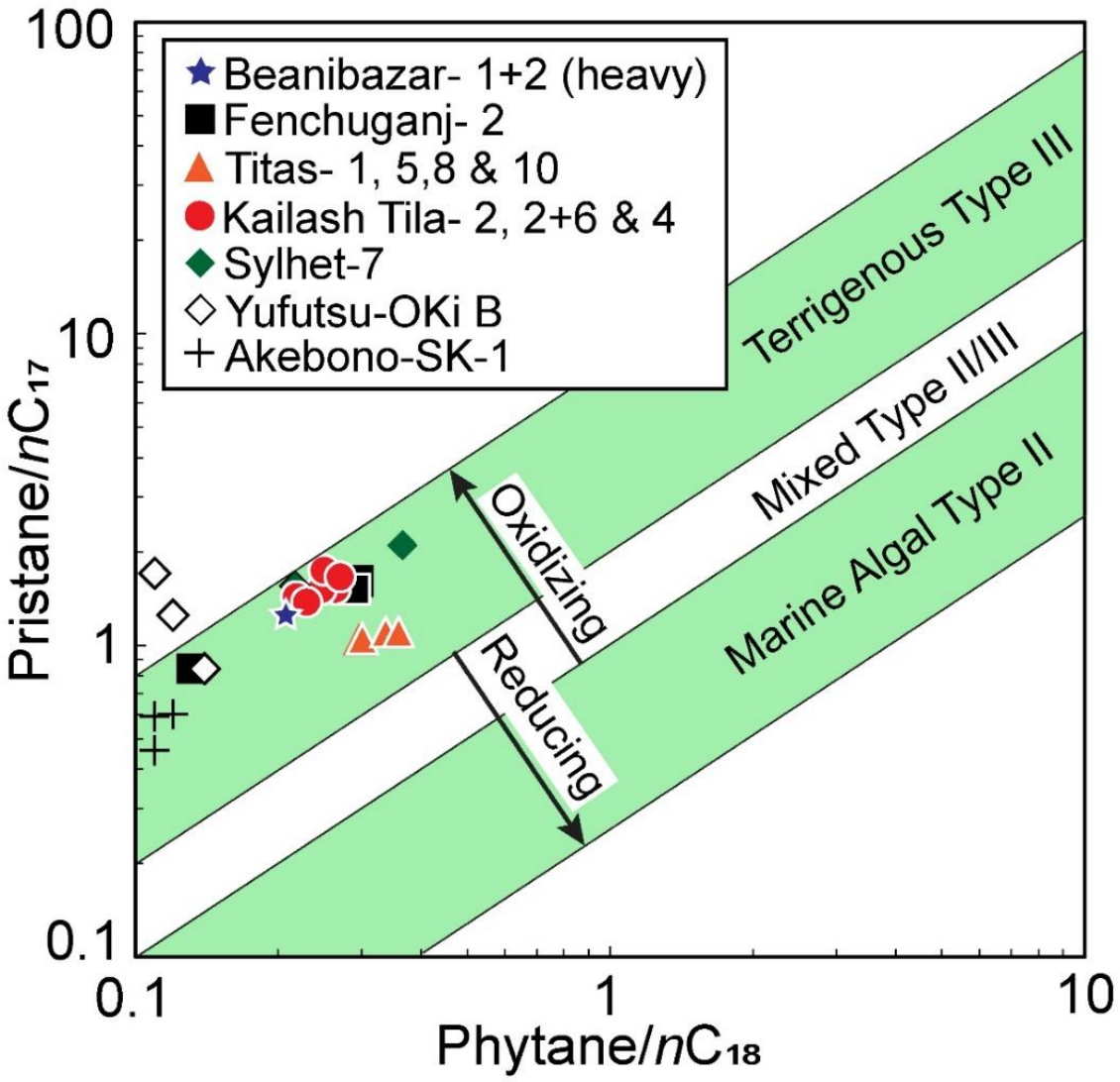

Fig. 5. Cross plot of pristane/*n*C$_{17}$ versus phytane/*n*C$_{18}$ for the evaluation of the source rock depositional environment (Hossain *et al*., 2014)

In contrast, 1,2,7-TMN was detected in all the study samples, although it was not fully separated from other compounds; it is thought to co-elute with 1,6,7-TMN and 1,2,6-TMN (Mrkic et al., 2011). Strachan et al. (1988) proposed that 1,2,7-TMN is derived directly from the structural degradation of an oleanane-type triterpenoid, which is a typical angiosperm biomarker. They reported increased relative abundances of 1,2,5-TMN and 1,2,7-TMN in immature Cretaceous and younger sediments associated with type III organic matter, and the relative abundance of these two isomers decreased with increasing maturity. In contrast, sediments older than Cretaceous with type III kerogen contain a higher relative abundance of 1,2,5-TMN and lower relative abundance of 1,2,7-TMN, suggesting a relationship to angiosperm evolution since the Early Cretaceous.

The presence of 1,2,7-TMN in all the oil samples suggests that a part of the source organic matter was derived from higher land plants. A very low concentration or absence of 1,2,5-TMN might be due to the higher maturity level of the oil samples. Only the oils from Titas field contained a detectable amount of 1,2,5-TMN (Fig. 7). Titas oils were also rich in cadalene compared to the other oils, indicating a significant contribution by vascular land plants to the source rock (Bendoraitis, 1974; Radke et al., 1984; Simoneit, 1986). However, apart from the Titas oils, the other oil samples are comparatively poor in cadalene. This could be due to the higher maturity level of the oils in the north to central Surma basin compared to the Titas oils, because cadalene can be thermally decomposed at higher maturities as suggested by Alexander et al. (1994b). By contrast, abundant bicadinanes in oils and condensates from the Surma basin suggest a significant input of vascular land plants to the source rocks (Alam and Pearson, 1990; Curiale et al., 2002; Takeda et al., 2011).

4.1.3. Depositional environment

The relative abundance of pristane and phytane can provide useful information on the palaeo-depositional environment of the source rock and the type of source organic matter. Pr/ph and pr/nC$_{17}$ ratios of oils from the Surma basin ranged between 5.3–11.9 and 0.8–2.1, respectively (Table 1), suggesting a terrestrial depositional environment. On a cross plot of pr/nC$_{17}$ versus ph/nC$_{18}$ (Fig. 5), all the oil samples plot within the field corresponding to an oxic environment, and organic matter derived from humic Type III

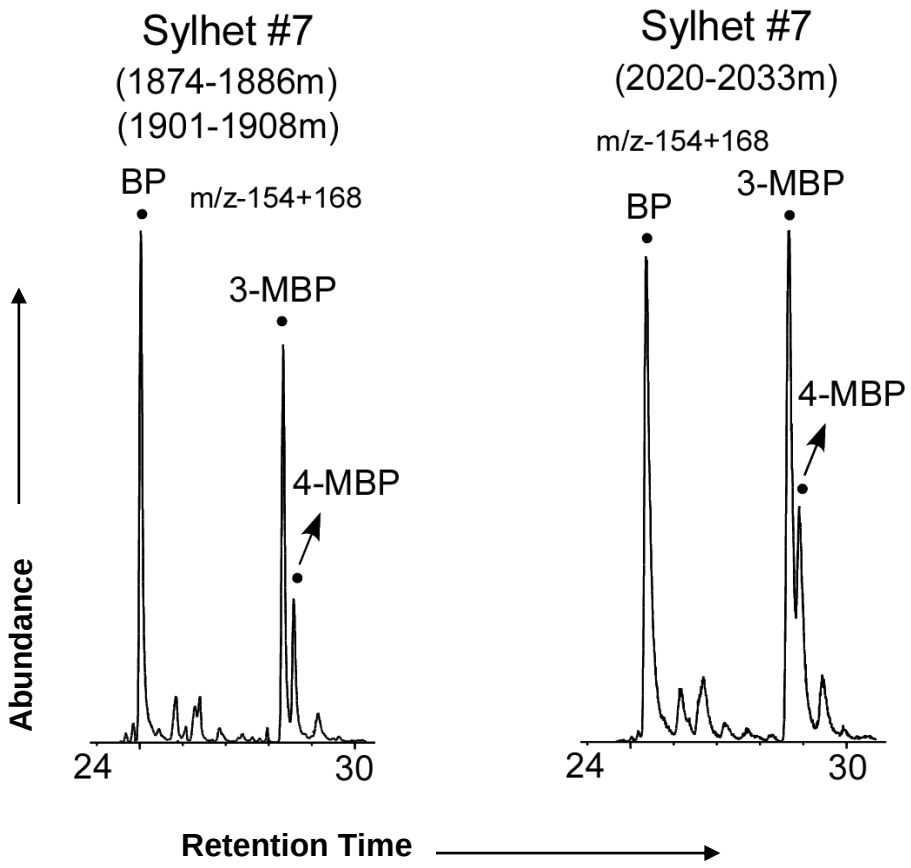

Fig. 6. Biphenyl and alkylbiphenyl distribution. BP, biphenyl; MBP, methylbiphenyl.

Continue Fig. 6.

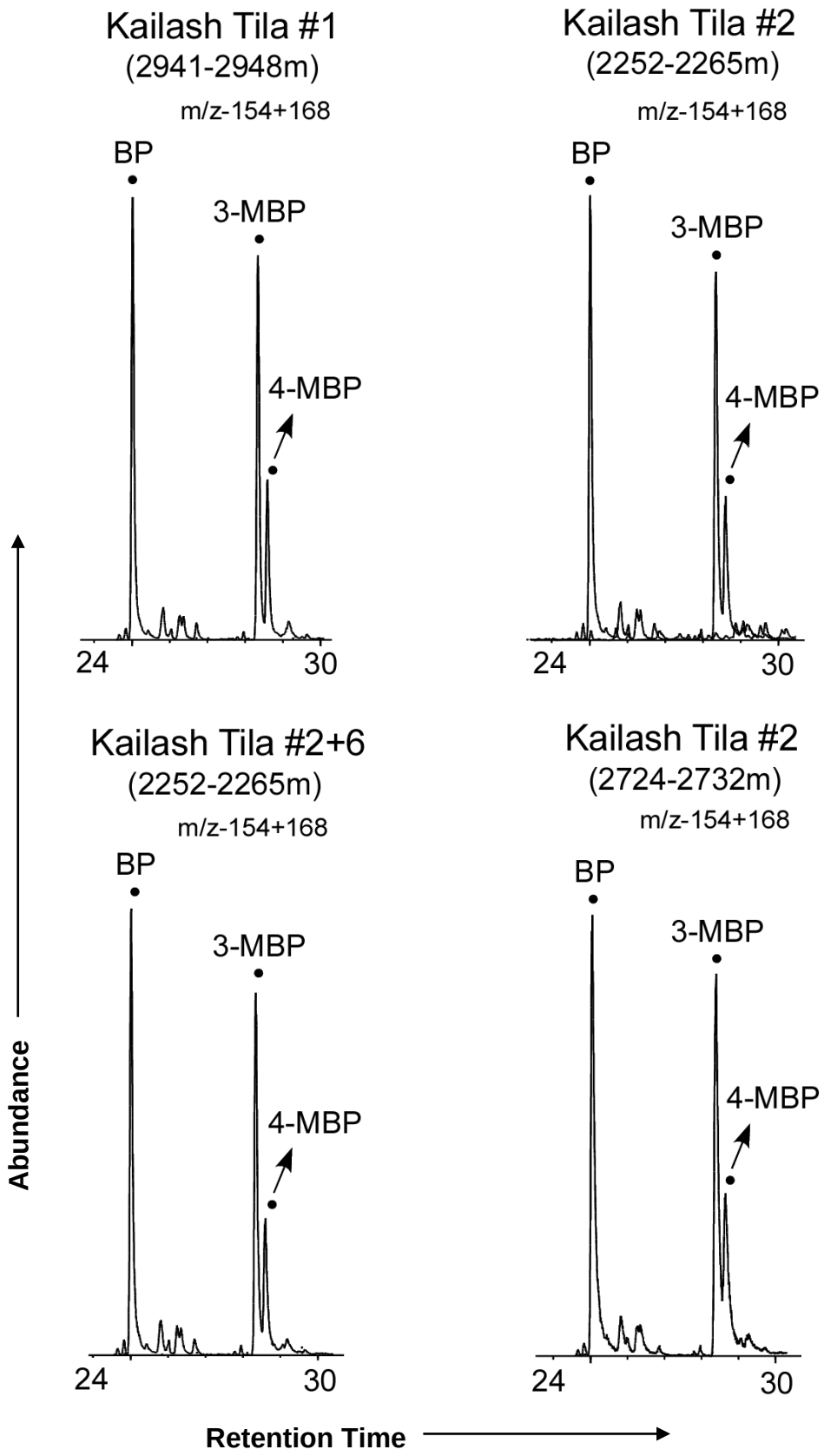

Continue Fig. 6.

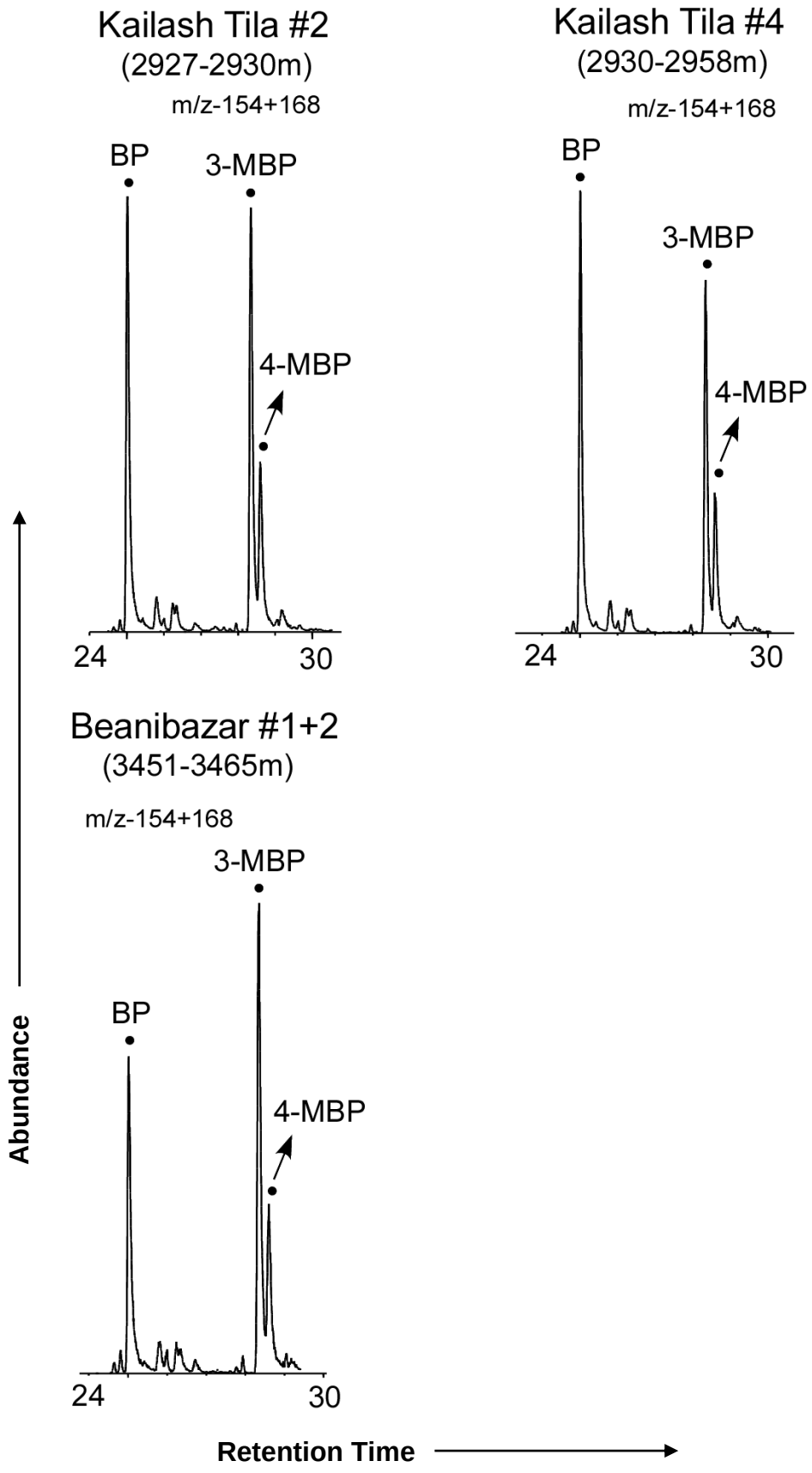

Continue Fig. 6.

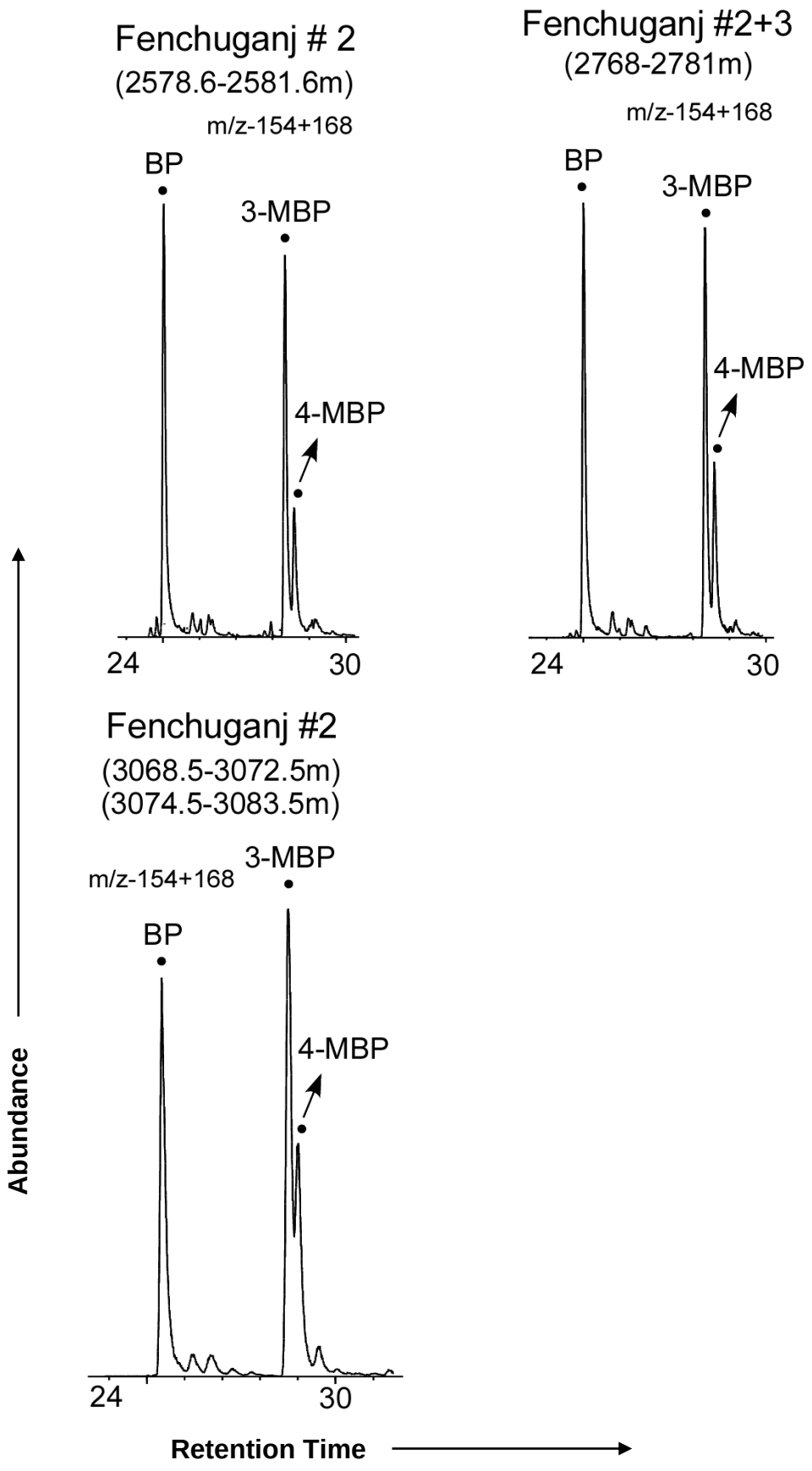

Continue Fig. 6.

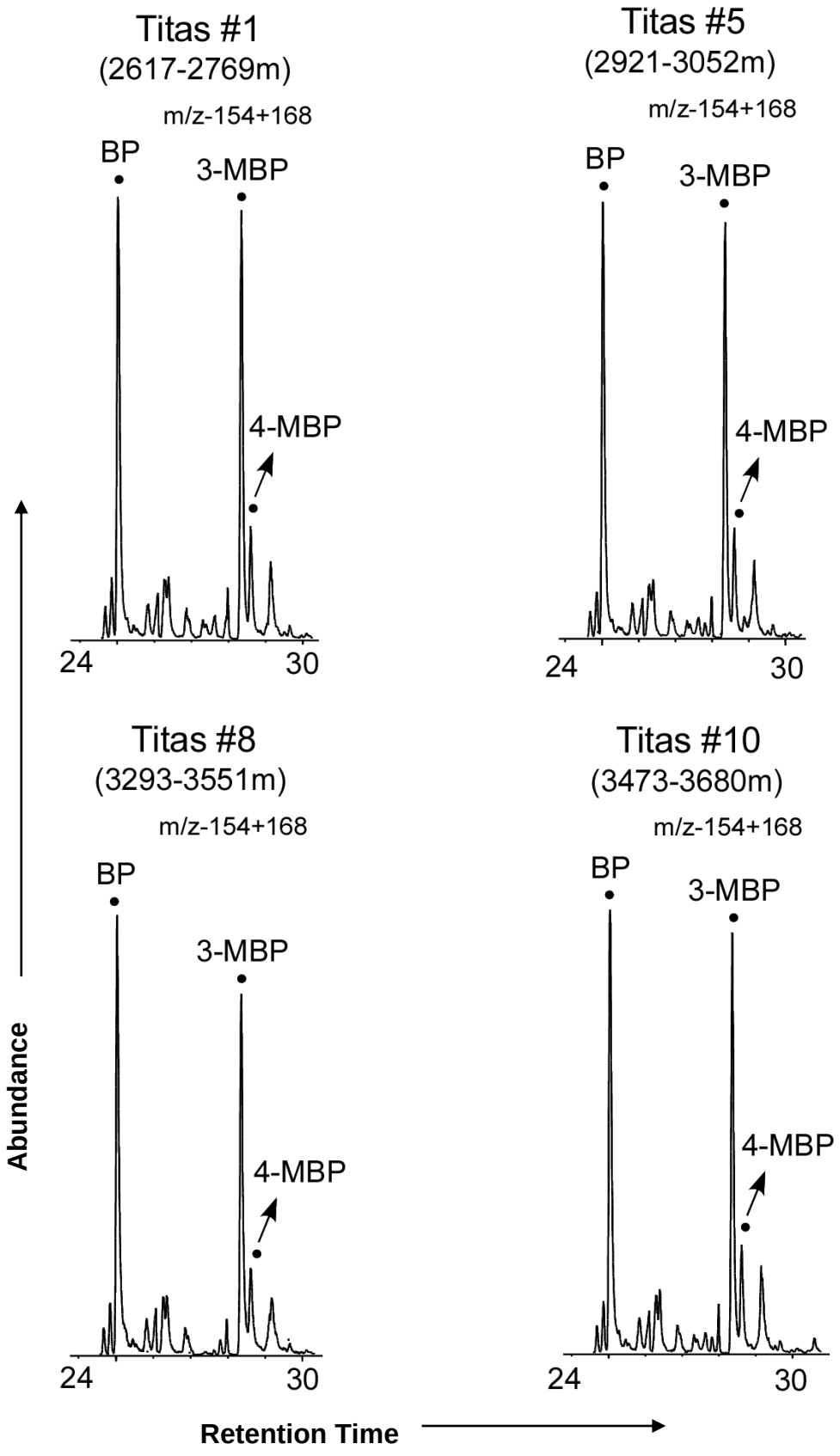

kerogen, consistent with oils and condensate from Yufutsu oil and gas fields, Hokkaido, Japan also plotted in the same figure. Based on several biomarkers, Yassalina et al. (2006) suggested that oils and condensates from Yufutsu oil and gas fields were derived from higher land plants organic matter. The Titas oils, however, plot closer to the field indicating a mixed kerogen type (Type II+III), suggesting a possible contribution of algal organic matter to the source rock for these oils.

4.1.4. Estimated maturity levels of the oils

The maturity levels of the crude oils and condensates in the Surma basin can be assessed by the calculated vitrinite reflectance (R_c, %), estimated by the methylnaphthalene ratio (MNR), trimethylnaphthalene ratio-2 (TNR-2) (Radke et al., 1984, 1994), methylphenanthrene ratio (MPR) and methylphenanthrene index-1 (MPI-1) (Radke et al., 1984) and MAI (%) (Chen et al., 1996). Calculated R_c values based on MNR, TNR-2, MPR and MPI-1 ranged from 1.0–1.3%, 0.8–1.0%, 1.1–1.3%, and 0.9–1.3%, respectively (Table 3). The maturity indices MNR, TNR-2, MPR and MPI-1 could not be determined for the biodegraded oils and condensates because they are very poor in aromatic hydrocarbons. By contrast, MNR and TNR-2 were determined for most of the oils and condensates except for the biodegraded oils.

Both R_c values calculated from MNR and TNR-2 varied consistently, although the R_c value from MNR generally tended to be 0.2 to 0.3% higher than the R_c value from TNR-2. The differences in R_c values determined from MNR and TNR-2 could be due to the rapid rate of temperature increase in the Surma basin. The rate of temperature increase since the Pliocene is estimated to be approximately 15 to 20°C/million years based on the stratigraphic age of Miocene-Pliocene boundary (Fig. 11) and the bottom-hole temperatures (95 to 121°C) of boreholes Beanibazar #1X, #2 and Atgram #1X in the Surma basin. Among the investigated oil samples, R_c values from alkylnaphthalene indices for the Titas oils were significantly lower than those from the Sylhet, Kailash Tila, Beanibazar and Fenchuganj wells in the north to central Surma basin (Table 3; Fig. 8). The R_c values from MNR of the Titas oils were about 1.0%, whereas the R_c values of the other oils were about 1.2–1.3% (Table 3). R_c values from TNR-2 of Titas oils were about

0.8%, also significantly lower than the R_c values from TNR-2 of the other oils (about 0.95–1.0%).

4.2. Characterization of the severely biodegraded oils

High concentrations of diamondoid hydrocarbons were detected in the severely biodegraded condensates, and adamantane and alkyladamantanes were present as major compounds (Fig. 3). The distributions of adamantane and alkyladamantanes in both biodegraded and non-biodegraded oils from the Surma basin were similar (Fig. 9), suggesting that all the crude oils and condensates in the study area originated from a similar type of source rocks rich in terrigenous organic matter. According to Chen et al. (1996), the relationship between the methyladamantane index (MAI%) and the R_c in non-biodegraded hydrocarbons can be used to evaluate the maturity levels of severely biodegraded oils. The MAI (%) of the severely biodegraded oils was also almost identical to those of the non-biodegraded oils, cross plot of MAI (%) versus R_c (from MNR) and R_c (from TNR) demonstrating that both the biodegraded and non-biodegraded oils were expelled at a similar maturity level (Fig. 10 A-B).

4.3. Possible source rocks and timing of oil expulsion

The Atgram #1X well, the deepest well (4961 m) drilled so far in Bangladesh, is located in the NE of the Surma basin (Fig. 1). An approximately 260 m thick section of the Oligocene Jenam Shale was drilled at this location (Hiller and Elahi, 1984). The TOC content of mudstones from the Jenam Shale (mean Ro= ca. 0.65%) ranged from 0.6 to 2.4%, and that of the overlying Miocene Bhuban Shale (mean Ro= ca. 0.5) was 0.2–0.7% (Shamsuddin and Abdullah, 1997). The comparatively low maturity level of the potential source rocks in the Jenam and Bhuban Formations may be because the wells were drilled on an anticlinal structure, or because of the basin margin location. Thus source rocks in the adjacent synclinal area may be more mature.

Abundant organic matter derived from higher land plants (dominated by angiosperms) was deposited during the Middle Eocene–Early Miocene, during deposition of the thick sedimentary sequences of the Jaintia and Barail Groups (Hossain et al., 2009). TOC content (0.15 to 0.9%), Rock-Eval pyrolysis data (S1 and S2) and the maturity level

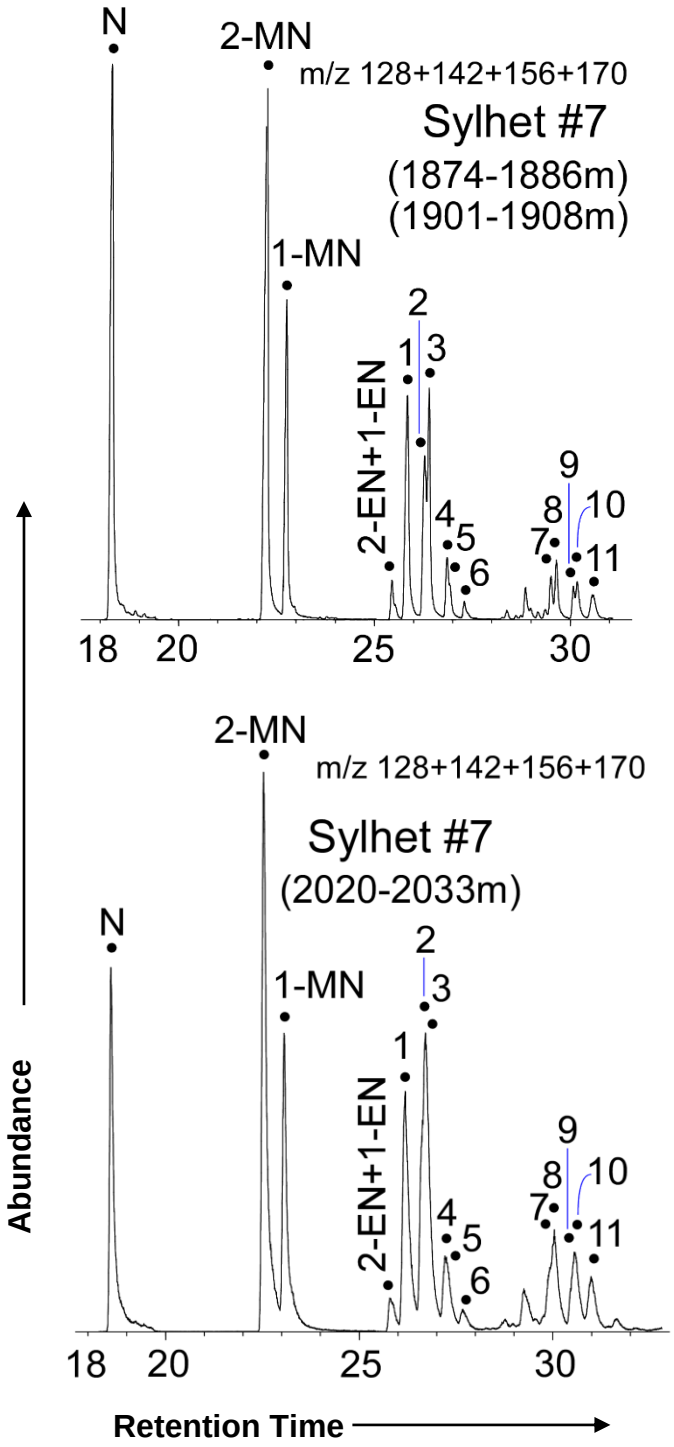

Fig. 7. Naphthalene and alkylnaphthalene distribution. N, naphthalene; MN, methylnaphthalene; EN, ethylnaphthalene, 1, 2,6 + 2,7-dimethylnaphthalene (DMN); 2, 1,3 + 1,7-DMN; 3, 1,6-DMN; 4, 1,4 + 2,3-DMN; 5, 1,5-DMN; 6, 1,2- DMN; 7, 1,3,7-trimethylnaphthalene (TMN); 8, 1,3,6- TMN; 9, 1,3,5 + 1,4,6- TMN; 10, 2,3,6- TMN; 11, 1,2,7 + 1,6,7 + 1,2,6- TMN; 12, 1,2,5- TMN.

Continue Fig. 7.

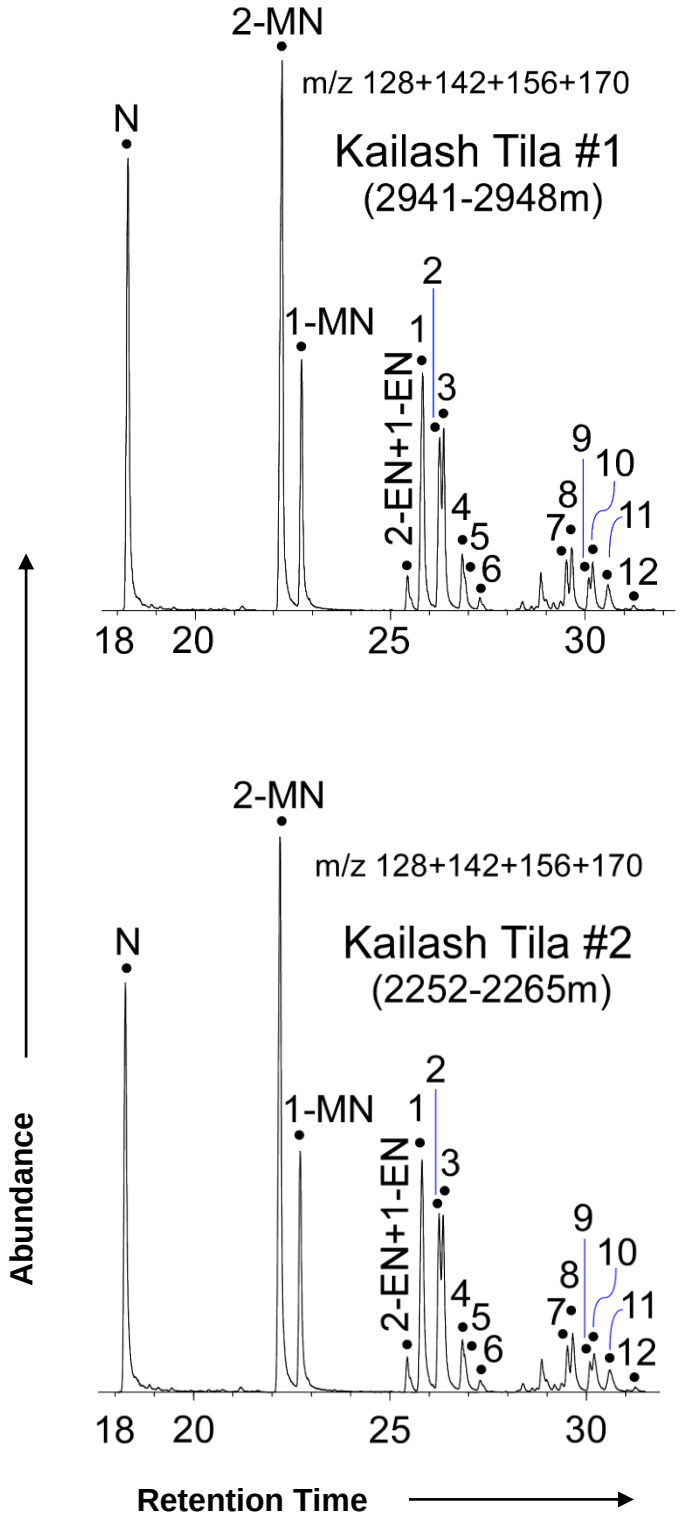

Continue Fig. 7.

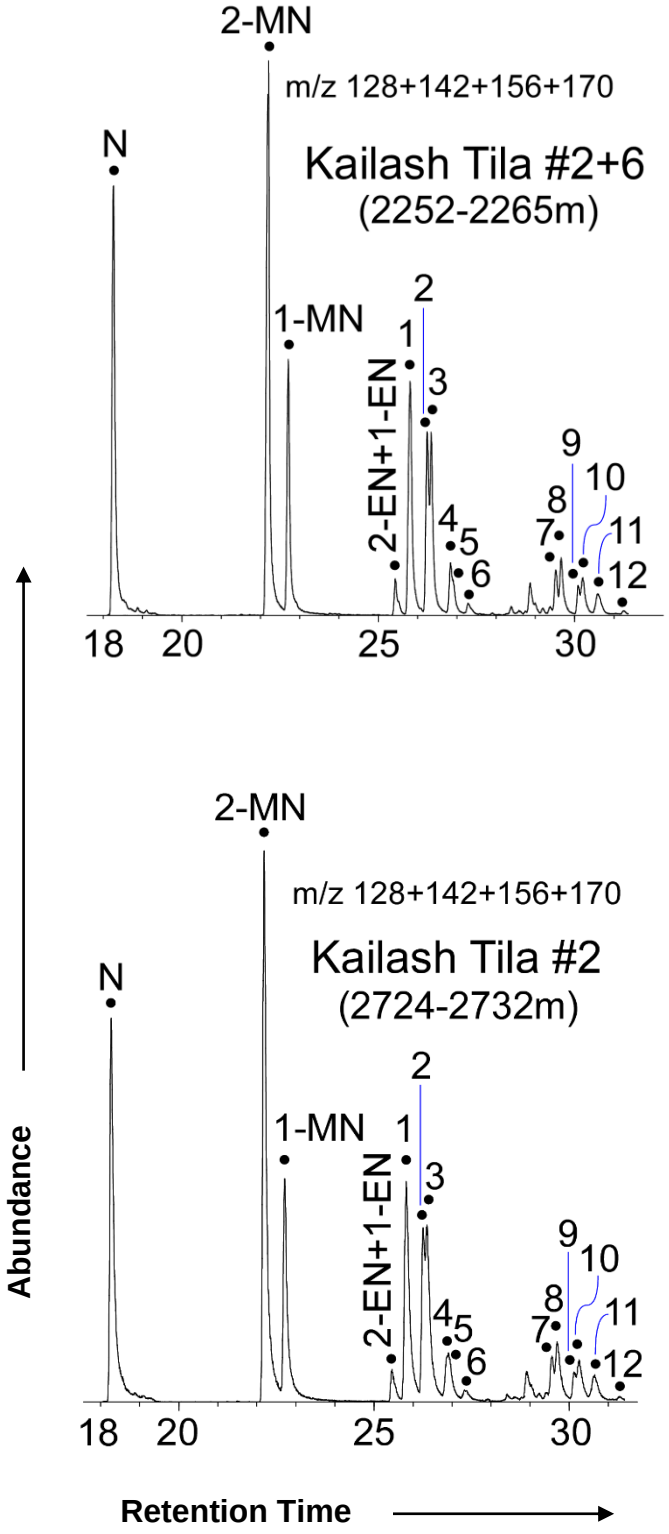

Continue Fig. 7.

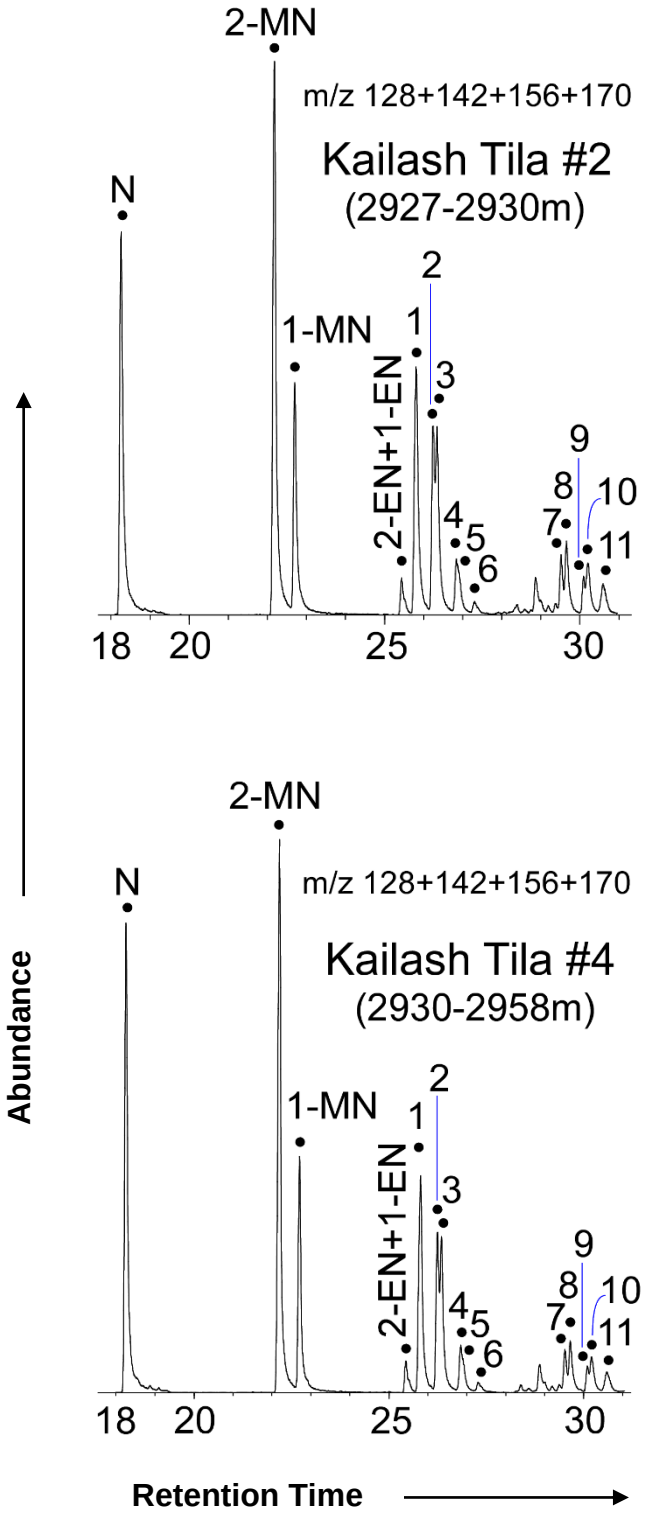

Continue Fig. 7.

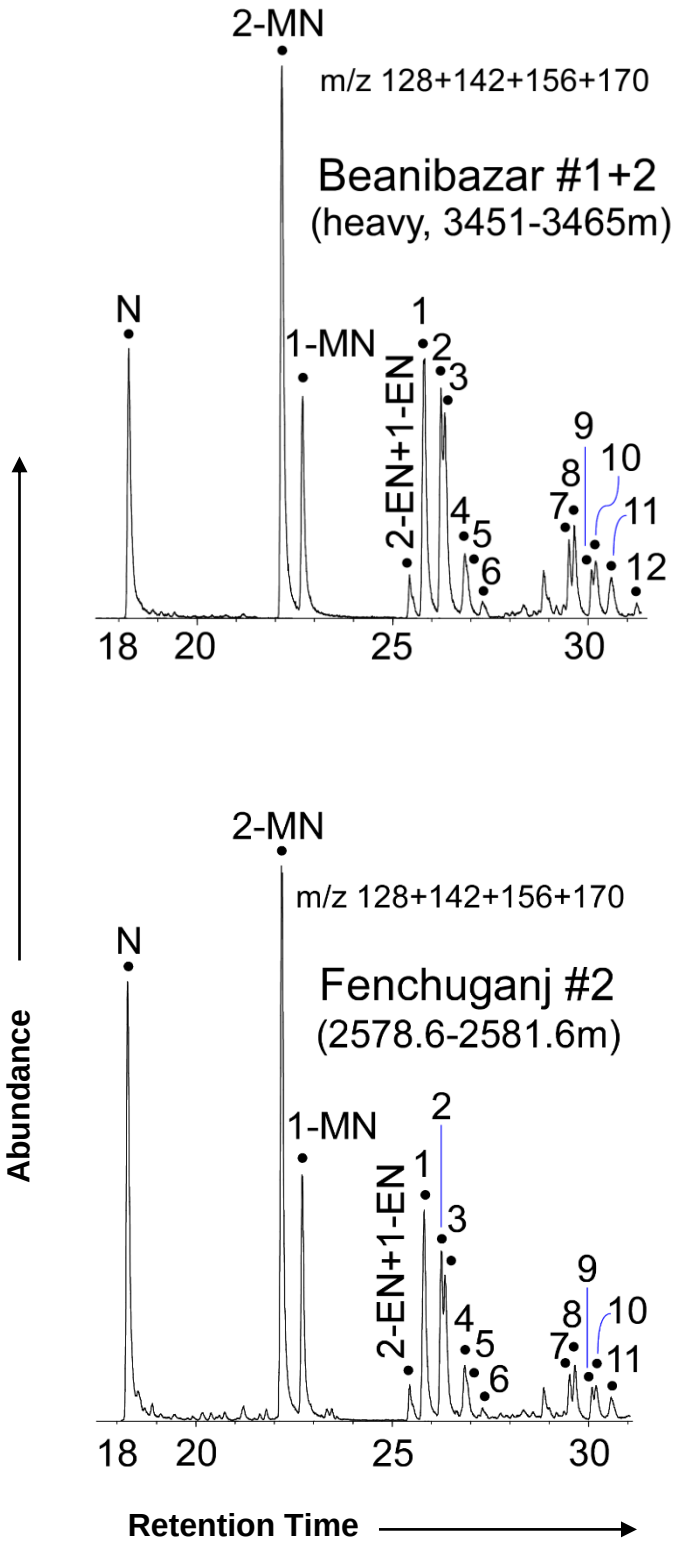

Continue Fig. 7.

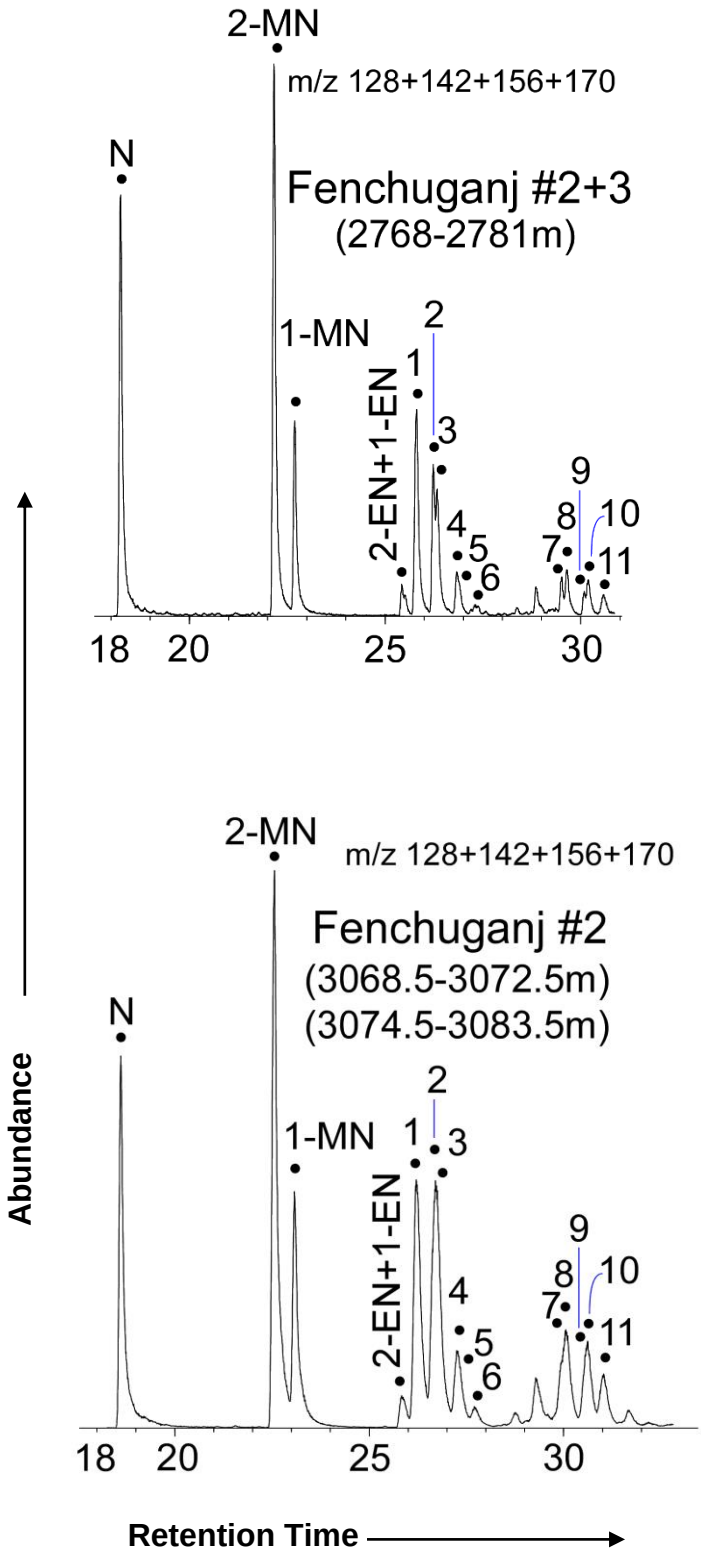

Continue Fig. 7.

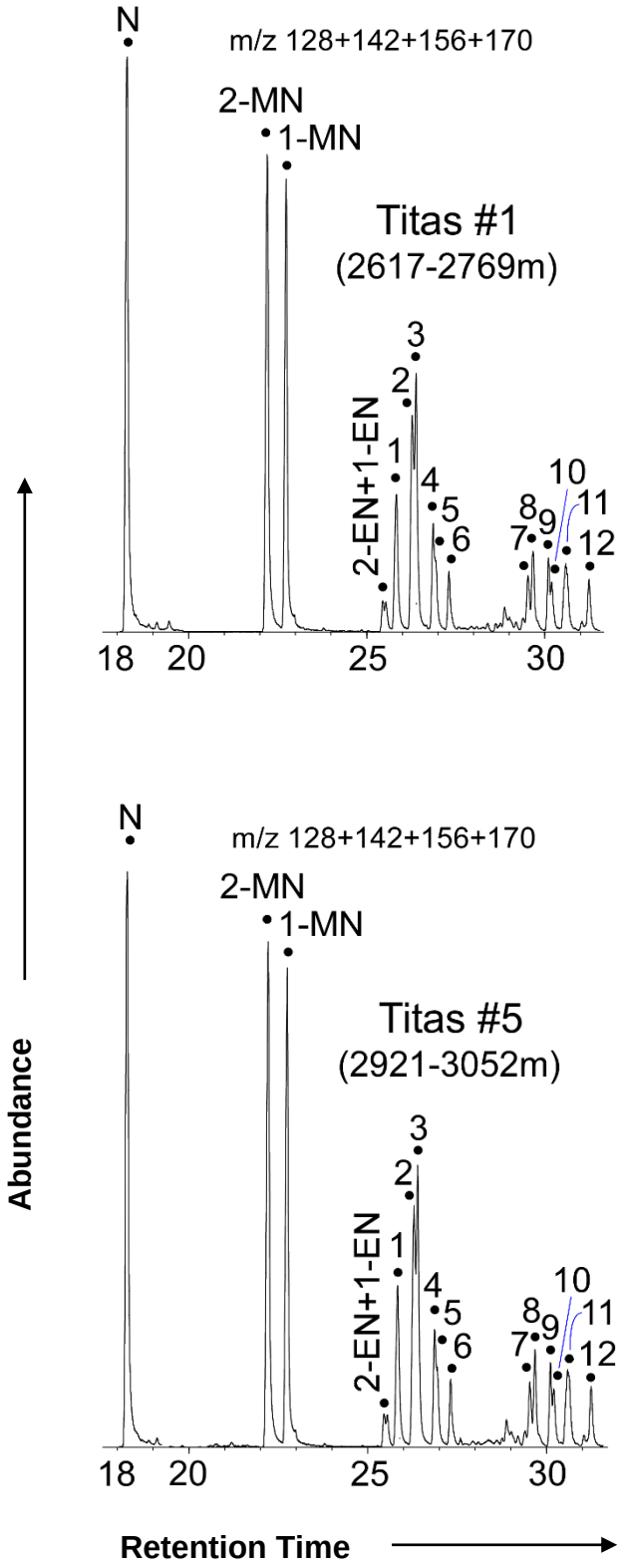

Continue Fig. 7.

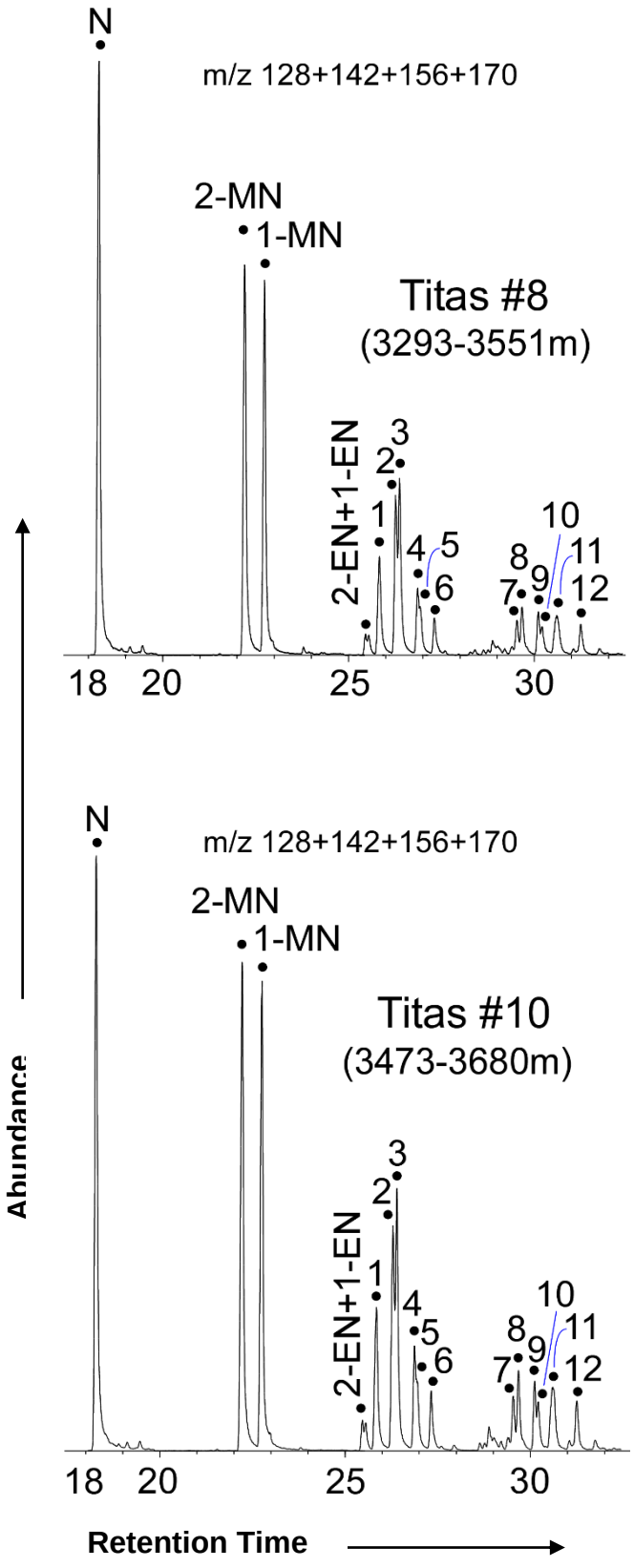

of the Miocene rocks (R_o=ca. 0.45–0.76%) (Shamsuddin and Khan, 1991; Farhaduzzaman et al., 2012) suggest the lower generation potential and lower maturity of the Middle Miocene–Pleistocene Surma, Tipam and Dupi Tila Groups. Hiller and Elahi (1984) suggested a geothermal gradient ranging from 1.8 to 2.2°C/100 m and non-balanced heat flows in the Surma basin, because of the very young and rapid burial history. The maximum R_o in the Early Miocene Bhuban Formation in Beanibazar #1X was approximately 0.58% at a depth close to the total depth (TD) at 4109 m. R_o increased to 0.7% in the Middle Oligocene Jenam Formation in well Atgram #1X at a depth close to the TD at 4961 m, near the threshold of the oil window. In addition, an R_o value of 0.73% at 3810 m in the Lower Bhuban Formation in well Atgram #1X was recorded, but is considered to be due to the reworking of older vitrinite (Hiller and Elahi, 1984).

However a relatively constant R_o of approximately 0.45–0.65% has been observed in the Surma and Barail Groups in the Surma basin (Shamsuddin and Khan, 1991; Shamsuddin and Abdullah, 1997). This suggests a similar thermal maturity level for rocks in the drilled section in the Surma basin, or the reworking of vitrinite macerals with similar R_o values. The calculated vitrinite reflectance values of the Titas oils (R_c=0.8–1.0%) and other oils from the Surma basin (R_c=1.0–1.3%) were significantly higher than those of the Oligocene and Miocene rocks. Major reservoir rocks are present in the Bhuban and Bokabil Formations of the Miocene–Early Pliocene Surma Group. Considering the lower maturity level of the sedimentary rocks in the Surma Group, the maturity levels as indicated by the R_c values of the oils are thought to show the timing of oil expulsion from the source rocks. On the basis of the time–temperature and R_o relationship (Suzuki et al., 1993), the geothermal gradient of 1.8–2.2°C/100 m in the Surma basin (Hiller and Elahi, 1984; Ismail and Shamsuddin, 1991), and the estimated R_c values of the oils and condensates (0.8–1.3%) (Fig. 11), the burial depth of the source rock at the time of hydrocarbon expulsion was estimated to be 5000–6000 m for the Titas oils and 6000–7000 m for the other oils in the north to central Surma basin.

The Oligocene Barail Group were reported at depths of 4700–4961 m and 4010–4595 m in the Atgram #1X and Rashidpur #2 wells, respectively (Johnson and Alam, 1991). Sedimentary strata older than the Oligocene Barail Group have not yet been drilled

in the Surma basin. In the northwest part of the Surma basin, the cumulative thickness of the Late Eocene Kopili Formation and the Oligocene Barail Group was estimated to be about 1400 m, although it varies within the basin (Johnson and Alam, 1991). According to a study of fossil assemblages by Banerji (1984), the depositional environment of the lower and upper divisions of the Kopili Shale Formation in Meghalaya (northern Surma basin) gradually changed from an open-marine to brackish and almost freshwater estuarine environment. On the other hand, the Jenam Formation of the Barail Group was deposited in a fluvio-deltaic environment (Johnson and Alam, 1991) suggesting a transition of marine to a starting of terrestrial depositional environment at the end of the Eocene time. The TOC of the Middle Oligocene Jenam Shale is 0.6–2.7% (Shamsuddin and Abdullah, 1997), suggesting significant source rock potential. However, the mean R_o value of the Middle Oligocene Jenam Shale is about 0.65% (Shamsuddin and Abdullah, 1997), which is lower than the estimated maturity levels of R_c=0.8–1.0% for the Titas oils and R_c=1.0–1.3% for the other oils in the north to central Surma basin. Although the geochemical data-set for the Oligocene and older sedimentary sequences is limited, upper part of the Eocene Kopili Shale to lower part of the Oligocene Jenam Shale rich in land-derived organic matter are interpreted to be most possible source rocks for the oils and condensates in the Surma basin.

4.4. In-reservoir phase separation, tertiary migration and re-accumulation of the oils

Source and maturity parameters of oils and condensates from the Surma basin suggest that all the oils (except the Titas oils) were generated from a similar source rock with significant amounts of terrigenous organic matter. The Titas oils are inferred to be derived from terrigenous source rocks with a significant contribution of marine organic matter. The maturity of the Titas oils is significantly lower than that of the oils from the north to central Surma basin. Except for the Titas samples, the oils show limited maturity levels as indicated by R_c values ranging from 1.0 to 1.3%. However, a significant diversity in the distribution of *n*-alkanes has been observed in the oils from the Surma basin (Figs. 4).

The *n*-alkane distribution in two oil samples, from 2578.6–2581.6 m and 2768–2781 m depths, in well Fenchuganj #2 ranged from C_7–C_{27} with a maximum at around

Table 3. Maturity parameters (Hossain *et al*., 2014).

MNR, methylnaphthalene ratio; TNR, trimethylnaphthalene ratio; MPR, methylphenanthrene ratio; MPI, methylphenanthrene index; Rc, calculated vitrinite reflectance; MAI, methyladamantane index. MNR=(2-MN/1-MN), Radke et al. (1982b), Rc (%) from MNR = (0.17 X MNR + 0.82); TNR-2 = (2,3,6 + 1,3,7-TMN) / (1,4,6 + 1,3,5 + 1,3,6-TMN), Radke et al. (1986); Rc (%) from TNR-2 = {0.4 + (0.6 x TNR-2)}; MPR = (2-MP/1-MP), Radke et al. (1982b), Rc (%) from MPR = (0.99 x log MPR + 0.94); MPI-1 = 1,5 [2-MP + 3-MP] /[P + 9-MP + 1-MP], Radke et al. (1982a), Rc (%) from MPI-1 = (0.6 x MPI-1 + 0.4) for Ro< 1.35; MAI (%) = 1-MA / (1-MA + 2-MA) (%), Chen et al. (1996).

Serial no.	Well name	Depth (m)	MNR	Rc (%) From MNR	TNR-2	Rc (%) From TNR-2	MPR	Rc (%) From MPR	MPI-1	Rc (%) From MPI-1	MAI (%)
1	Sylhet #7	1874-1886 1901-1908	2.30	1.21	0.92	0.95	nd	nd	nd	nd	66.8
2	Sylhet #7	2020-2033	2.02	1.16	0.94	0.96	1.46	1.10	1.13	1.08	61
3	Kailash Tila #1	2941-2948	2.58	1.26	1.00	1.00	2.46	1.33	0.87	0.92	66.5
4	Kailash Tila #2	2252-2265	2.62	1.27	1.00	1.00	nd	nd	nd	nd	66
5	Kailash Tila #2+6	2252-2265	2.55	1.25	1.01	1.01	nd	nd	nd	nd	63
6	Kailash Tila #2	2724-2732	2.69	1.28	0.98	0.99	2.18	1.27	1.01	1.00	69
7	Kailash Tila #2	2927-2930	2.43	1.23	1.04	1.02	2.12	1.26	1.18	1.10	65.8
8	Kailash Tila #4	2930-2958	2.55	1.25	1.02	1.01	nd	nd	nd	nd	67
9	Beanibazar #1+2 (heavy)	3451-3465	2.74	1.29	0.91	0.95	nd	nd	nd	nd	70.7
10	Beanibazar #1+2 (light)		nd	nd	nd	nd	nd	nd	nd	nd	nd
11	Fenchuganj #2	2578.6-2581.6	2.51	1.25	0.91	0.95	nd	nd	nd	nd	73
12	Fenchuganj #2+3	2768-2781	2.90	1.31	1.06	1.03	nd	nd	nd	nd	73
13	Fenchuganj #2	3068.5-3072.5 3074.5-3083.5	2.21	1.20	1.06	1.04	1.98	1.23	1.55	1.33	67
14	Rashidpur #1	1401-1418 1421-1445	nd	nd	nd	nd	nd	nd	nd	nd	70.5
15	Habiganj #1	1417-1428	nd	nd	nd	nd	nd	nd	nd	nd	73
16	Habiganj #3+4	1328-1487 (3) 1363-1489 (4)	nd	nd	nd	nd	nd	nd	nd	nd	72.7
17	Titas #1	2617-2769	1.21	1.03	0.72	0.83	nd	nd	nd	nd	66.7
18	Titas #5	2921-3052	1.20	1.02	0.69	0.81	nd	nd	nd	nd	66.7
19	Titas #8	3293-3551	1.19	1.02	0.71	0.82	nd	nd	nd	nd	68.8
20	Titas #10	3473-3680	1.17	1.02	0.69	0.81	nd	nd	nd	nd	66

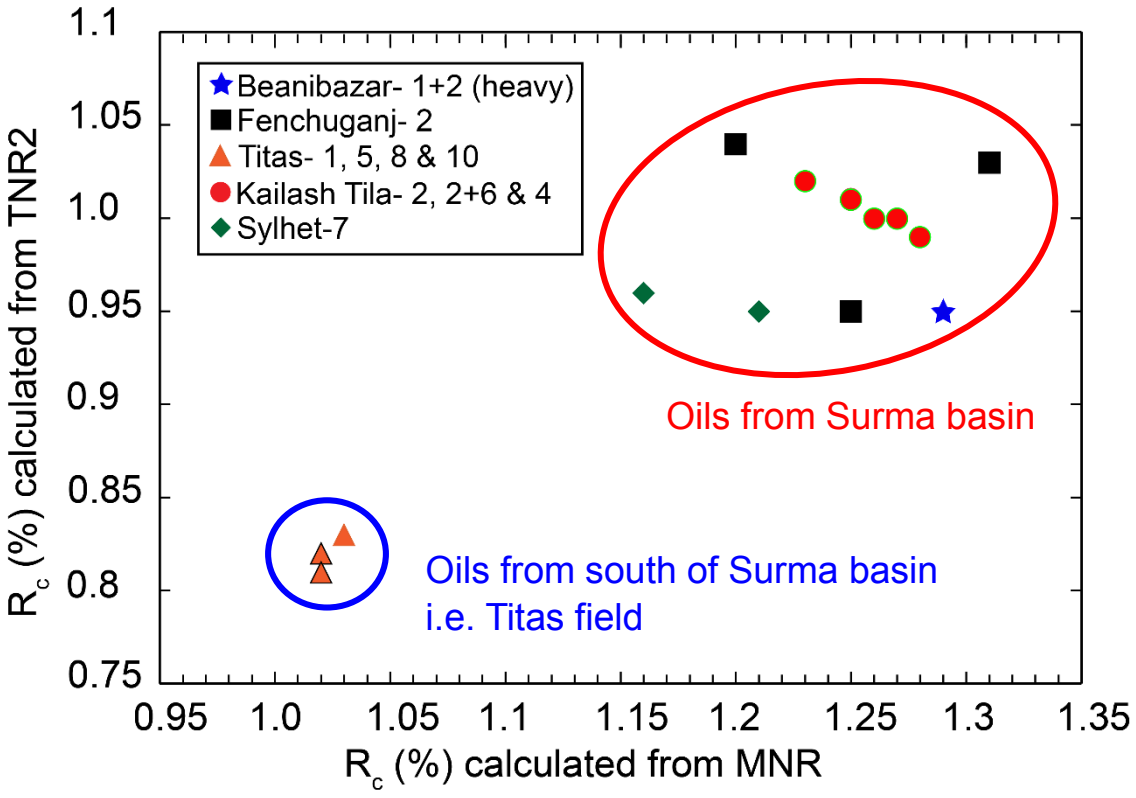

Fig. 8. Cross plot of R_c (%) calculated from methylnaphthalene ratio (MNR) versus R_c (%) calculated from trimethylnaphthalene ratio (TNR2).

C_{10}-C_{11}. Deeper oils from the same well, from 3068.5–3072.5 m and 3074.5–3083.5 m, showed an *n*-alkane distribution ranging from C_7–C_{35} with a maximum at around C_{25}–C_{27} (Fig. 4). The latter oil samples are waxy at room temperature and are dark yellow in colour. A similar variation in the distribution of *n*-alkanes was observed in two oils from well Sylhet #7 (Fig. 4). In this well, oils from 1874–1886 m and 1901–1908 m showed *n*-alkane distributions in the range of C_7–C_{22} with a maximum at C_{10}. Oil from a depth of 2020–2033 m contains *n*-alkanes ranging from C_7–C_{35} with a maximum at around C_{17}–C_{22}; this oil is waxy at room temperature and has a dark yellow colour. Six oil samples from Kailash Tila gas field were characterized by a similar *n*-alkane distribution ranging from C_7–C_{28} with a maximum at C_{10} (Fig. 4), and varied from colourless to light yellow. Four samples from Titas also showed a similar *n*-alkane distribution ranging from C_7–C_{25} with a maximum at around C_{11}–C_{13} (Fig. 4) and likewise varied from colourless to light yellow. The colourless oil sample from Beanibazar #1+2 (heavy) contained *n*-alkanes ranging from C_7–C_{31} with a maximum at C_{10} (Fig. 4).

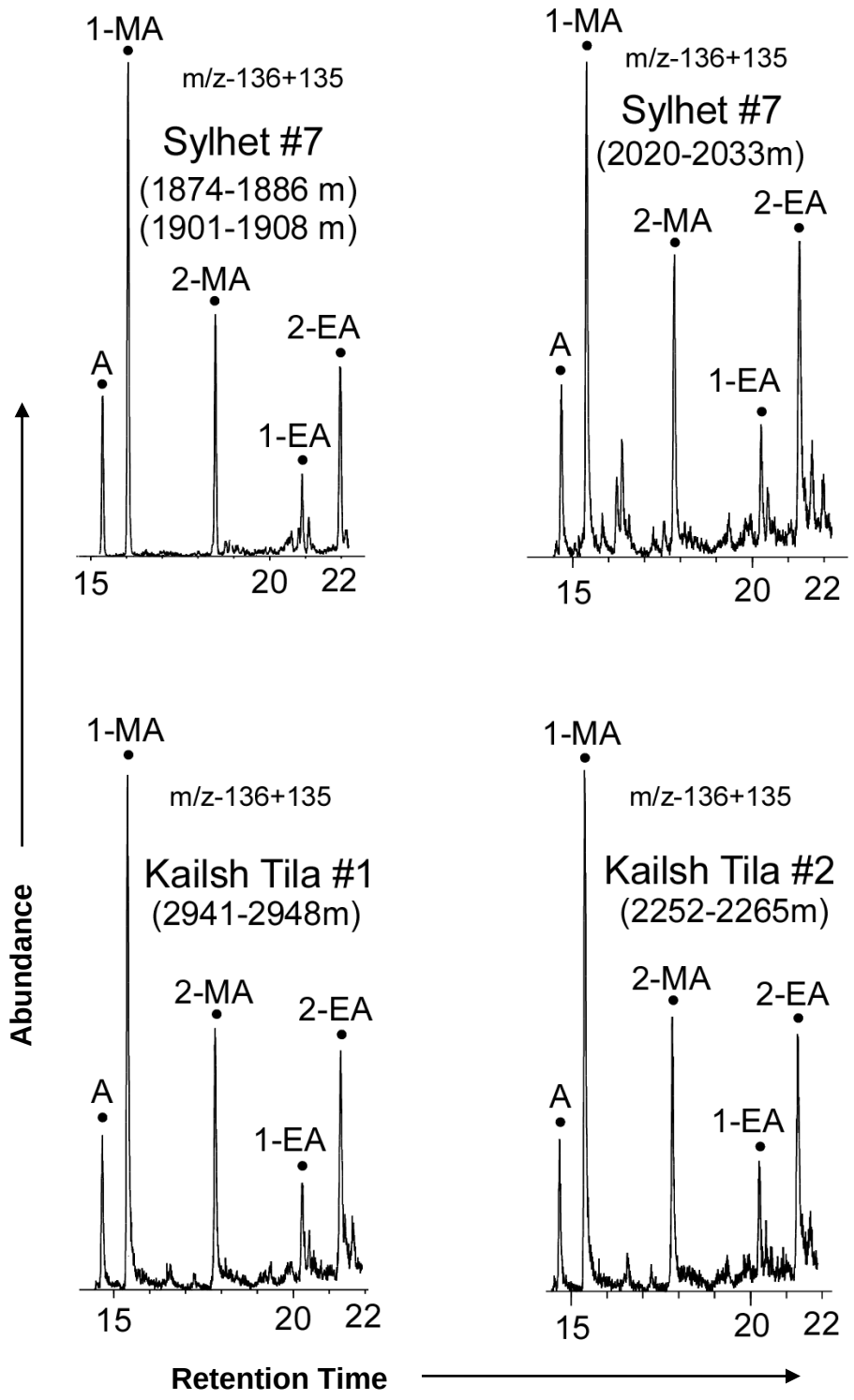

Fig. 9. Adamantane and alkyladamantane distribution of the oil and condensates. A, adamantane; MA, methyladamantane; EA, ethyladamantane.

Continue Fig. 9.

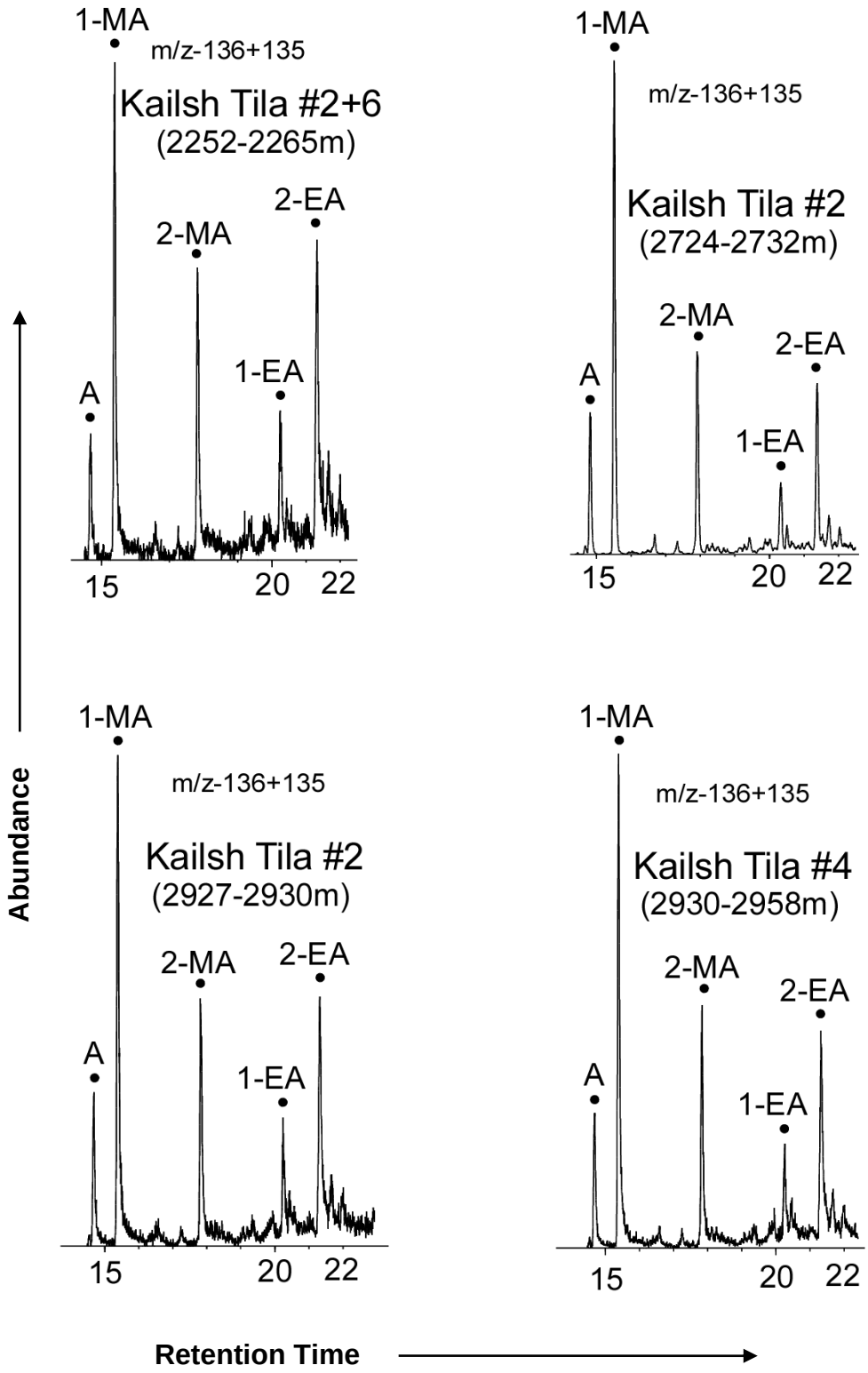

Continued Fig. 9.

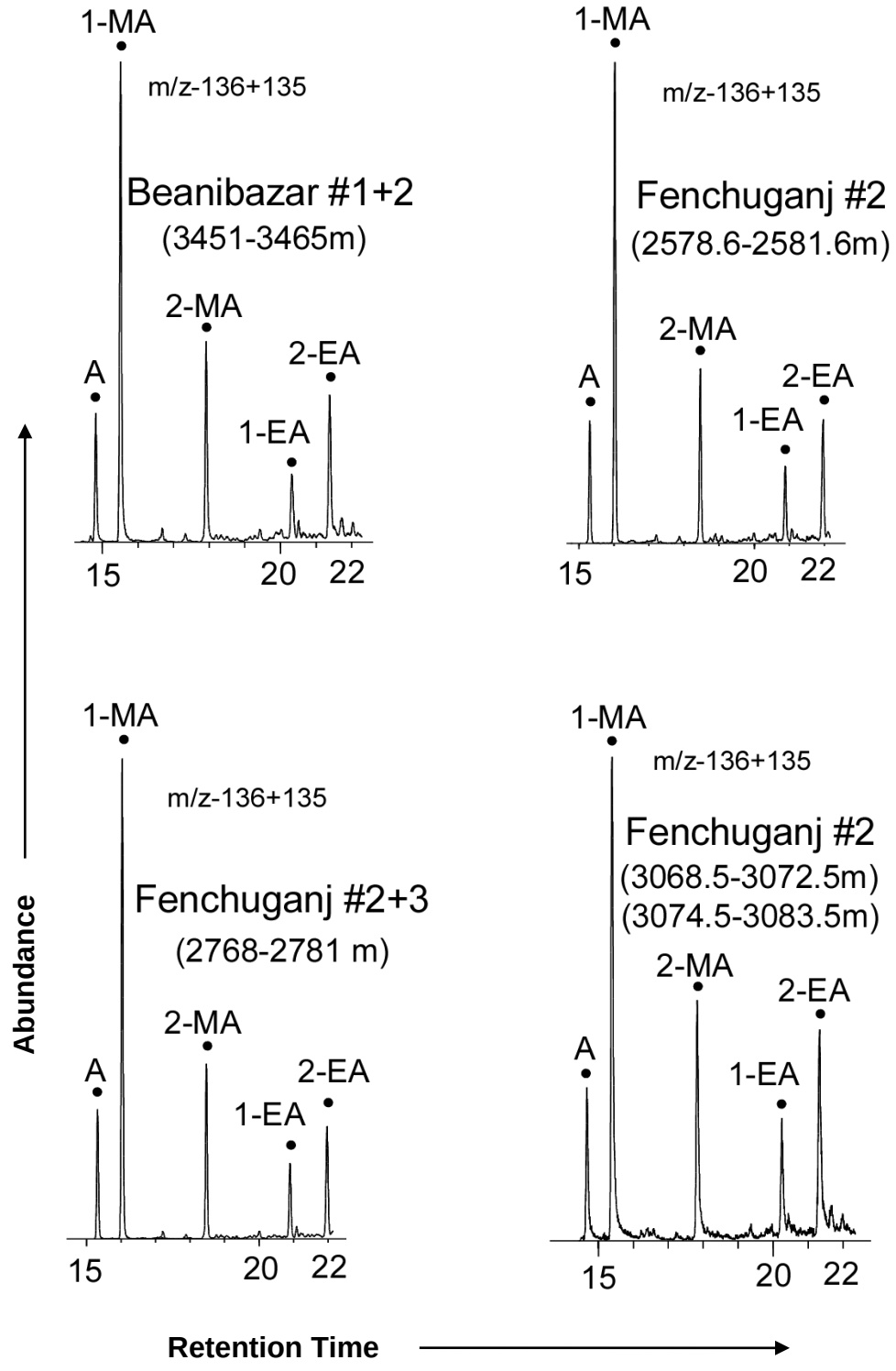

Continue Fig. 9.

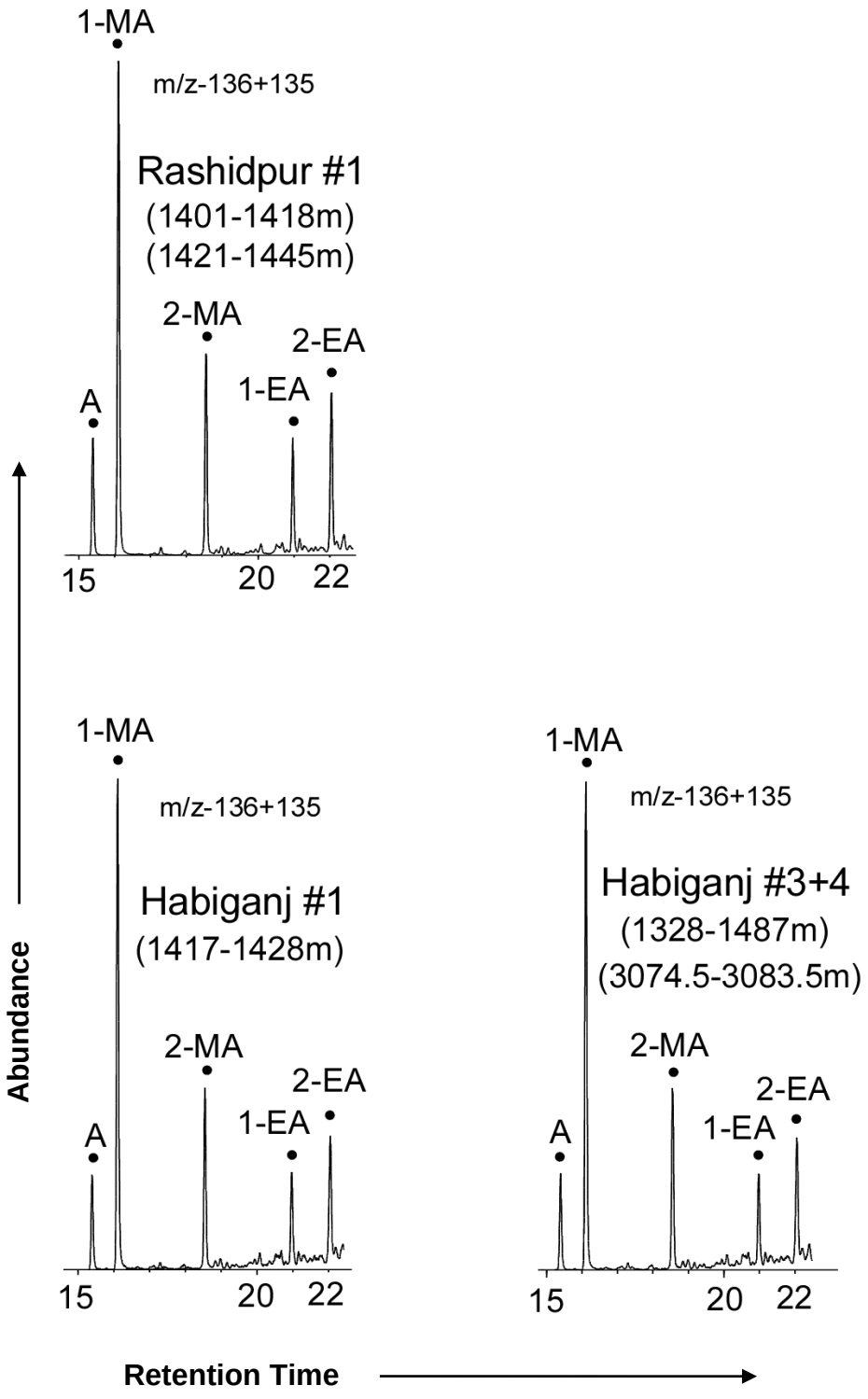

Continue Fig. 9.

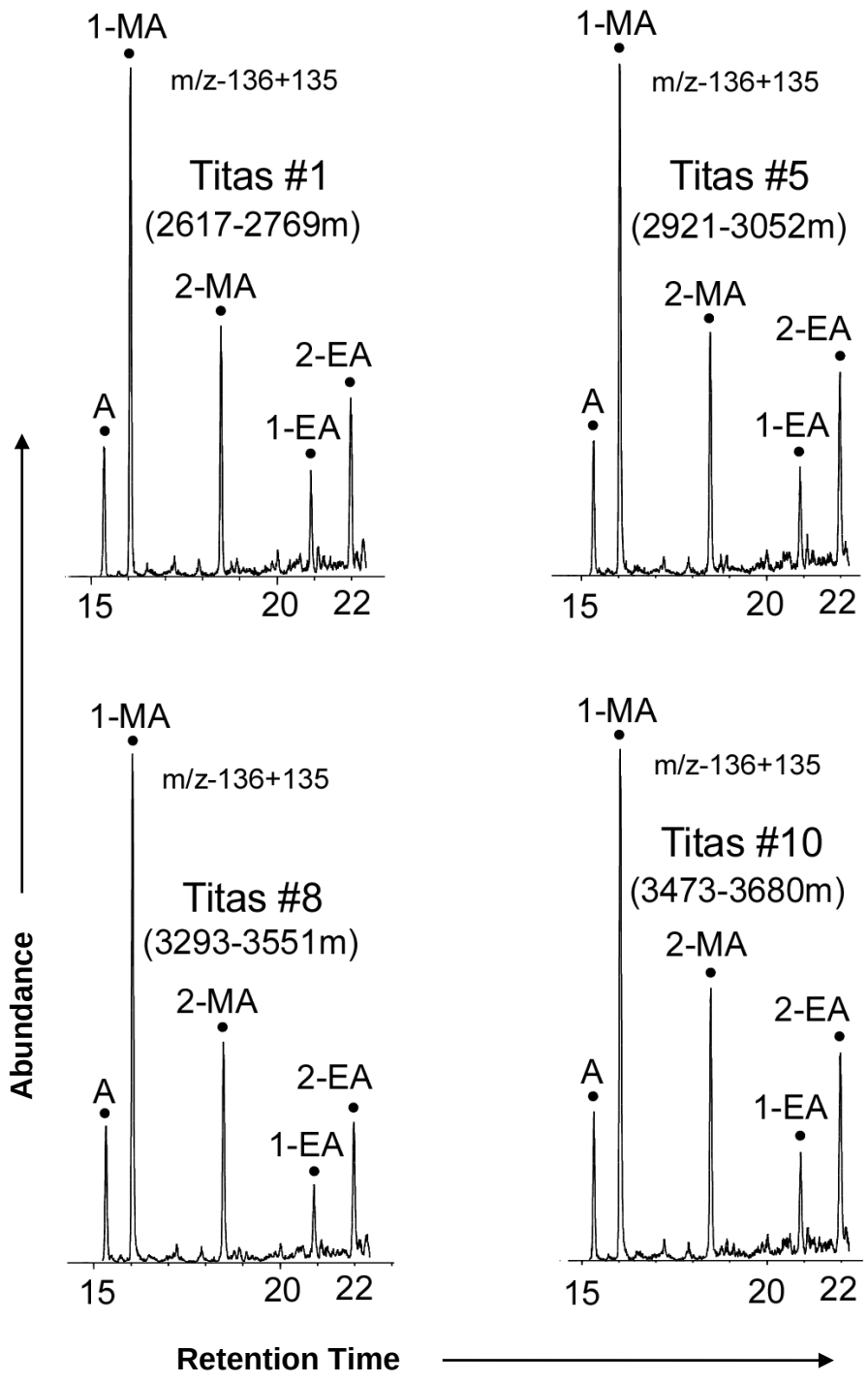

API gravities of the studied oils were 26.2 to 48.3°, except for two waxy oils from Fenchuganj #2 and Sylhet #7 (Takeda et al., 2011). API gravities of waxy oils from 3068.5–3072.5 m and 3074.5–3083.5 m depths in Fenchuganj #2 and 2020–2033 m in Sylhet #7 were reported to be 17.2° and 28.3°, respectively (Ahmed et al., 1991).

These variations, particularly in the oils from the north to central Surma basin, cannot be interpreted to be due to differences in source rock type and/or maturity levels, because the oils are derived from similar terrigenous source rocks and show similar maturity levels. After the original accumulation of oil in a reservoir, the oil composition can be modified as a result of processes such as thermal degradation, deasphaltening, water washing and tertiary migration. As detailed above, waxy oils are generally located at greater depths than lighter condensates. This difference in distribution may suggest that evaporative fractionation of the reservoired oil has occurred, followed by upward migration of lighter hydrocarbons. Lighter hydrocarbons may be selectively vaporized and expelled from a reservoir rock due to changes in reservoir temperature and pressure resulting from tectonic activity. These lighter hydrocarbons may migrate to a neighboring reservoir to form a gas-condensate accumulation. Residual oil remaining in the reservoir will then become heavier and waxy. Thompson (1987) demonstrated evaporative fractionation in laboratory experiments which investigated the nature of the products (condensates and residual oil) and the original oil.

The experiments showed that progressive evaporation can result in oils which are lighter, more paraffinic and less aromatic than the original oils. In addition, the depletion of lower molecular weight *n*-alkanes and a change in the dominant *n*-alkanes from lighter to heavier in the residual oil were observed. Thompson (1987) proposed a plot of aromaticity (toluene/nC$_7$) versus. paraffinicity (nC$_7$/methylcyclohexane) to illustrate the progressive evaporative fractionation process. The aromaticity and paraffinicity of the oil samples from the Surma basin were determined, based on the relative abundances of toluene, methylcyclohexane and nC$_7$, and aromaticity was plotted versus paraffinicity (Fig. 12).

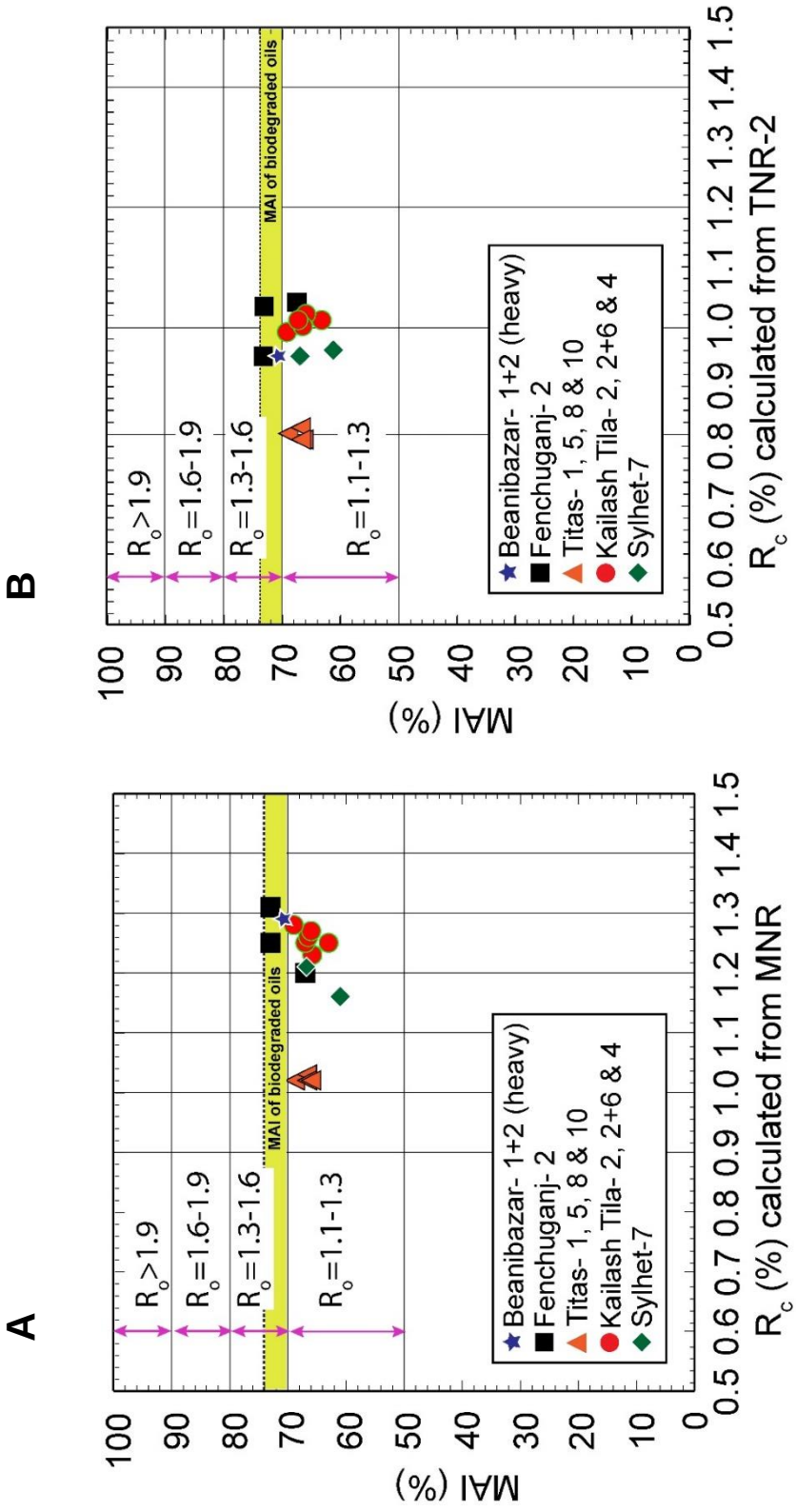

Fig. 10. Cross plot of methyladamantane index (MAI, %) versus (A) R_c (%) calculated from methylnaphthalene ratio (MNR) and (B) R_c (%) calculated from trimethylnaphthalene ratio (TNR-2).

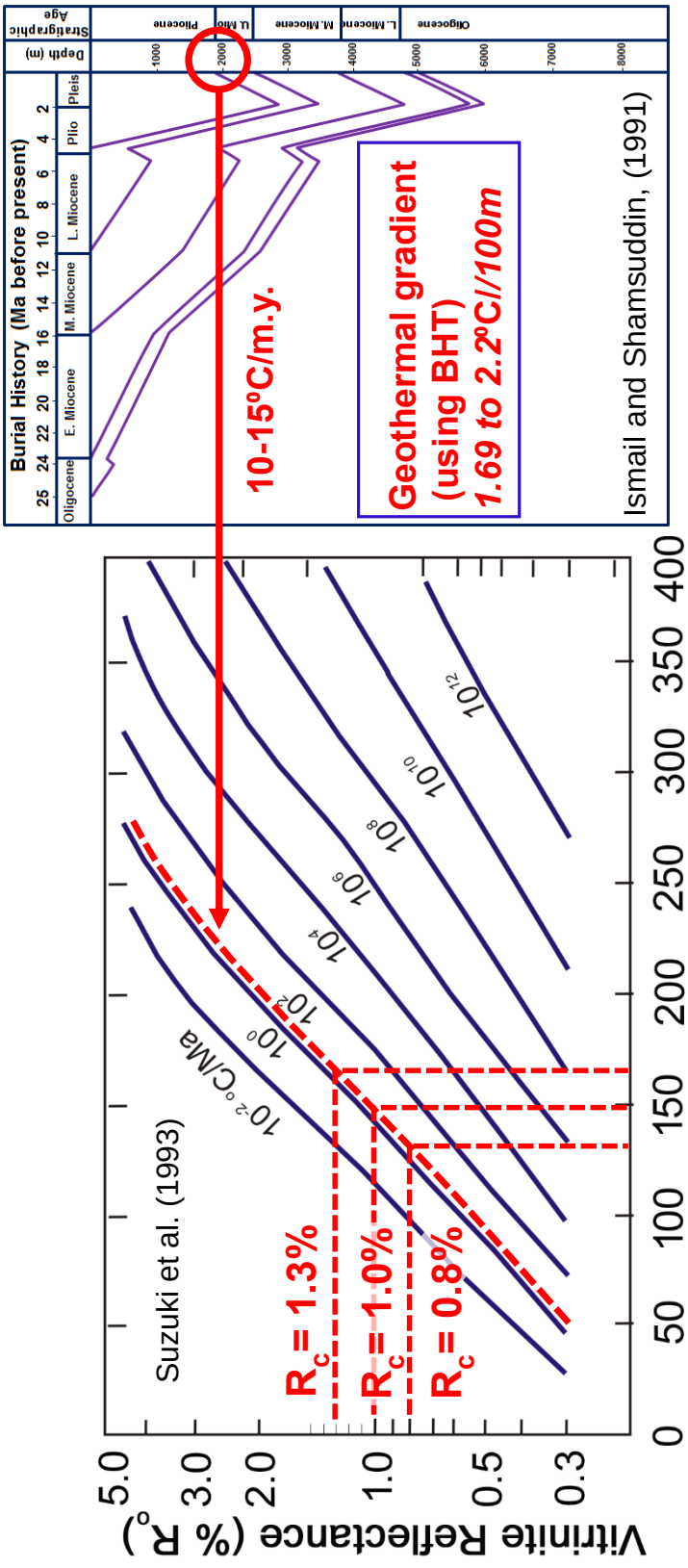

Fig. 11. Geothermal gradient (°C/100meter) of the Surma basin have been calculated using bottom hole temperature (BHT), temperature increment per million year have been calculated at the Miocene-Pliocene boundary and plotted in the time-temperature and vitrinite reflectance relationship curve (Suzuki et al., 1993) to determine the maximum temperature correspond to the calculated vitrinite reflectance (R_c).

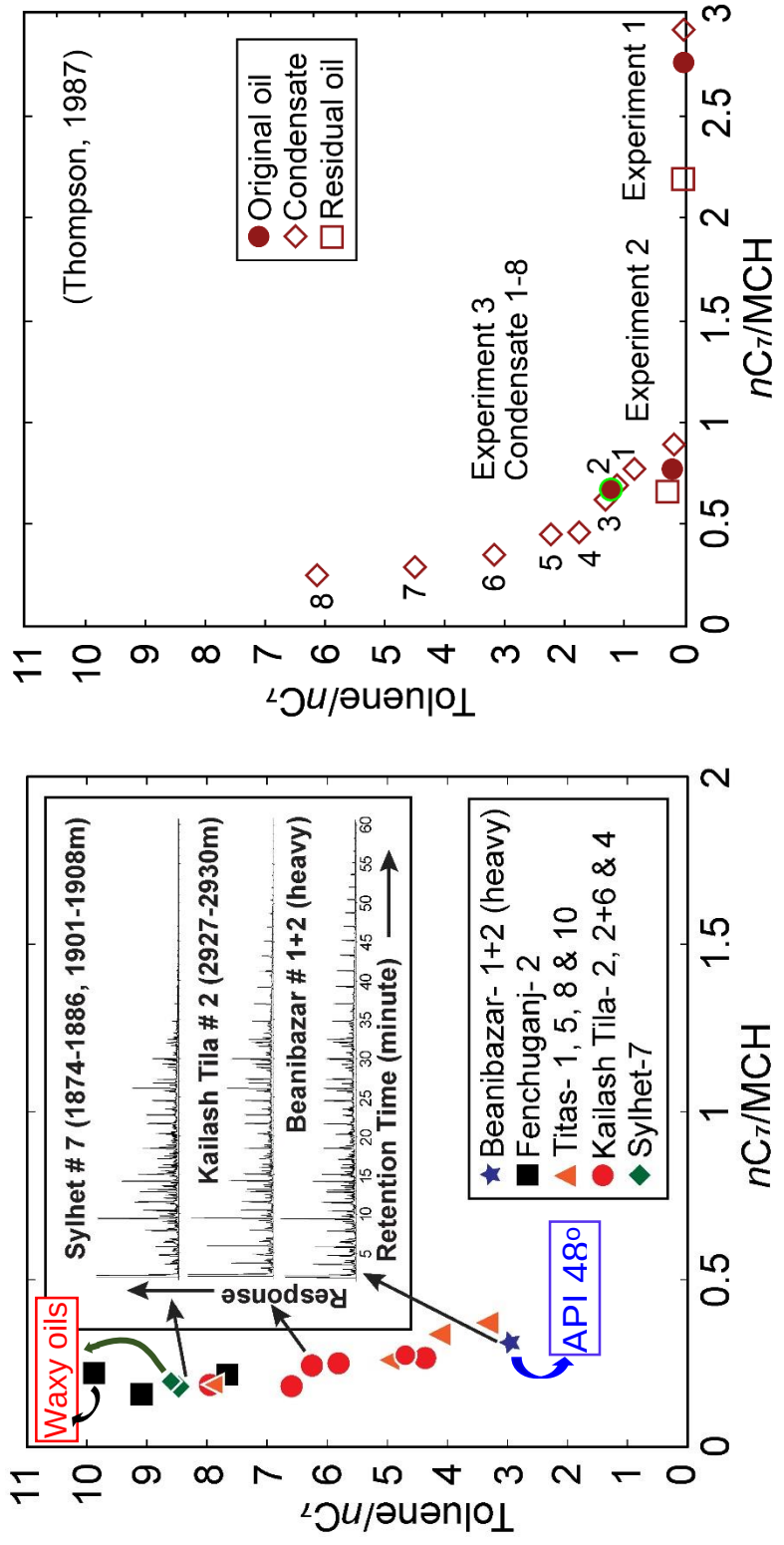

Fig. 12. Aromaticity (toluene/nC7) versus paraffinicity (nC7/ methylcyclohexane) of oils from the Surma basin. In-reservoir phase separation after the accumulation of oils resulted in the formation of diverse oils, as shown by the whole oil chromatograms.

Waxy oils from wells Fenchuganj #2 and Sylhet #7 were characterized by higher aromaticity compared to condensates which had accumulated in reservoir units overlying the waxy oil reservoir. Condensates from Beanibazar #1+2, which have the lowest API gravity (48.3°), showed the lowest aromaticity and highest paraffinicity among all the oil samples. Oils from Kailash Tila and Titas plotted between the waxy oils and the condensates from Beanibazar #1+2. The significantly different aromaticity and paraffinicity observed in similar terrigenous oils with similar maturities strongly suggest that evaporative fractionation has taken place following initial oil accumulation in the reservoir. Tertiary migration and re-accumulation of lighter hydrocarbons is expected to have taken place during and after the formation of traps and anticlinal folds in the Pliocene. The API gravity values of oils in the Surma basin increases with decreasing reservoir depth, corresponding closely to changes in the aromaticity and paraffinicity of the oils. This trend was especially evident in the Fenchuganj #2 and Sylhet #7 wells.

The Tipam and Dupi Tila Formations are characterized by thick fluvial to deltaic sedimentary successions deposited during rapid subsidence of the Surma basin due to overthrusting of the Shillong Plateau during the Pliocene (Johnson and Alam, 1991). Large-scale tectonic movements along the Dauki Fault and in the Himalaya and Indo-Burman Ranges occurred during the Pliocene, resulting in the formation of the present-day basin architecture (Alam, 1989; Imam and Hussain, 2002). Structural dislocation of pre-existing reservoirs occurred in the Surma basin as a result of this Pliocene tectonism, and evaporative fractionation, tertiary migration and re-accumulation of hydrocarbons resulted in the compositional diversity of petroleum which is observed. The occurrence of many oil and gas seepages in the Surma basin suggests that tertiary migration continues at the present day.

5. Conclusions

Twenty oils and condensate samples from seven oil and gas fields in the Surma basin, Bangladesh, were analysed and were found to have highly diverse *n*-alkane distributions. The relative abundance of pristane, phytane and adjacent *n*-alkanes and abundant biphenyls, cadalene, and bicadinanes suggested that most of the oils and condensates were derived from source rocks rich in terrigenous organic matter. A cross-plot of pr/nC$_{17}$

versus ph/nC$_{18}$ for oils from the Titas field, however, suggested a possible contribution of algal organic matter. Maturities of the oils and condensates were estimated based on the polyaromatic hydrocarbons, and showed that oils can be classified into two groups. Oils from the north to central Surma basin are characterized by relatively high R_c values (1.0–1.3%), whereas R_c values of oils from the Titas well in the southern margin are 0.8–1.0%. Oil samples from the Rashidpur and Habiganj wells were severely biodegraded. However, diamondoid hydrocarbons were identified in both the biodegraded oils and non-biodegraded samples. The distribution of adamantanes and the methyladamantane index of the severely biodegraded oils were almost identical to those of non-biodegraded oils, indicating a similar type of source rocks and similar maturity levels of all the oils in the north to central Surma basin.

Taking into account the time–temperature history of the Surma basin and the estimated maturity levels of the oils and condensates, the burial depth of the source rocks at the major stage of hydrocarbon expulsion is estimated to be between 5000–6000 m for the Titas oils and 6000–7000 m for the other oils in the Surma basin. Although the geochemical data set for the Oligocene and older sedimentary sequences is limited, the top of the Eocene Kopili Shale to lower Jenam Shale of early Oligocene sedimentary rocks rich in terrigenous organic matter are identified as possible source rocks. The aromaticity and paraffinicity of the oils, as evaluated by toluene, methylcyclohexane and nC$_7$, indicated progressive subsurface evaporative fractionation after initial accumulation of oil in the reservoir. This resulted in separate accumulations of relatively light condensates and heavier waxy oils. Tertiary migration is interpreted to have occurred during and after the Pliocene, when pre-existing reservoirs were dislocated by large-scale tectonic activity.

References

AHMED. M., KHAN, S.I. AND SATTAR, M.A., 1991. Geochemical characterization of oils and condensates in the Bengal Foredeep, Bangladesh. *Journal of Southeast Asian Earth Sciences*, **5**, 391-399.

ALAM, M., 1989. Geology and depositional history of Cenozoic sediments of the Bengal Basin of Bangladesh. *Palaeogeography, Palaeoclimatology, Palaeoecology*, **69**, 125-139.

ALAM, M., ALAM, M.M., CURRAY, J.R., CHOWDHURY, M.L.R., GANI, M.R., 2003. An overview of the sedimentary geology of the Bengal Basin in relation to the regional tectonic framework and basin-fill history. *Sedimentary Geology*, **155**, 179-208.

ALAM, M. and PEARSON, M.J., 1990. Bicadinanes in oils from the Surma Basin, Bangladesh. *Org. Geochem*, **15**, 461-464.

ALEXANDER, R., BAKER, R.W., KAGI, R.I. and WARTON, B., 1994a. Cyclohexyl benzenes in crude oils. *Chemical Geology*, **113**, 103-115.

ALEXANDER, R., KAGI, R.I., SINGH, R.K. and SOSROWIDJOJO, I.B., 1994b. The effect of maturity on the relative abundances of cadalene and isocadalene in sediments from the Gippsland Basin, Australia. *Organic Geochemistry*, **21**, 115-120.

BANERJI, R.K., 1981. Cretaceous-Eocene sedimentation, tectonism and biofacies in the Bengal Basin, India. *Palaeogeography, Palaeoclimatology, Palaeoecology*, **34**, 57-85.

BANERJI, R.K., 1984. Post-Eocene biofacies, palaeoenvironments and palaeogeography of the Bengal Basin, India. *Palaeogeography, Palaeoclimatology, Palaeoecology*, **45**, 49-73.

BENDORAITIS, J.G., 1974. Hydrocarbons of biogenic origin in petroleum-Aromatic triterpenes and bicyclic sesquiterpenes. In: TISSOT B. AND BIENNER F. (eds), *Advances in Organic Geochemistry, Technip, Paris*, 209-224. Technip, Paris.

CHEN, J., FU, J., SHENG, G., LIU, D. and ZHANG, J., 1996. Diamondoid hydrocarbon ratios: novel maturity indices for highly mature crude oils. *Organic Geochemistry*, **25**, 179-190.

CUMBERS, K.M., ALEXANDER, R., KAGI, R.I., 1987. Methylbiphenyl, ethylbiphenyl and dimethylbiphenyl isomer distributions in some sediments and crude oils. *Geochimica et Cosmochimica Acta*, **51**, 3105-3111.

CURIALE, J.A., COVINGTON, G.H., SHAMSUDDIN, A.H.M., MORELOS, J.A. and SHAMSUDDIN, A.K.M., 2002. Origin of petroleum in Bangladesh. *AAPG Bulletin*, **86**, 625-652.

FARHADUZZAMAN, M., WAN HASIAH, A., ISLAM, M. A. and PEARSON, M. J., 2012. Source rock potential of organic-rich shales in the Tertiary Bhuban and Boka Bil Formations, Bengal Basin, Bangladesh. *Journal of Petroleum Geology*, **35**, 357-376.

GRICE, K., ALEXANDER, R., KAGI, R.I., 2000. Diamondoid hydrocarbon ratios as indicators of biodegradation in Australian crude oils. *Organic Geochemistry*, **31**, 67-73.

HILLER, K., ELAHI, M., 1984. Structural development and hydrocarbon entrapment in the Surma Basin/Bangladesh (northwest Indo-Burman fold belt). In: Fifth Offshore South East Asia Conference, Singapore, 650-663.

HOSSAIN, MD. A., SUZUKI, N., MATSUMOTO, K., SAKAMOTO, R., and TAKEDA, N., 2014: In-reservoir fractionation and the accumulation of oil and condensates in the Surma basin, NE Bangladesh. *Journal of Petroleum Geology*, **37(3)**, 269-286.

HOSSAIN, H.M.Z., SAMPEI, Y., ROSER, B.P., 2009. Characterization of organic matter and depositional environment of Tertiary mudstones from the Sylhet Basin, Bangladesh. *Organic Geochemistry*, **40**, 743-754.

IMAM, M.B., 2005. Energy resources of Bangladesh. University Grants Commission of Bangladesh, Dhaka, Bangladesh.

IMAM, M.B. and HUSSAIN, M., 2002. A review of hydrocarbon habitats in Bangladesh. *Journal of Petroleum Geology*, **25**, 31-52.

ISMAIL, M. and SHAMSUDDIN, A.H.M., 1991. Organic matter maturity and its relation to time, temperature and depth in the Bengal Foredeep, Bangladesh. *Journal of Southeast Asian Earth Sciences*, **5**, 381-390.

JOHNSON, S.Y. and NUR ALAM, A.M., 1991. Sedimentation and tectonics of the Sylhet trough, Bangladesh. *Geological Society of America Bulletin*, **103**, 1513-1527.

MAIR, B.J. and MAYER, T.J., 1964. Composition of the dinuclear aromatics, C12 to C14, in the light gas oil fraction of petroleum. *Anal. Chem*. **36**, 351-362.

MRKIC, S., STOJANOVIC, K., KOSTIC, A., NYTOFT, H.P., SAJNOVIC, A., 2011. Organic Geochemistry of Miocene source rocks from the Banat Depression (SE Pannonian Basin, Serbia). *Organic Geochemistry*, **42**, 655-677.

RADKE, M., LEYTHAEUSER, D. and TEICHMULLER, M., 1984. Relationship between rank and composition of aromatic hydrocarbons for coals of different origins. *Organic Geochemistry*, **6**, 423-430.

RADKE, M., WELTE, D.H. and WILLSCH, H., 1982a. Geochemical study on a well in the Western Canada Basin: relation of the aromatic distribution pattern to maturity of organic matter. *Geochimica et Cosmochimica Acta*, **46**, 1-10.

RADKE, M., WILLSCH, H., LEYTHAEUSER, D. and TEICHMULLER, M., 1982b. Aromatic components of coal: relation of distribution pattern to rank. *Geochimica et Cosmochimica Acta*, **46**, 1831-1848.

RADKE, M., WELTE, D.H. and WILLSCH, H., 1986. Maturity parameters based on aromatic hydrocarbons: influence of the organic matter type. *Organic Geochemistry*, **10**, 51-63.

RADKE, M., RULLKOTTER, J. and VRIEND, S.P., 1994. Distribution of naphthalenes in crude oils from the Java Sea: Source and maturation effects. *Geochimica et Cosmochimica Acta*, **58**, 3675-3689.

RAO, A.R., 1983. Geology and hydrocarbon potential of a part of Assam-Arakan basin and its adjacent region: *Pet. Asia J*. **6**, 127-158.

SHAMSUDDIN, A.H.M. and ABDULLAH, S.K.M., 1997. Geologic evolution of the Bengal Basin and its implication in hydrocarbon exploration in Bangladesh. *Indian Journal of Geology*, **69**, 93-121.

SHAMSUDDIN, A.H.M. and KHAN, S.I., 1991. Geochemical criteria of migration of natural gases in the Miocene sediments of the Bengal Foredeep, Bangladesh. *Journal of Southeast Asian Earth Sciences*, **5**, 89-100.

SIMONEIT, B.R.T., 1986. Cyclic terpenoids of the geosphere. In: JOHNS, R.B. (eds.), Biological Markers in the Sedimentary Record. 43-82, Elsevier, Amsterdam.

STRACHAN, M.G., ALEXANDER, R. and KAGI, R.I., 1988. Trimethylnaphthalenes in crude oils and sediments: Effects of source and maturity. *Geochimica et Cosmochimica Acta*, **52**, 1255-1264.

SUZUKI, N., MATSUBAYASHI, H. and WAPLES, D.W., 1993. A simpler kinetic model of vitrinite reflectance. *AAPG Bulletin*, **77(9)**, 1502-1508.

TAKEDA, N., KATO, S., FUJIWARA, M., ALAM, M. N., HOSSAIN, M.M., KAHN, M.A.E., RAHMAN, M.M. and SARKER, M.A.H., 2011. Geochemistry of Gas and Condensate in the Surma Basin, Bangladesh. Petroleum Geology Conference & Exhibition (PGCE) 2011 Program Book. Kuala Lumpur Convention Center.

TEGELAAR, E.W., DE LEEUW, J.W., LARGEAU, C. and DERENNE, S., SCHULTEN, H. R. and MULLER, R., BOON, J.J. and NIP, M., SPRENKELS, J. C. M., 1989. Scope and limitations of several pyrolysis methods in the structural elucidations of a macromolecular plant constituent in the leaf cuticle of Agave Americana L. *Journal of Analytical and Applied Pyrolysis*, **15**, 29-54.

THOMPSON, K.F.M., 1987. Fractionated aromatic petroleums and the generation of gas-condensates. *Organic Geochemistry*, **11**, 573-590.

TROLIO, R., ALEXANDER, R., KAGI, R.I., 1996. Alkyldiphenylmethanes in crude oils. *Polycyclic Aromatic Compounds*, **9**, 137-142.

TROLIO, R., GRICE, K., FISHER, S.J., ALEXANDER, R., KAGI, R.I., 1999. Alkylbiphenyls and alkyldiphenylmethanes as indicators of petroleum biodegradation. *Organic Geochemistry*, **30**, 1241-1253.

UDDIN, A., LUNDBERG, N., 2004. Miocene sedimentation and subsidence during continent - continent collision, Bengal basin, Bangladesh. *Sedimentary Geology*, **164**, 131-146.

VAN AARSSEN, B.G.K., BASTOW, T.P., ALEXANDER, R., KAGI, R.I., 1999. Distributions of methylated naphthalenes in crude oils: indicators of maturity, biodegradation and mixing. *Organic Geochemistry*, **30**, 1213-1227.

WENGER, L.M., ISAKSEN, G.H., 2002. Control of hydrocarbon seepage intensity on level of biodegradation in sea bottom sediments. *Organic Geochemistry*, **33**, 1277-1292.

WHITE, C.M. and LEE, M.L., 1980. Identification and geochemical significance of some aromatic components of coal. *Geochimica et Cosmochimica Acta*, **44**, 1825-1832.

WINGERT, W.S., 1992. G.c-m.s. analysis of diamondoid hydrocarbons in Smackover petroleums. *Fuel*, **71**, 37-43.

YESSALINA, S., SUZUKI, N., NISHITA, H. and WASEDA, A., 2006. Higher Plant Biomarkers in Paleogene crude oils from the Yufutsu oil-and gas field and offshore wildcats, Japan. *Journal of Petroleum Geology*, vol. **29(4)**, pp 327-336.

YEW, F.F.H. and MAIR, B.J., 1966. Isolation and Identification of C13 to C17 alkylnaphthalenes, alkylbiphenyls and alkyldibenzofurans from the 275° to 305° C. dinuclear aromatic fraction of petroleum. *Analytical Chemistry*, **38**, 231-237.

ZHANG, M. and PHILP, P., 2010. Geochemical characterization of aromatic hydrocarbons in crude oils from the Tarim, Qaidam and Turpan Basins, NW China. *Petroleum Science*, **7**, 448-457.

Chapter 2

Carbon and hydrogen isotope composition of individual *n*-alkanes in crude oils and condensates

Abstract

The relative abundance of C_7 aromatic, cyclic, and straight chain hydrocarbons in oil/condensates and other molecular parameters inferred a large diversity of the petroleum from waxy crude oils to condensates in the Surma basin, Bangladesh. This diversity of petroleum is thought to be due to in-reservoir evaporative fractionation, resulting in residual waxy oils and lighter condensates which subsequently underwent tertiary migration and re-accumulation in the deltaic basin. Stable carbon and hydrogen isotope of individual *n*-alkane in oil/condensate samples have been analyzed for further understanding the origin and compositional fractionation of petroleum.

The $\delta^{13}C$ values of individual *n*-alkanes ranging from -32 to -25 ‰ tends to decrease with increasing carbon number. The $\delta^{13}C$ profile of *n*-alkanes showing nearly similar distribution pattern in all the crude oil/condensate samples. The $\delta^{2}H$ value of individual *n*-alkane ranges from -128 to -70‰ and linearly increases with increasing carbon number. However, the relationship between carbon number and $\delta^{2}H$ value is notably different among the oil/condensate samples. Waxy oils are remarkably depleted in ^{2}H with increasing carbon number compared to all other condensates. This variation in $\delta^{2}H$ value of *n*-alkanes clearly distinguishes lighter condensates from heavy waxy oils.

Both source organic type and maturity level of oil are related to $\delta^{13}C$ values of *n*-alkanes in oils. Taking into account the similar maturity levels of oils as suggested by molecular parameters, the similar distribution of $\delta^{13}C$ values of *n*-alkanes elucidate that all the oil/condensates were generated from similar source organic matter, being consistent with our previous molecular study.

A comparatively large variation in $\delta^{2}H$ values of *n*-alkanes in oils from the Surma basin is thought to be related to the subsurface evaporative fractionation. Vaporization of non-polar compounds like *n*-alkanes is partly related to the intermolecular dispersion force (a sort of Van der Waals force) caused by induction of a dipole moment. Intermolecular dispersion force of non-polar compound with ^{2}H is weaker than the same compound without ^{2}H because of weak polarizability of ^{2}H. Consequently, vaporization of non-polar *n*-alkane with ^{2}H occurs easily compared to that without ^{2}H. Isotopically

heavier compound with ^{2}H, therefore, would be expected to be concentrated in vapor phase. This effect termed as "inverse isotope fractionation". We report on the possible first observation of inverse hydrogen isotope fractionation of *n*-alkanes associated with in-reservoir phase separation, migration, and re-accumulation in the natural petroleum system. On the other hand, nearly similar $\delta^{13}C$ values of long chain *n*-alkanes suggests a minor effect of evaporative fractionation on the $\delta^{13}C$ value of *n*-alkane.

6. Introduction

Petroleum in the Paleogene to Neogene Surma basin, northeast Bangladesh (part of the Bengal Basin) ranges from waxy crude oils to condensates. The diversity of the petroleum in the Surma basin was thought to be due to evaporative fractionation, resulting in residual waxy oils and lighter condensates which subsequently underwent tertiary migration and re-accumulation in the deltaic basin (Hossain et al., 2014). Compound specific isotope composition of *n*-alkanes in oils now a days being a widespread used parameter in the geochemical research of petroleum correlation. Carbon isotope composition of individual *n*-alkane in oils are considered a major correlating tool especially in source organic matter, depositional environment and maturity. Several studies e.g. Clayton, 1991; Bjoroy et al., 1990; 1994a, b; Mycke et al., 1994 illustrated that, subtle variation in source materials and maturity levels can influence $\delta^{13}C$ value of individual *n*-alkanes in oils and condensates.

Likewise, hydrogen isotope composition of individual *n*-alkane in oils also can be used as a powerful tool to reconstruct the paleo-hydrology. The $\delta^{2}H$ values of individual *n*-alkanes of oils and sediment extracts are reported to be the suitable candidate to preserve initial $\delta^{2}H$ values of their precursor water (Dawson et al., 2004; Schimmelmann et al., 2006; Kikuchi et al., 2010). In particular, $\delta^{2}H$ values of *n*-alkanes were found as almost constant through diagenesis to the stage of peak oil generation. On the other hand, aromatic hydrocarbons and acyclic isoprenoids become significantly rich in ^{2}H at the starting of oil window and at the peak oil generation stage respectively as a result of carbon bound H exchange reaction with sediment pore water associate with increasing maturity (Kikuchi et al., 2010). However, ^{2}H enrichment of *n*-alkane with increasing maturity in oils also reported by Li et al., 2001. Apart from these, in-reservoir phase separation, subsurface evaporative fractionation and/or migration fractionation effects on both the carbon and hydrogen isotopic compositions of petroleum are not well documented yet. Aim of the present study is to characterize the crude oils and condensates based on stable carbon and hydrogen isotope compositions of individual *n*-alkanes and to investigate the influence of subsurface evaporative fractionation on carbon and hydrogen isotope composition of individual *n*-alkane.

Dzou and Hughes (1993) have reported that, individual *n*-alkanes of condensates that derived by the way of evaporative fractionation are generally depleted in ^{13}C compared to that of the residual waxy oils. However, Graas et al. (2000) reported, no effect and/or very small variation in carbon isotope composition of oils and condensates during laboratory experiment of petroleum phase separation. In addition, Xiao et al., 2012, reported 'normal carbon isotope fractionation' e.g. progressive enrichment in ^{13}C of residual liquid low molecular weight hydrocarbon (C_6-C_8 range) during vaporization experiment in laboratory.

On the other hand, hydrogen isotope fractionation of *n*-alkanes during vaporization has been studied in the laboratory, showing that residual liquid *n*-alkanes become depleted in ^{2}H and is significant with increasing molecular weight (Wang and Huang, 2003, Bai et al., 2013). This hydrogen isotope fractionation of *n*-alkanes is termed as "inverse isotope fractionation". There are, however, few studies on the hydrogen isotope fractionation of *n*-alkanes due to evaporative fractionation of oils in the sedimentary basin.

7. Materials and methods

7.1. Samples

A total 16 crude oil/condensate samples (Table 4) have been selected from five oil and gas fields located in north to central and southern margin of the Surma basin, Bangladesh (Fig. 1): Sylhet, Kailash Tila, Beanibazar, Fenchuganj and Titas.

7.2. Analysis of stable carbon isotope of individual n-alkanes

Aliphatic fractions were separated from crude oil/condensates using silica gel column chromatography (Fig.13). Aliphatic fractions were then treated by the way of urea adduct to separate straight chain *n*-alkanes from branched and cyclic hydrocarbons.

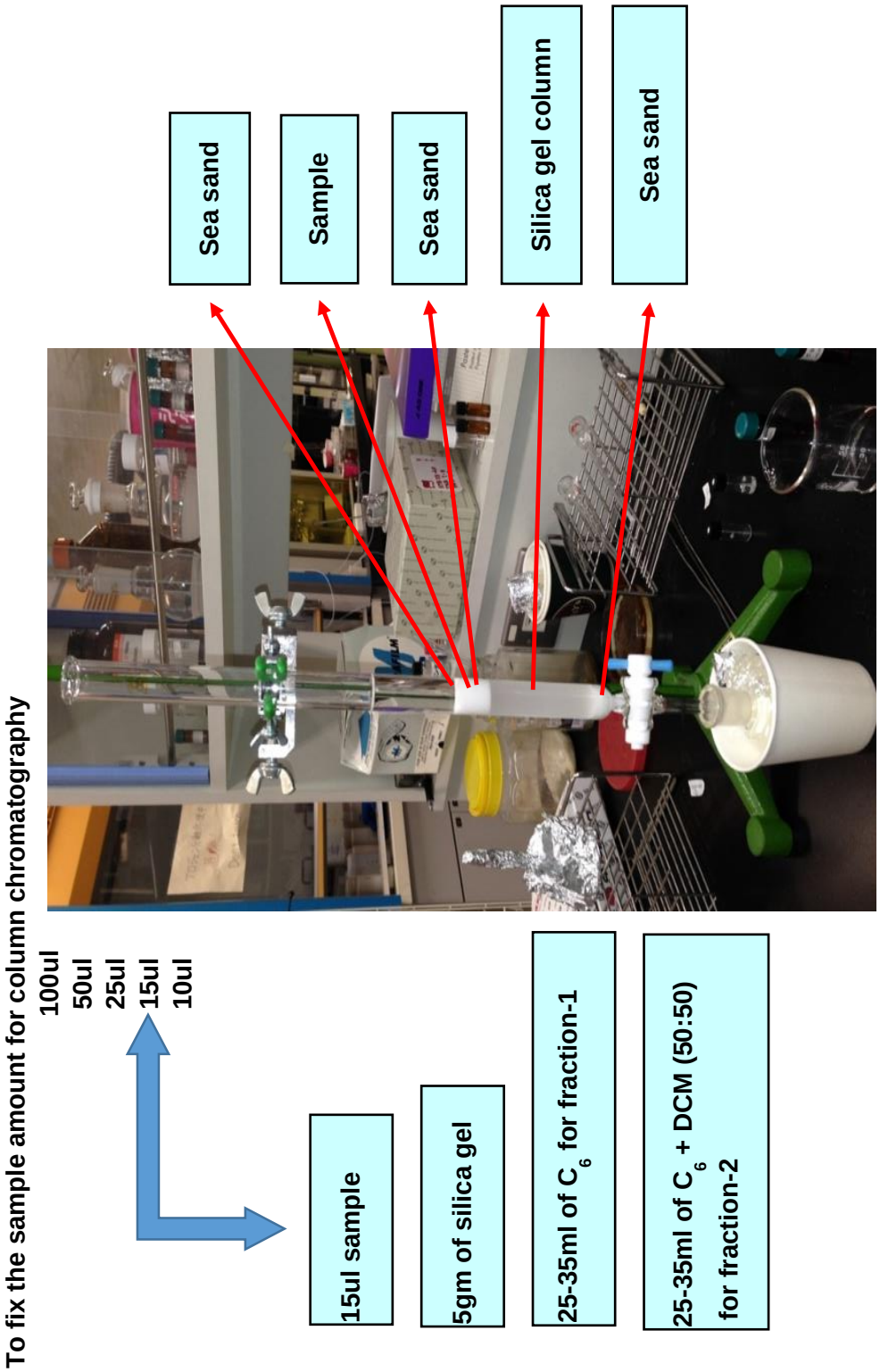

Fig. 13. Silica gel column chromatography.

Table 4. Physical and molecular properties of crude oils and condensates from the Surma basin.

Well name	Field name	Depth (m)	Formation	*n*-Alkane Range	API Gravity (°)	Color	Under room condition
Sylhet #7	Sylhet	1874-1886 1901-1908	Upper Bhuban	C_7 - C_{23}	43.1[b]	Color less	Liquid
Sylhet #7		2020-2033	Bhuban	C_7 - C_{35}	28.3[a]	Dark yellow	**Waxy**
Kailash Tila #1	Kailash Tila	2941-2948	Bhuban	C_7 - C_{27}	44.8[b]	Color less	Liquid
Kailash Tila #2		2252-2265	Bokabil	C_7 - C_{24}	43.2[b]	Color less	Liquid
Kailash Tila #2+6		2252-2265	Bokabil	C_7 - C_{23}	46.4[b]	Light yellow	Liquid
Kailash Tila #2		2724-2732	Bhuban	C_7 - C_{26}	43.4[b]	Color less	Liquid
Kailash Tila #2		2927-2930	Bhuban	C_7 - C_{29}	39.7[b]	Light yellow	Liquid
Kailash Tila #4		2930-2958	Bhuban	C_7 - C_{26}	44.8[b]	Color less	Liquid
Beanibazar #1+2 (heavy)	Beanibazar	3451-3465	Bokabil	C_7 - C_{31}	48.3[b]	Color less	Liquid
Fenchuganj #2	Fenchuganj	2578.6-2581.6		C_7 - C_{27}	42.4[b]	Light yellow	Liquid
Fenchuganj #2+3		2768-2781	Upper Bhuban	C_7 - C_{27}	41.1[b]	Color less	Liquid
Fenchuganj #2		3068.5-3072.5 3074.5-3083.5		C_7 - C_{35}	17.2[a]	Dark yellow	**Waxy**
Titas #1	Titas	2617-2769	Upper Bhuban	C_7 - C_{25}	40[b]	Color less	Liquid
Titas #5		2921-3052	Bhuban	C_7 - C_{25}	38.8[b]	Color less	Liquid
Titas #8		3293-3551	Bhuban	C_7 - C_{24}	42.9[b]	Color less	Liquid
Titas #10		3473-3680	Bhuban	C_7 - C_{25}	39.7[b]	Light yellow	Liquid

a- Ahmed et al., 1991**; b-** Takeda et al., 2011

Saturated *n*-alkanes were analyzed by gas chromatography/mass spectrometry (GC/MS) using HP6890/HP5973 instrument equipped with a fused silica capillary column DB35MS (30m x 0.25 mm J&W). The oven temperature of the GC/MS was initially programmed to 40ºC and held isothermally for 5 minutes; to 300ºC at a rate of increase 4ºC/min and held isothermally for 5 minutes. Helium was used as the carrier gas with a flow rate of 0.6 ml/min. Carbon isotope composition of the individual *n*-alkanes were analyzed by gas chromatography–combustion–isotope ratio mass spectrometry (GC–C–IRMS) using HP6890 GC. GC was equipped with capillary column DB35MS (30m x 0.25 mm J&W) coupled with a Finnigan MAT-252 isotope mass spectrometry and a Finnigan MAT interface GC-combustion III. The initial oven temperature of the GC was 40ºC and held isothermally for 2 minutes; followed by 10ºC/min to 120ºC, subsequently at a rate of 4ºC/min to 300ºC and held isothermally for 20 minutes. Helium was used as carrier gas with a flow rate of 1.5 ml/min. The carbon isotope values were reported in δ-notation relative to Vienna Pee Dee Belemnite (VPDB) standard. $^{13}C/^{12}C$ ratio value of the reference CO_2 gas was estimated by comparison with the standard *n*-alkanes with known $\delta^{13}C$ values (C_{27} – 28.45‰, C_{32} – 29.29‰, and C_{36} – 26.99‰). All the samples have at least two runs (replicated) and in case of large difference (>2‰) of $\delta^{13}C$ value of single *n*-alkane between two runs, samples have been analyzed three (triplicate) times and getting the average value.

7.3. Analysis of stable hydrogen isotope of individual n-alkanes

Saturated *n*-alkanes were analyzed by gas chromatography/mass spectrometry (GC/MS) using HP6890/HP5973 instrument equipped with a fused silica capillary column DB5HT (30m x 0.25 mm J&W). The oven temperature of the GC/MS was initially programmed to 40ºC and held isothermally for 4 minutes; to 300ºC at a rate of increase of 4ºC/min and held isothermally for 20 minutes. Helium was used as the carrier gas with a flow rate of 0.6 ml/min. Hydrogen isotope composition of individual *n*-alkane were then analyzed by gas chromatography–thermal conversion–isotope ratio mass spectrometry (GC–TC–IRMS, Thermo Electron Corporation DELTA V Advantage). GC was equipped with a fused silica capillary column DB5HT (30m x 0.25 mm J&W). The oven temperature was same as GC/MS. Helium was used as the carrier gas with a flow rate of 1.3 ml/min.

Table 5. Carbon isotope composition of individual *n*-alkanes (‰, VPDB).

Well name	Depth (m)	C_8	C_9	C_{10}	C_{11}	C_{12}	C_{13}	C_{14}	C_{15}	C_{16}	C_{17}	C_{18}	C_{19}	C_{20}	C_{21}	C_{22}	C_{23}	C_{24}	C_{25}	C_{26}	C_{27}	C_{28}	C_{29}	C_{30}	C_{31}	C_{32}	C_{33}	C_{34}
Sylhet #7	1874-1886 1901-1908	nd	-27	-27	-29	-29	-28	-29	-29	-30	-30	-30	-29	nd	nd	nd	nd	nd	nd	nd	nd	nd	nd	nd	nd	nd	nd	nd
Sylhet #7	2020-2033	nd	nd	nd	-28	-29	-29	-30	-30	-30	-30	-30	-30	-31	-30	-31	-30	-31	-30	-31	-32	-31	-31	-31	-31	-31	-32	-32
Kailash Tila #1	2941-2948	-27	-30	-31	-30	-30	-30	-31	-30	-30	-30	-29	-30	-29	-30	-30	-29	nd	nd	nd	nd	nd	nd	nd	nd	nd	nd	nd	nd
Kailash Tila #2	2252-2265	nd	-28	-30	-32	-35	-36	-38	-36	-34	-34	-31	-30	-30	-30	nd	nd	nd	nd	nd	nd	nd	nd	nd	nd	nd	nd	nd	nd
Kailash Tila #2+6	2252-2265	nd	-27	-27	-29	-31	-31	-32	-33	-35	-33	-33	-32	-31	30	30	nd	nd	nd	nd	nd	nd	nd	nd	nd	nd	nd	nd	nd
Kailash Tila #2	2724-2732	nd	-27	-28	-29	-30	-31	-32	-31	-30	-30	-30	-31	-31	-31	-30	-30	-30	-29	nd	nd	nd	nd	nd	nd	nd	nd	nd	nd
Kailash Tila #2	2927-2930	nd	-27	-28	-29	-30	-30	-30	-30	-31	-30	-31	-31	-31	-31	-31	-31	-31	-30	-30	-30	nd	nd	nd	nd	nd	nd	nd	nd
Kailash Tila #4	2930-2958	nd	-27	-27	-30	-29	-30	-29	-30	-30	-30	-30	-30	-31	-30	-30	-30	-30	-29	nd	nd	nd	nd	nd	nd	nd	nd	nd	nd
Beanibazar #1+2 (heavy)	3451-3465	-25	-27	-27	-29	-30	-30	-28	-29	-29	-29	-29	-30	-30	-30	-29	-30	-30	-30	-30	-30	-30	-30	nd	nd	nd	nd	nd	nd
Fenchuganj #2	2578.6-2581.6	-26	-27	-26	-29	-29	-30	-29	-29	-29	-29	-29	-30	-29	-29	-29	-30	-29	-29	nd	nd	nd	nd	nd	nd	nd	nd	nd	nd
Fenchuganj #2+3	2768-2781	-25	-27	-26	-28	-30	-31	-29	-29	-29	-29	-29	-29	-29	-29	-29	-29	-29	nd	nd	nd	nd	nd	nd	nd	nd	nd	nd	nd
Fenchuganj #2	3068.5-3072.5 3074.5-3083.5	nd	nd	nd	nd	nd	nd	nd	nd	nd	-27	-28	-29	-29	-30	-31	-31	-31	-31	-30	-31	-31	-32	-32	-32	-32	-32	-31
Titas #1	2617-2769	-25	-25	-26	-27	-27	-29	-29	-29	-28	-27	-28	-29	-27	-26	-27	nd	nd	nd	nd	nd	nd	nd	nd	nd	nd	nd	nd	nd
Titas #5	2921-3052	-25	-26	-27	-29	-29	-29	-27	-27	-28	-28	-28	-27	-28	-26	nd	nd	nd	nd	nd	nd	nd	nd	nd	nd	nd	nd	nd	nd
Titas #8	3293-3551	-25	-27	-27	-28	-28	-28	-29	-31	-29	-27	-27	-27	-29	-26	nd	nd	nd	nd	nd	nd	nd	nd	nd	nd	nd	nd	nd	nd
Titas #10	3473-3680	-27	-27	-27	-29	-29	-30	-28	-29	-28	-28	-27	-28	-27	-28	-27	-28	nd	nd	nd	nd	nd	nd	nd	nd	nd	nd	nd	nd

nd, not detected

Table 6. Hydrogen isotope composition of individual *n*-alkanes (‰ , VSMOW).

Well name	Depth (m)	C_{11}	C_{12}	C_{13}	C_{14}	C_{15}	C_{16}	C_{17}	C_{18}	C_{19}	C_{20}	C_{21}	C_{22}	C_{23}	C_{24}	C_{25}	C_{26}	C_{27}	C_{28}	C_{29}	C_{30}	C_{31}	C_{32}	C_{33}	C_{34}
Sylhet #7	1874-1886 1901-1908	-128	-123	-123	-122	-115	-116	-116	-112	-116	-114	nd	nd	nd	nd	nd	nd	nd	nd	nd	nd	nd	nd	nd	nd
Sylhet #7	2020-2033	nd	-115	-123	-120	-123	-118	-122	-120	-119	-118	-114	-116	-116	-113	-115	-113	-117	-118	-109	-109	-110	-92	nd	nd
Kailash Tila #1	2941-2948	nd	-117	-111	-109	-109	-107	-108	-106	-106	-101	-98	-93	-89	nd	nd	nd	nd	nd	nd	nd	nd	nd	nd	nd
Kailash Tila #2	2252-2265	-122	-120	-115	-112	-111	-108	-111	-107	-106	-101	-99	-87	nd	nd	nd	nd	nd	nd	nd	nd	nd	nd	nd	nd
Kailash Tila #2+6	2252-2265	-120	-119	-112	-102	-100	-97	-103	-102	-101	-95	-91	-85	-71	nd	nd	nd	nd	nd	nd	nd	nd	nd	nd	nd
Kailash Tila #2	2724-2732	-121	-120	-115	-111	-101	-101	-102	-101	-103	-99	-101	-94	-92	-88	-87	-75	nd	nd	nd	nd	nd	nd	nd	nd
Kailash Tila #2	2927-2930	-115	-114	-112	-111	-109	-109	-110	-111	-108	-106	-103	-105	-97	-98	-97	-91	-91	nd	nd	nd	nd	nd	nd	nd
Kailash Tila #4	2930-2958	-122	-116	-116	-114	-114	-111	-112	-108	-108	-102	-100	-100	-94	-92	-94	-79	nd	nd	nd	nd	nd	nd	nd	nd
Beanibazar #1+2 (heavy)	3451-3465	-121	-115	-115	-111	-111	-109	-108	-106	-109	-101	-100	-103	-100	-93	-92	-94	-82	-87	-75	nd	nd	nd	nd	nd
Fenchuganj #2	2578.6-2581.6	-121	-116	-116	-118	-117	-120	-116	-113	-116	-107	-105	-104	-99	-97	-96	-86	-81	nd	nd	nd	nd	nd	nd	nd
Fenchuganj #2+3	2768-2781	nd	-114	-107	-109	110	-108	-106	-109	-106	-94	-101	-97	-89	-83	nd	nd	nd	nd	nd	nd	nd	nd	nd	nd
Fenchuganj #2	3068.5-3072.5 3074.5-3083.5	nd	nd	-107	-113	-106	-106	-109	-111	-111	-109	-107	-107	-108	-107	-105	-104	-103	-100	-97	-96	-95	-94	-90	-89
Titas #1	2617-2769	-119	-115	-112	-112	-110	-110	-109	-105	-101	-100	-94	-87	-82	-80	nd	nd	nd	nd	nd	nd	nd	nd	nd	nd
Titas #5	2921-3052	-121	-116	-108	-104	-102	-98	-100	-98	-96	-92	-90	-85	nd	nd	nd	nd	nd	nd	nd	nd	nd	nd	nd	nd
Titas #8	3293-3551	nd	-108	-108	-104	-103	-102	-101	-95	-91	-84	-82	-82	nd	nd	nd	nd	nd	nd	nd	nd	nd	nd	nd	nd
Titas #10	3473-3680	-123	-118	-117	-112	-110	-110	-108	-105	-101	-97	-95	-91	-76	nd	nd	nd	nd	nd	nd	nd	nd	nd	nd	nd

nd, not detected

$^{2}H/^{1}H$ value of the reference hydrogen gas was estimated by comparison with the standard *n*-alkanes with known $\delta^{2}H$ values (C_{24} – 52.704‰, C_{25} – 114.738‰, C_{28} – 232.937‰, and C_{30} – 33.562‰). The hydrogen isotope values ($^{2}H/^{1}H$) were reported in δ-notation relative to Vienna Standard Mean Ocean Water (VSMOV).

8. Results and discussion

Petroleum in the Paleogene to Neogene Surma basin, northeast Bangladesh (part of the Bengal Basin) ranges from waxy crude oils to condensates. Taking into account the physical and geochemical characteristics of oils, all the samples in the present study can be divided into two groups i.e. one as heavy waxy oils and the other as lighter condensates (Table 4). A significant diversity of *n*-alkanes distribution has been observed in the crude oils/condensate samples from the Surma basin. The diversity of the petroleum in the Surma basin was thought to be due to evaporative fractionation, resulting in residual waxy oils and lighter condensates which subsequently underwent tertiary migration and re-accumulation in the deltaic basin (Hossain et al., 2014).

8.1. Stable carbon isotope composition of individual n-alkane

The $\delta^{13}C$ value of individual *n*-alkane ranging as a whole from -32 to -25 ‰ (Table 5). The plot of $\delta^{13}C$ versus carbon number showing nearly similar distribution pattern of $\delta^{13}C$ in all the oil/condensate samples (Fig. 14). Oils and condensates from the Surma basin tends to decrease in ^{13}C with increasing carbon number (Fig. 14 and 15) in other words, negative slope of individual *n*-alkane $\delta^{13}C$ profile. Two condensates from the Kailash Tila field i.e. Kailash Tila #2 (2251-2265 m) and Kailash Tila #2+6 (2251-2265 m) showing significant depletion of ^{13}C upto -37 ‰ in the range of $C_{11\text{-}19}$ (Fig. 14). This unusual depletion in ^{13}C cannot be interpreted by the effects of biodegradation, water washing and/or in-reservoir phase separation fractionation. Among these two samples Kailash Tila #2 (2251-2265 m) is more depleted in ^{13}C compared to the mixed samples of Kailash Tila #2+6 (2251-2265 m) suggesting a possibility of contamination in the preservation tank in the field and/or during sample collection.

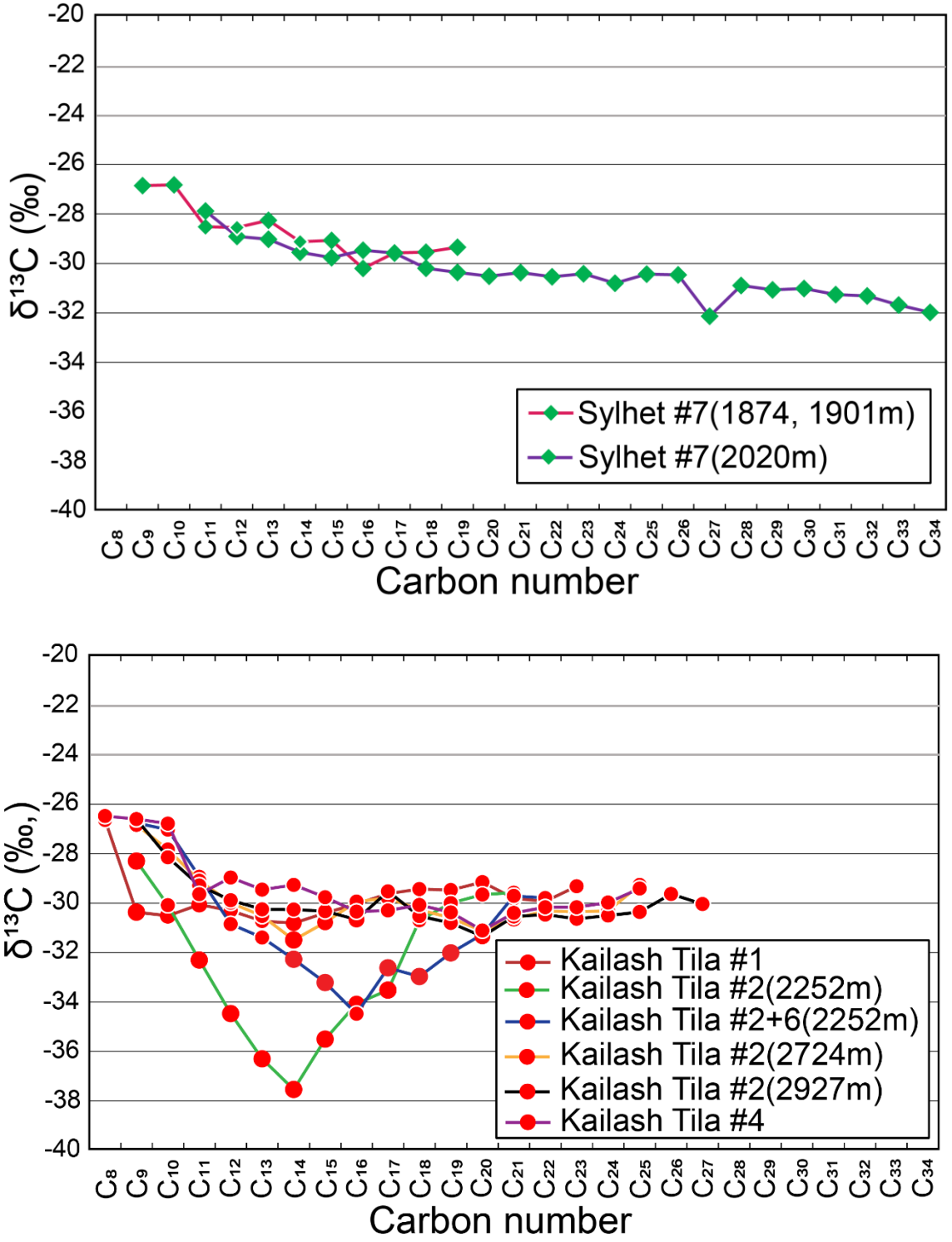

Fig. 14. Relationship between $\delta^{13}C$ value and carbon number of individual *n*-alkanes in oils and condensates from the Surma basin

Continue Fig. 14.

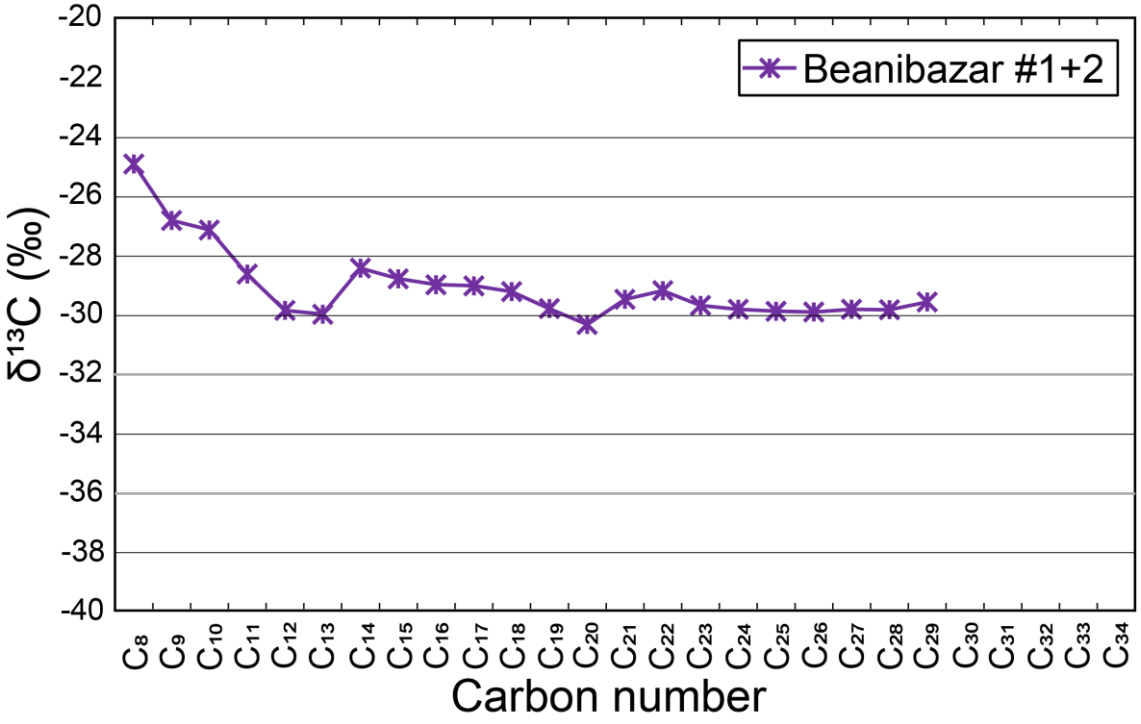

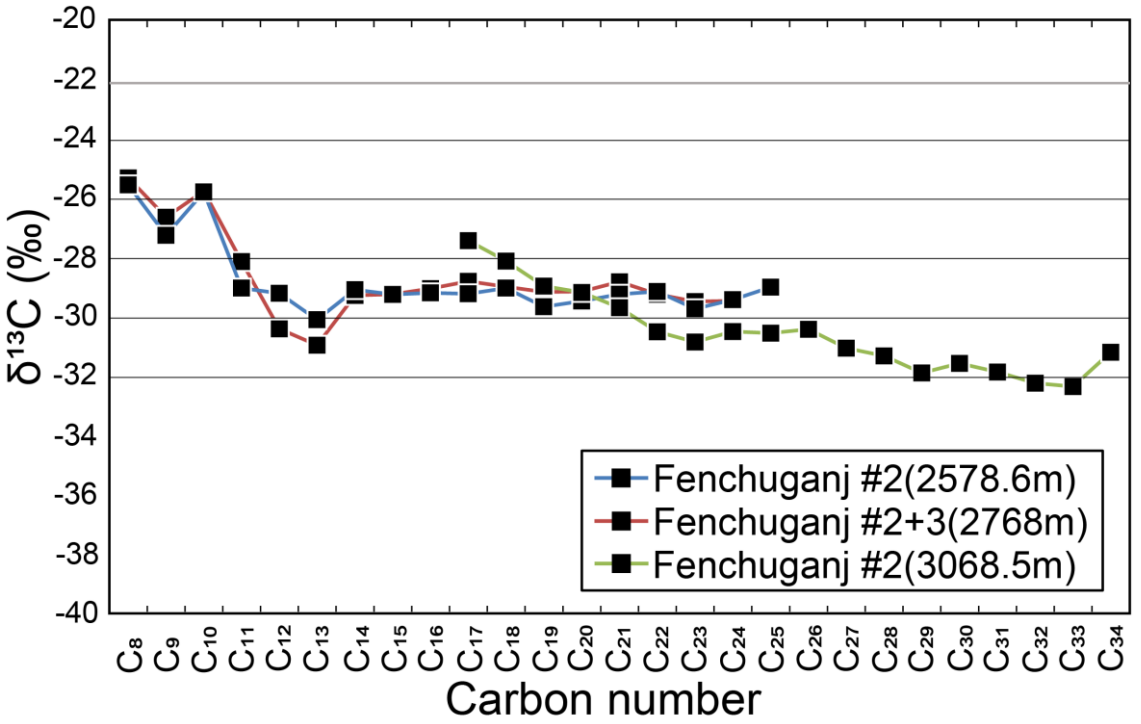

Continue Fig. 14.

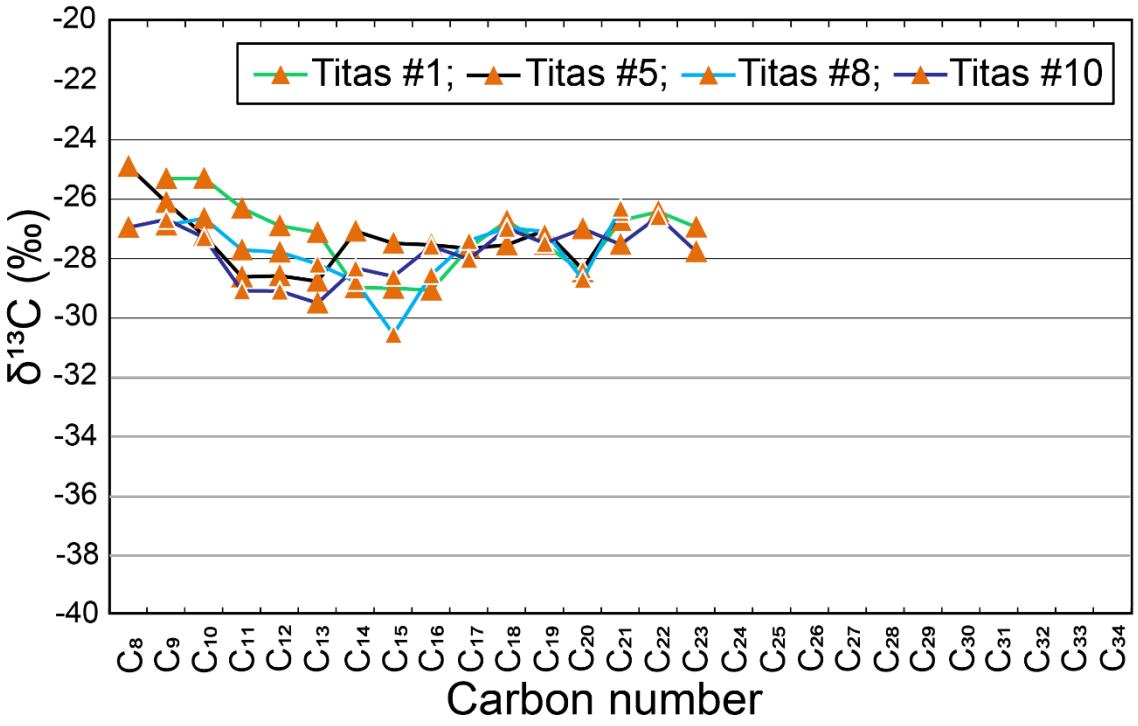

Therefore, carbon isotope composition of these two samples were not considered in the main discussion. In addition, the δ^{13}C profile of *n*-alkanes in condensates from the Titas field located in the southern margin of the Surma basin tends to increase in ^{13}C with increasing carbon number showing relatively flat and/or positive slope of δ^{13}C (Fig. 15). Source organic type and maturity level of oil are related to δ^{13}C values of *n*-alkanes in oils (Clayton, 1991; Bjoroy et al., 1991; 1994a; Odden et al., 2002; Xiong et al., 2005). Considering the similar maturity levels of oils and condensates as suggested by molecular parameters, the similar distribution of δ^{13}C values of *n*-alkanes elucidate that all the oils and condensates from the Surma basin were derived from the similar type of source organic matter and at similar maturity level, being consistent with molecular study (Hossain et al., 2014). Oils and condensates from the Surma basin tends to decrease in ^{13}C with increasing carbon number (Fig. 14) i.e. negative slope of the δ^{13}C profile suggest fluvio-deltaic and fresh water transitional environment of deposition (Bjoroy et al., 1991; Murray et al., 1994; Samuel et al., 2009).

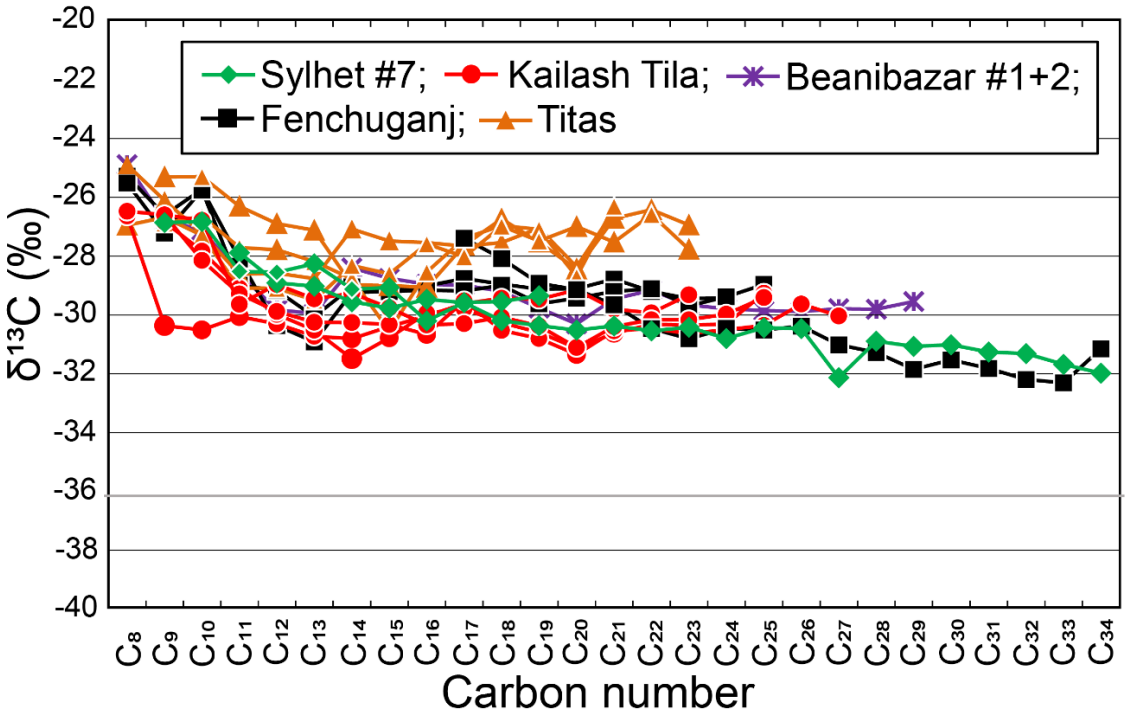

Fig. 15. Cross plot of $\delta^{13}C$ vs. carbon number, combining all the study samples

On the other hand, relatively flat and/or positive slope of *n*-alkane $\delta^{13}C$ profile in the condensates from Titas field that located in the southern margin of the Surma basin suggest marine influenced depositional environment as well as comparatively lower level of maturity (Clayton, 1991; Bjoroy et al., 1991; Murray et al., 1994; Samuel et al., 2009) also being consistent with the cross plot of pr/nC_{17} versus ph/nC_{18} (Fig. 5, chapter 1) and maturity parameters (Hossain et al., 2014).

8.2. Stable hydrogen isotope composition of individual n-alkane

The $\delta^{2}H$ value of individual *n*-alkanes ranges from -128 to -70 ‰ (Table 6) and linearly increases with increasing carbon number (Fig. 16). The relationship between carbon number and $\delta^{2}H$ value is notably different among the oil/condensate samples. Waxy oils from Sylhet #7 and Fenchuganj #2 showed remarkable depletion in ^{2}H with increasing carbon number compared to all other condensates. The distribution of $\delta^{2}H$ value of *n*-alkanes clearly distinguishes condensates from heavy waxy oils (Fig. 17). This large variation in $\delta^{2}H$ values of individual *n*-alkane in oils and condensates from the Surma

basin could be related to in-reservoir phase fractionation of the original oils, resulting in residual waxy oils and lighter condensates which subsequently underwent tertiary migration and re-accumulation in the deltaic basin (Hossain et al., 2014).

Vaporization of non-polar compounds like *n*-alkanes is partly related to intermolecular dispersion force (a sort of van der Waals force) caused by induction of a dipole moment. Intermolecular dispersion force of non-polar compound with ^{2}H is weaker than the same compound without ^{2}H because of weak polarizability of ^{2}H (Ramirez et al., 1998; Schulte et al., 2001). Consequently, vaporization of non-polar *n*-alkane with ^{2}H occurs easily compared to that without ^{2}H. Isotopically heavier compound with ^{2}H, therefore, would be expected to be concentrated in vapour phase. This effect termed as "inverse isotope fractionation" is significant with increasing molecular weight and has been observed in the laboratory (Wang and Huang, 2003; Bai et al., 2013). Probable mechanism of less polarizability of ^{2}H can be discussed in the following.

Influence of nuclear quantum fluctuation on isotopic substitution have been studied based on Feynman path integral Monte Carlo (PIMC) simulation associated with Hartree-Fock Hamiltonian (HF) calculation (Ramirez et al., 1998; Bohm and Saal, 2000; Schulte et al., 2001). PIMC simulation mainly based on Born-Oppenheimer approximation (BO) which introduced that molecular Hamiltonian (total energy= nuclear + electronic) can be separated. Hartree-Fock calculation described the decomposition of total energy E_{tot} to $\bar{E}_i$ ($\bar{E}_i$ represents their ensemble average value of i, where, i=kinetic energy of electron; i=nuclear-nuclear repulsion; i=electron-electron repulsion; i=electron-nuclear attraction; i=total electronic energy and i=potential energy of electron Hamiltonian etc.). The ensemble energy $\bar{E}_i$ are defined at the ground state of electron and relative to a single nuclear configuration at the zero point energy surface where Ei is zero (Fig. 18 and 19 respectively).

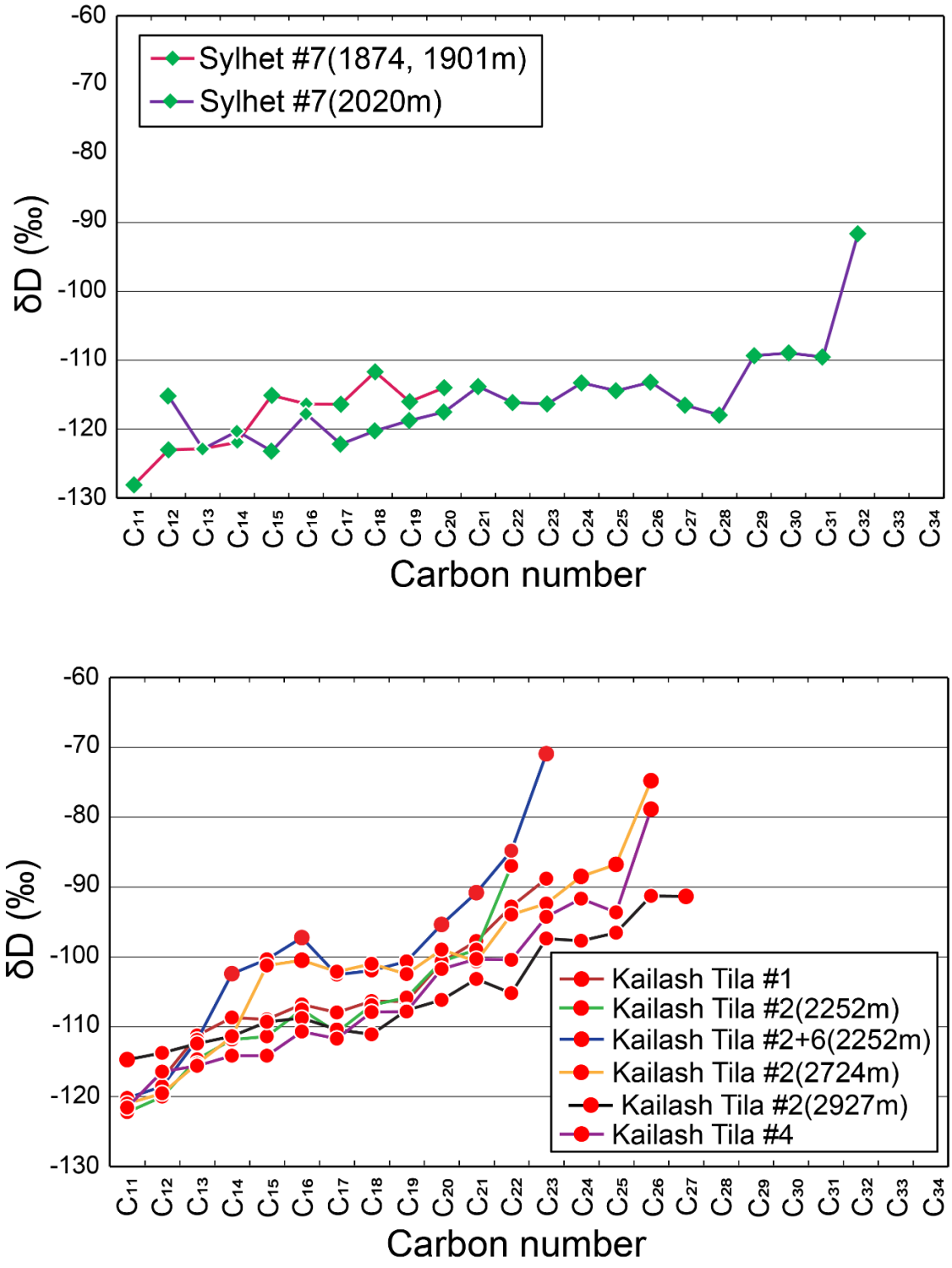

Fig. 16. Relationship between δ^2H value and carbon number of individual *n*-alkanes in oils and condensates from the Surma basin

Continue Fig. 16.

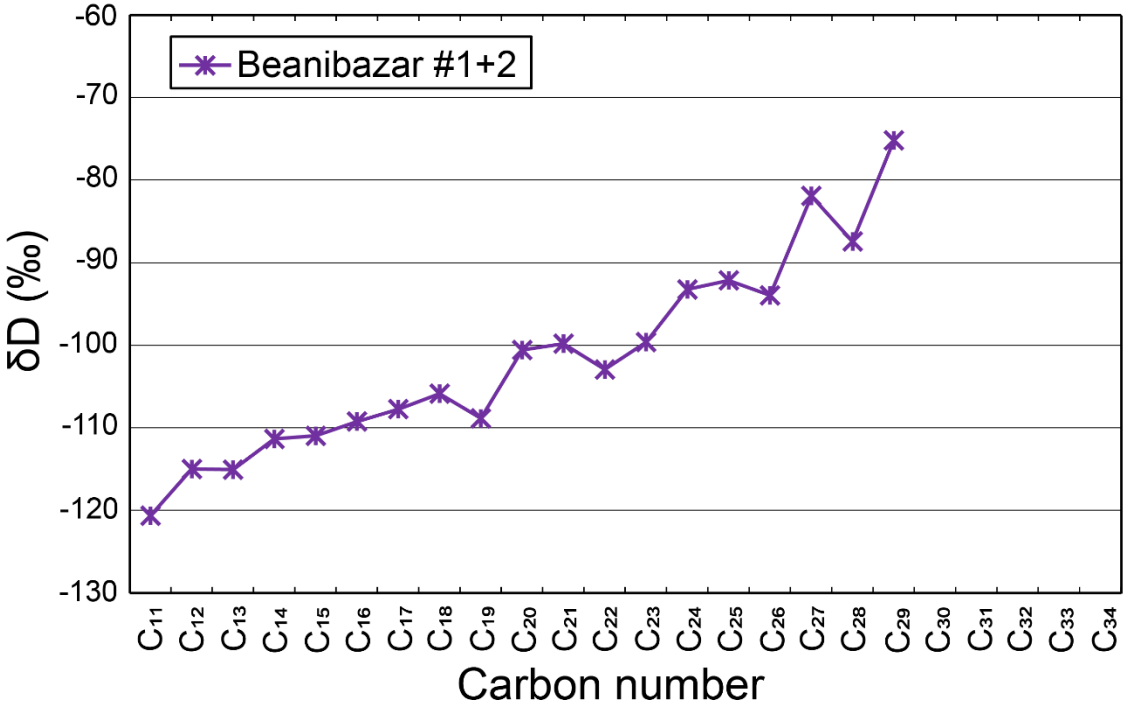

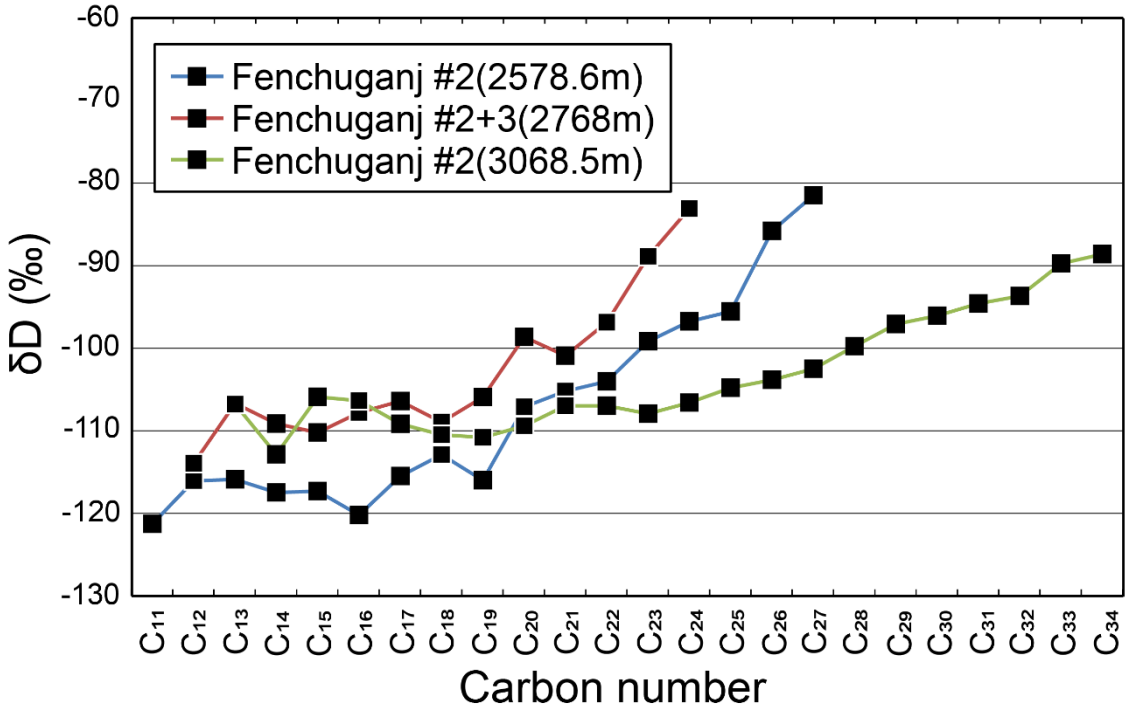

Continue Fig. 16.

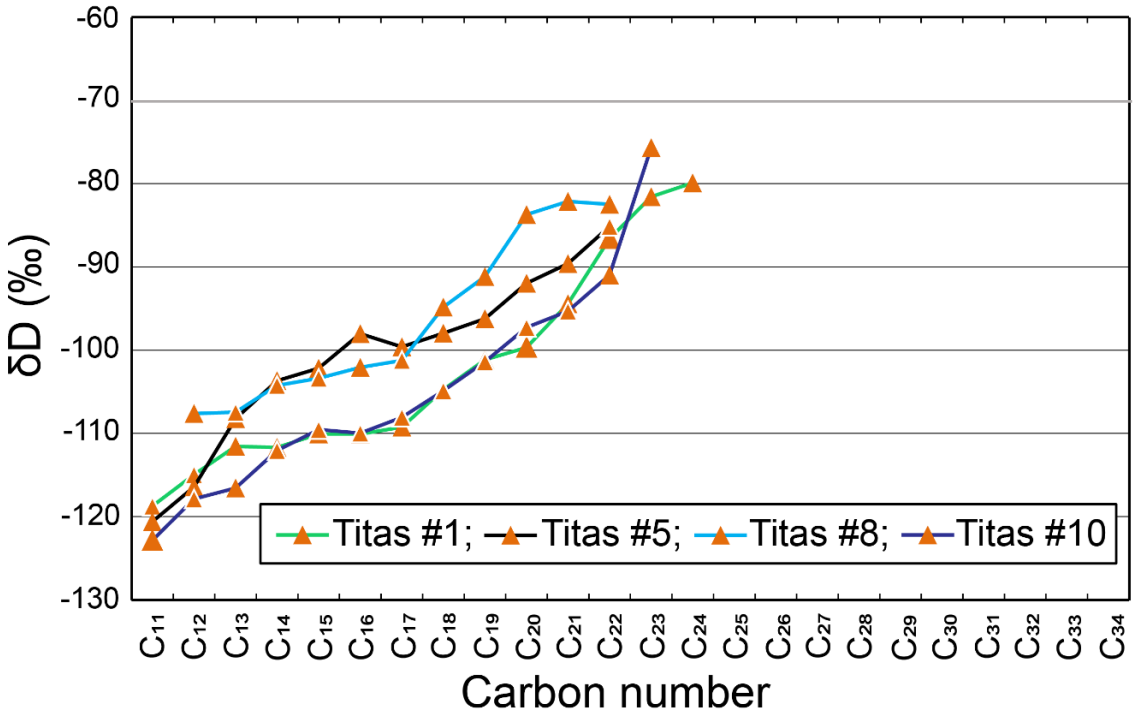

Probability distribution function of nuclei for manifold configuration (about more than 6000 configuration for benzene and ethylene) demonstrate sizeable spatial fluctuation of atomic nuclei. The nuclear fluctuation increases with decreasing atomic mass (e.g. H relative to C), results increasing ability to induce dipole moment (Schulte et al., 2001). In addition average value of instantaneous dipole moment $|\bar{\mu}|$ of non-polar compound with ^{2}H and without ^{2}H have been derived and found that, substitution of ^{1}H by ^{2}H reduces its dipole moment. Therefore, non-polar compound like *n*-alkane with ^{2}H is considered to be weaker than that of the compound without ^{2}H.

9. Inverse hydrogen isotope fractionation of n-alkanes

The $\delta^{2}H$ value of individual *n*-alkane in all the condensates from the Surma basin and Titas field linearly increases with increasing carbon number. *n*-Alkanes in condensates are rich in ^{2}H, whereas those in residual waxy oils are obviously depleted in ^{2}H. This variations in $\delta^{2}H$ value of waxy oils and condensates cannot be interpreted to be due to the differences in source rock type, maturity levels and/or paleo-hydrology.

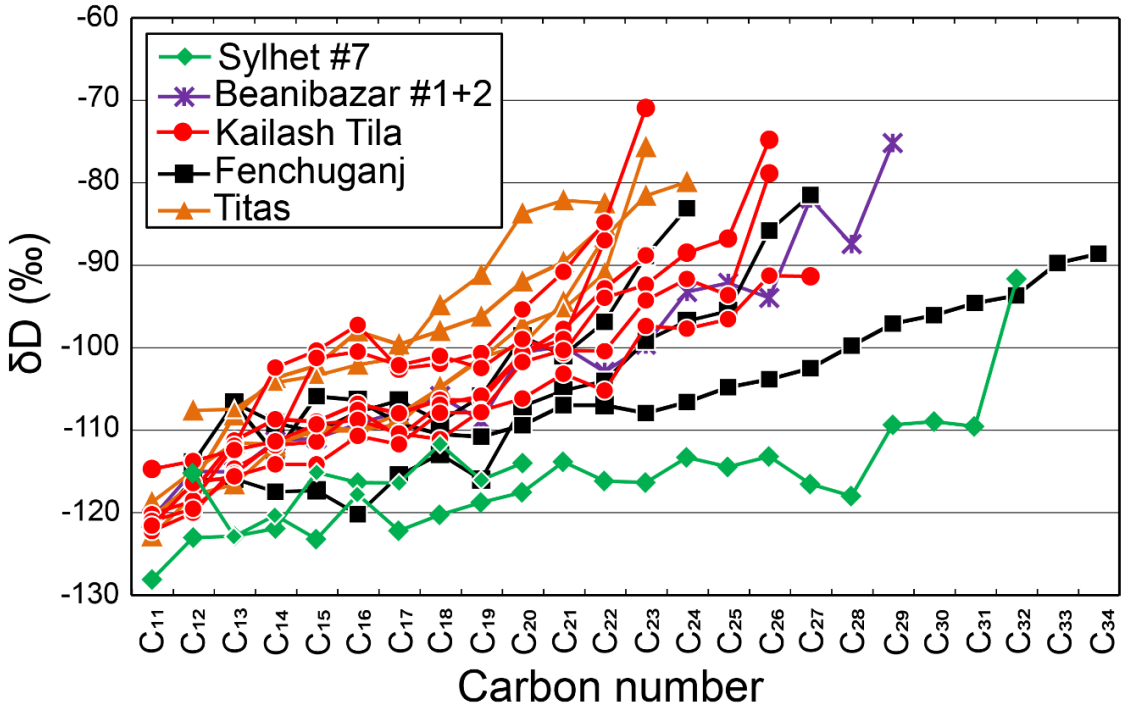

Fig. 17. δ^2H vs. carbon number, combining all the study samples

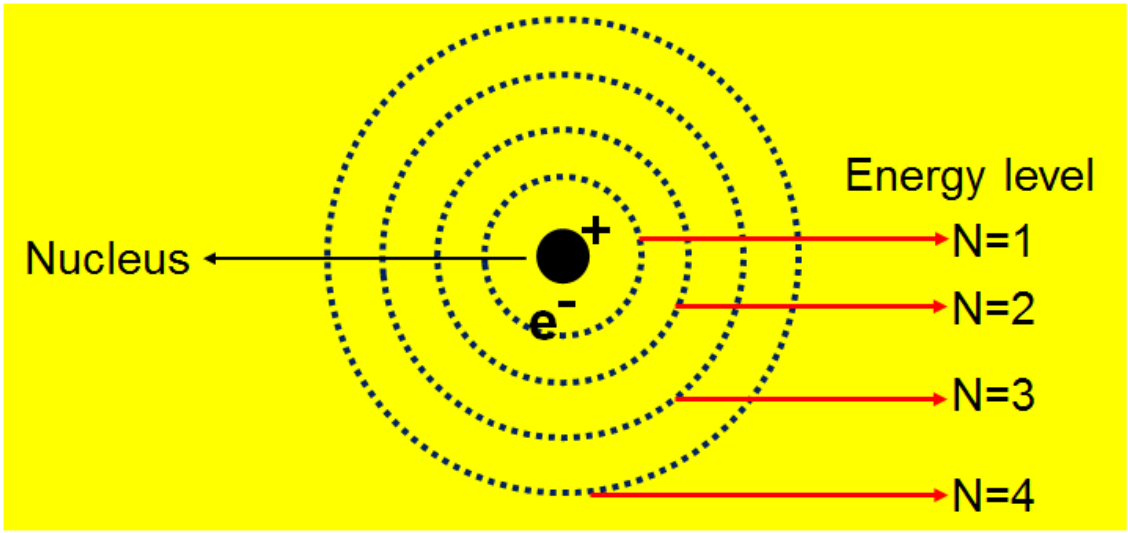

Fig. 18. Ground state of electron i.e. electron located close to the nucleus.

Since, the molecular investigation suggest that, crude oils and condensates specially from the Surma basin were derived from the similar terrestrial source rocks and expulsion of hydrocarbons from source rock took place at the identical level of maturity (Hossain et al., 2014). The large variation in δ^2H values of *n*-alkanes in oils/condensates from the study area is thought to be the possible first observation of "inverse hydrogen isotope fractionation" of *n*-alkanes associated with in-reservoir phase separation, migration, and re-accumulation in the natural petroleum system. On the other hand, small variation in δ^{13}C values of *n*-alkanes suggests a minor effect of phase separation on δ^{13}C value of *n*-alkanes. The evaluation of petroleum fractionation due to gas injection and phase separation needs various supporting data as discussed by Peters et al. (2005). The δ^2H value of *n*-alkanes in oil/condensates from the Surma basin, Bangladesh can be a useful data set for the evaluation of evaporative fractionation of petroleum in the sedimentary basin.

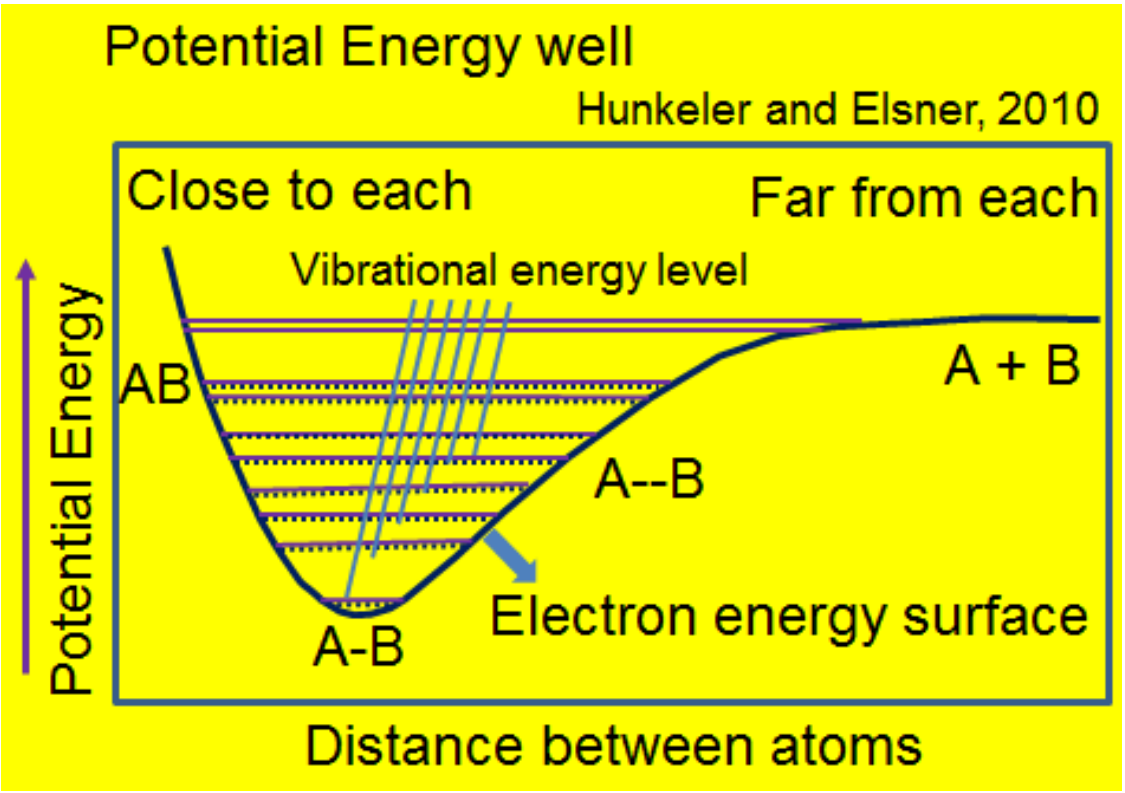

Fig. 19. Zero point energy surface well for a di-atomic (A and B) molecule.

10. Conclusions

Similar maturity levels of oils as suggested by molecular parameters and the similar distribution of $\delta^{13}C$ values of *n*-alkanes elucidate that all the oils and condensates were generated from the similar type of source rock rich in terrigenous organic matter and at the identical maturity level. Depletion in ^{13}C value of *n*-alkanes with increasing carbon number (negative slope) suggest that, source rocks were deposited under fluvio-deltaic environment. On the other hand, relatively flat and/or positive slope of *n*-alkane $\delta^{13}C$ profile in the condensates from Titas field that located in the southern margin of the Surma basin suggest marine influenced depositional environment as well as oils were derived comparatively lower level of maturity.

The distribution of $\delta^{2}H$ value of *n*-alkanes clearly distinguishes condensates from heavy waxy oils. *n*-Alkanes in condensates are rich in $\delta^{2}H$, whereas those in residual waxy oils are obviously depleted in $\delta^{2}H$. The remarkable variation in $\delta^{2}H$ values of *n*-alkanes in oils/condensates from the Surma basin is the possible first observation of "inverse hydrogen isotope fractionation" of *n*-alkanes associated with in-reservoir phase separation, migration, and re-accumulation in the natural petroleum system. On the other hand, small variation in $\delta^{13}C$ values of *n*-alkanes suggests a minor effect of phase separation fractionation on $\delta^{13}C$ value of *n*-alkanes. The evaluation of petroleum fractionation due to gas injection and phase separation needs various supporting data. Therefore, the $\delta^{2}H$ value of *n*-alkanes can be a useful data set for the evaluation of evaporative fractionation of petroleum in the sedimentary basin.

11. Synopsis of the thesis

Petroleum in the Surma basin, NE Bangladesh (part of the Bengal Basin) ranges from waxy crude oils to condensates. The relative abundance of pristane, phytane, and adjacent *n*-alkanes, and the abundance and similar distribution of biphenyls, cadalene and bicadinanes in most of the oils and condensates from the Surma basin suggest that, oils were derived from the terrestrial source rocks and expelled at the maturation stage of R_o=1.0–1.3%. Oils from the southern margin of the Surma basin were derived from marine influenced terrestrial source rock and at a relatively low maturity levels (Ro=0.8–1.0%). Diamondoid hydrocarbons can be used to characterize the severely biodegraded oils. Relationship of time-temperature, vitrinite reflectance and estimated maturity levels of the oil/condensate from the Surma basin associated with depositional environment suggested based on biostratigraphic study, non-marine deposits ranging from the late Eocene upper Kopili Shale to the early Oligocene lower Jenam Formation can be the most possible source rocks of the study oils and condensates. The relative abundance of C_7 aromatic, cyclic, and straight chain hydrocarbons in condensate to waxy oils and other molecular parameters suggeste evaporative fractionation due to in-reservoir phase separation.

Similar maturity levels of oil/condensates and the similar distribution of $\delta^{13}C$ values of *n*-alkanes elucidate that all the oils and condensates from the Surma basin were generated from the similar type of source rock rich in terrigenous organic matter and at the identical maturity level. Decreasing $\delta^{13}C$ value of *n*-alkanes with increasing carbon number (negative slope) suggest that, source rocks were deposited under fluvio-deltaic environment. On the other hand, relatively flat and/or positive slope of $\delta^{13}C$ profile in the condensates from Titas field indicates marine influenced depositional environment and comparatively lower level of maturity. The distribution of $\delta^{2}H$ value of *n*-alkanes clearly distinguishes condensates from heavy waxy oils. *n*-Alkanes in condensates are rich in $\delta^{2}H$, whereas those in residual waxy oils are obviously depleted in $\delta^{2}H$. The remarkable variation in $\delta^{2}H$ values of *n*-alkanes in oils/condensates from the Surma basin is thought to be the possible first observation of "inverse hydrogen isotope fractionation" of *n*-alkanes associated with in-reservoir phase separation, migration, and re-accumulation in the natural petroleum system. On the other hand, nearly similar $\delta^{13}C$ values of *n*-alkanes suggests a minor effect of phase separation on $\delta^{13}C$ value of *n*-alkanes.

Acknowledgement

First of all, I am very grateful to the Government of Japan for giving me the opportunity to continue my doctoral course in Hokkaido University by the support of 'MEXT' scholarship. Also, I am grateful to the authority of my employer 'Bangladesh Petroleum Exploration & Production Company Ltd (BAPEX)' for giving me the permission to come to Japan.

I am highly indebted and would like to express my sincere gratitude to my supervisor Noriyuki SUZUKI, Professor and Dean, Graduate School of Science, Hokkaido University. The person, who gave me a tremendous support and guidance during my stay in Japan that made my research fruitful. He is very kind and friendly to all of his students. I feel proud of myself to be a student of him for his patience, motivation, enthusiasm, and immense knowledge.

I am thankful to all the honorable members of joint study between Bangladesh Petroleum Institute (BPI)/Bangladesh Oil, Gas & Mineral Corporation (Petrobangla)/Bangladesh Petroleum Exploration & Production Company Limited (BAPEX), Bangladesh and Mitsui Oil Exploration Company Limited (MOECO)/JGI Inc. and Hokkaido University, Japan for providing me the samples and necessary data.

Special thanks to Hiroyuki Saito, who helped and guided me in all aspects to do my research here especially in analyzing and handling the machines involved with my research. I would like to convey my gratitude to Mr. Ken Sawada and Tsuyoshi Watanabe the honorable staff members of our laboratory, for their valuable advice during my study. Thankful to all the 5G Members for their friendly attitude all the time.

Also, I am indebted to the secretaries (Ms. Miyabi Hirata, Ms. Michiko Magira, Ms. Mizue Asaarashi and Ms. Naoko Kanou) for their enormous support and kind co-operation. I am very much obliged to all of my family members and friends for their immense support from various aspects during my residing in Sapporo, Hokkaido, Japan. Everything became possible only by the blessings of almighty Allah. It is not possible to express in a few words my gratefulness to Allah, who gifted us our one and only son 'Ibtesum Manal' during my study (May 8, 2012) in Japan.

References

BAI, H., PENG, L., CAO, J., LIU, X., ZHANG, J., MU, L., 2013: Effects of volatilization on the hydrogen isotope composition of selected *n*-alknaes. *Atmospheric Research*, **132-133**, 164-172.

BJOROY, M., HALL, K. and JUMEAU, J., 1990: Stable carbon isotope ratio analysis on single components in crude oils by direct gas chromatography-isotope analysis. *Trends in analytical chemistry*, **9**, 1990.

BJOROY, M., HALL, K., GILLYON, P. and JUMEAU, J., 1991: Carbon isotope variations in *n*-alkanes and isoprenoids of whole oils. *Chemical Geology*, **93**, 13-20.

BJOROY, M., HALL, P. B. and MOE, R. P., 1994a: Variation in the isotopic composition of single components in the $C_4 – C_{20}$ fraction of oils and condensates. *Org. Geochem*. **21**, 761-776.

BOHM, M. C., SAAL, C., 2000: Quantum statistical analysis of superconductivity, fractional quantum hall effect, and aromaticity. *International Journal of Quantum Chemistry*, **79**, 125-162.

CLAYTON, C. J., 1991: Effect of maturity on carbon isotope ratios of oils and condensates. *Org. Geochem.* **17**, 887-899.

DAWSON, D., GRICE, K., WANG, S. X., ALEXANDER, R., RADKE, J., 2004: Stable hydrogen isotopic composition of hydrocarbons in torbanites (Late Carboniferous to Late Permian) deposited under various climatic conditions. *Organic Geochemistry*, **35**, 189-197.

DZOU, L. I. P. and HUGHES, W. B., 1993: Geochemistry of oils and condensates, K field Offshore Taiwan: a case study in migration fractionation. *Org. Geochem*. **20**, 437-462.

GRAAS, G. W. V., GILJE, A. E., ISOM, T. P., TAU, L. A., 2000: The effects of phase fractionation on the composition of oils, condensates and gases. *Organic Geochemistry*, **31**, 1419-1439.

HOSSAIN, MD. A., SUZUKI, N., MATSUMOTO, K., SAKAMOTO, R., and TAKEDA, N., 2014: In-reservoir fractionation and the accumulation of oil and condensates in the Surma basin, NE Bangladesh. *Journal of Petroleum Geology*, **37(3)**, 269-286.

Hunkeler, D., Elsner, M., 2010: Principles and mechanisms of isotope fractionation. In: Aelion, C. M., Hohener, P., Hunkeler, D., Aravena, R. (eds.) Environmental isotopes in biodegradation and bioremediation. CRC Press, Boca Raton.

KIKUCHI, T., SUZUKI, N., SAITO, H., 2010: Change in hydrogen isotope composition of *n*-alkanes, pristine, phytane, and aromatic hydrocarbons in Miocene siliceous mudstones with increasing maturity. *Organic Geochemistry*, **41**, 940-946.

LI, M., HUANG, Y., OBERMAJER, M., JIANG, C., SNOWDON, L. R., FOWLER, M. G., 2001: Hydrogen isotope compositions of individual alkanes as a new approach to petroleum correlation: case studies from the Western Canada Sedimentary Basin. *Organic Geochemistry*, **32**, 1387-1399.

MURRAY, A. P., SUMMONS, R. E., BOREHAM, C. J. and DOWLING, L. M., 1994: Biomarker and n-alkane isotope profiles for Tertiary oils: relationship to source rock depositional setting. *Org. Geochem*. **22**, 521-542.

MYCKE, B., HALL, K. AND LEPLAT, P., 1994: Carbon isotopic composition of individual hydrocarbons and associated gases evolved from micro-scale sealed vessel (MSSV) pyrolysis of high molecular weight organic material. *Org. Geochem*. **21**, 787-800.

ODDEN, W., BARTH, T., TALBOT, M. R., 2002: Compound-specific carbon isotope analysis of natural and artificially generated hydrocarbons in source rocks and petroleum fluids from offshore Mid-Norway. *Organic Geochemistry*, **33**, 47-65.

PETERS, K.E., WALTERS, C.C. and MOLDOWAN, J.M., 2005, The Biomarker Guide: Vol.1, Biomarkers and isotopes in the environment and human history. Cambridge Univ. Press, Cambridge.

RAMIREZ, R., HERNANDEZ, E., SCHULTE, J., BOHM, M. C., 1998: Nuclear quantum effects in the electronic structure of C2H4: a combined Feynman path integral – ab initio approach. *Chemical Physics Letters*, **291**, 44-50.

SAMUEL, O. J., CORNFORD, C., JONES, M., ADEKEYE, O. A., AKANDE, S. O., 2009: Improved understanding of the petroleum systems of the Niger Delta Basin, Nigeria. *Organic Geochemistry*, **40**, 461-483.

SCHIMMELMANN, A., SESSIONS, A. L. and MASTALERZ, M., 2006: Hydrogen isotopic (D/H) composition of organic matter during diagenesis and thermal maturation. *Annual Review of Earth and Planetary Science*, **34**, 501-533.

SCHULTE, J., RAMIREZ, R., BOHM, M. C., 2001: Isotope dependence of dispersion forces: a Feynman path integral – ab initio study. *Journal of Molecular Structure (Theochem)*, **536**, 277-287.

WANG, Y., HUANG, Y., 2003: Hydrogen isotopic fractionation of petroleum hydrocarbons during vaporization: implications for assessing artificial and natural remediation of petroleum contamination. *Applied Geochemistry*, **18**, 1641-1651.

XIAO, Q., SUN, Y., ZHANG, Y., CHAI, P., 2012: Stable carbon isotope fractionation of individual light hydrocarbons in the C_6-C_8 range in crude oil as induced by natural evaporation: Experimental results and geological implications. *Organic Geochemistry*, **50**, 44-56.

XIONG, Y., GENG, A., PAN, C., LIU, D., PENG, P., 2005: Characterization of the hydrogen isotopic composition of individual n-alkanes in terrestrial source rocks. *Applied Geochemistry*, **20**, 455-464.